NASA TM X-420

NASA TM X-420

NASA

TECHNICAL MEMORANDUM

X-420

COMPILATION OF PAPERS SUMMARIZING SOME RECENT NASA RESEARCH ON MANNED MILITARY AIRCRAFT

By Staff of the NASA

NATIONAL AERONAUTICS AND SPACE ADMINISTRATION
WASHINGTON 3
October 1960

NATIONAL AERONAUTICS AND SPACE ADMINISTRATION

TECHNICAL MEMORANDUM X-420

FOREWORD

The nine papers included in this volume were presented by NASA research staff members at the National Meeting on The Future of Manned Military Aircraft sponsored by the Institute of the Aeronautical Sciences and held in San Diego, Calif., from August 1 to August 3, 1960. Because, together, they provide a comprehensive summary of research by NASA in the areas covered, they have been compiled in this publication for the information of personnel concerned with the design and procurement of manned military aircraft.

CONTENTS

PRECEDING PAGE BLANK NOT FILMED.

NATIONAL AERONAUTICS AND SPACE ADMINISTRATION

TECHNICAL MEMORANDUM X-420

COMPILATION OF PAPERS SUMMARIZING SOME RECENT NASA RESEARCH ON MANNED MILITARY AIRCRAFT*

By Staff of the NASA

I. VTOL AIRCRAFT - STATE OF THE ART

By Robert H. Kirby

Langley Research Center

INTRODUCTION

During the last few years a large number and wide variety of VTOL aircraft types have been studied; some of them promising, some not so promising. The purpose of this paper is to summarize briefly the state of the art in this field and to indicate which of the types are most promising, to bring out applications where they are best suited and to indicate what is needed in the way of additional research and development.

DISCUSSION

Before the different types are considered individually, the factors that determine their logical areas of application are discussed.

A basic relationship that exists between the four propulsion types in hovering is shown in figure 1. Hovering effectiveness, which is defined as the amount of vertical lift produced by a given amount of power, is shown as a function of slipstream or jet velocity. The helicopter rotor moves a large mass of air downward at a low velocity whereas the turbojet accelerates a small mass of air to very high velocities. A good indication of the meaning of hovering effectiveness can be obtained from the fuel consumption of the different types. For hovering with a given payload, the propeller VTOL will use about 3 to 4 times the fuel used by the helicopter whereas the jet would use in the neighborhood of 25 times as much as the helicopter. Obviously, the hovering time of these higher performance aircraft has to be kept to a minimum.

The differences in the slipstream velocities shown in figure 1 are often cited as reasons for accepting or rejecting various VTOL configurations. It is probably true that the higher velocities associated with

*Title, Unclassified.

propeller, ducted-fan, and turbojet aircraft will increase the severity of the problems of ground erosion and recirculation of dust and debris that has been experienced with helicopters when operating from unprepared bases. Just how much more of a problem this will be, however, seems to be open to question.

Recent National Aeronautics and Space Administration downwash studies with models have indicated that good sod will not disintegrate under the impact of heavily loaded propeller slipstreams. Experience with the Short S.C. 1 in Ireland, has indicated that even turbojet-lifted airplanes can perform certain limited operations from substantial sod.

For logistic support or assault transport missions with propeller-driven aircraft, it would seem to be possible in most cases to find a grass field or a very hard dirt surface for the operation of VTOL aircraft and thereby avoid serious ground erosion problems. This problem is a localized problem right beneath the aircraft. In the surrounding area, the concern that high-velocity slipstreams will be more prone to blow over personnel and equipment some distance from the aircraft is contrary to existing experimental evidence, the reason being the very rapid dissipation of the energy in the smaller, higher velocity slipstreams. (See fig. 2.) Shown at the top of figure 2 is a helicopter and a typical four-propeller tilt wing, both weighing the same (about 30,000 pounds). The helicopter has a rotor diameter of 72 feet and therefore a disk loading of about 7.5. The propellers are 15 feet in diameter with a disk loading of 43 or about $5\frac{1}{2}$ times that of the helicopter. The sketches at the top of figure 2 show the rotor and propeller slipstreams as they flow down and then out along the ground. These velocities along the ground are plotted in figure 2 against distance out from the center of the aircraft and the plots show that the velocities decay as the distance increases. The solid line is the horizontal velocity of the propeller slipstream and the dashed line is for the helicopter. This plot shows that, although the propeller velocities are higher at the start, they decay so rapidly that in a very short distance, in this case about 18 feet from the tips, the velocity is less for the propeller than for the large rotor. It would not be expected that personnel or equipment would often be any closer than this crossover point to either of the machines during take-off or landing. It should also be pointed out that the slipstream from the small propeller is only about one-fourth as deep as that for the rotor. This discussion of ground effects is not intended to imply that the higher slipstream velocities will not cause operational problems in the field; certainly, ground erosion and related subjects are much in need of research and operational evaluation, but it does seem that the slipstream problem may not be as great as it is sometimes pictured to be.

As indicated earlier, the large rotor is the most effective way of producing vertical lift but this is only one part of the answer. When the mission calls for higher speed and longer range, an efficient forward flight system - something like that of the conventional airplane - is needed. The power-required curves of figure 3 show the shortcomings of the helicopter in this regard. There is a rapid increase in power required for the helicopter at low forward speeds. With some of the higher performance VTOL aircraft, such as propeller tilt-wing, ducted-fan, and turbojet types, the efficiency of the conventional airplane in cruising flight can be approached.

The following areas of application shown in figure 4 where hovering time is plotted against cruising speed were thus obtained: helicopter for long-hovering and low-speed missions, other rotor types for a little higher speed and range, propeller and ducted-fan VTOL aircraft where higher speed and range is a big factor, and turbojets where speed is the primary consideration.

These types will now be considered individually to determine the most promising ones in each area.

The helicopter, of course, is already well established and, with expected improvements, should continue to be the best VTOL for missions such as flying cranes, rescue, and forward-area operations where long hovering time is required and where low speed and short range are acceptable.

Figure 5 shows two other rotor types: the compound or dual propulsion on the left and the tilt rotor on the right. Here the disk loadings have increased only a little above the helicopter, about 8 or so on the compound and up to about 20 for the tilt rotor; thus, these are promising types for applications where a large amount of hovering and low-speed operation is still required but where somewhat higher cruising speed and range are needed than can be achieved with the helicopter.

The state of the art is further advanced for the compound helicopter than for the tilt-rotor machine, mainly because its development has been actively pursued in England as the Rotodyne. It appears that a machine of the Rotodyne type may operate reasonably satisfactorily as a commercial transport provided certain operating problems, such as the high noise level and high operating cost, can be solved. The development of a military version of this aircraft would seem to be a fairly straightforward procedure.

The technical feasibility of the tilt rotor has been demonstrated successfully. A few objectionable handling qualities have been discovered but they seem to be largely functions of the very lightly loaded rotors

of the research machines and might not be such serious problems on a transport-size aircraft with more heavily loaded rotors. Although it does appear possible to develop an operational tilt-rotor machine, interest in this type seems to be limited because of strong competition from two other VTOL types, the compound helicopter which could be available for operational use sooner and propeller configurations which offer better cruising performance.

Propeller-driven VTOL's (particularly tilting wing and deflected slipstream types) have received much attention. Figure 6 illustrates a configuration that combines the two types somewhat by having a tilting wing with a large chord slotted flap and results in a configuration that is considered to be one of the most promising VTOL types, particularly, for use on short or medium transport missions. A configuration like this would take off and land in a short distance (STOL) where possible, such as from rear supply areas and for ferry hops, but would have the vertical take-off and landing (VTOL) capability where needed. For one particular mission, that of a small logistic support transport which was studied in connection with an ASR (Army Service Requirement) program, a tilt-wing configuration of this type seemed to offer very promising performance in terms of payload, range, and operating cost.

Fairly extensive wind-tunnel and flying-model research on advanced configurations such as this type have indicated solutions to most of the peculiarities of the early propeller test beds. It is now felt that there are no technical barriers to the design and construction of a machine of this type for obtaining operational experience. Of course, additional research and development is still needed.

To date, ducted-fan VTOL aircraft have appeared to be generally less promising than other types but there are three ducted-fan applications for military use that should be mentioned. The first configurations are for a special low-speed application and have been termed flying platforms and light combat aerial vehicles (sometimes called aerial jeeps). These machines are the result of an effort to give the Army a utility machine that would be simple, compact, and easy to fly. Research to date, however, has not revealed any configurations likely to meet the requirement of being simple and easy to fly and the machines tested to date have been restricted in forward-flight performance.

The second ducted-fan applications are the fan-in-wing and fan-in-fuselage configurations. These aircraft have ducted fans buried in the wing or fuselage for vertical take-off and landing and for cruising flight the fans are covered over and conventional turbojet propulsion is used. Recent research has revealed an unexpectedly severe problem in the transition speed range for both these submerged fan types and for lifting-jet engine configurations. The problem arises from the interference of the fan or jet exhaust with the free-stream airflow. Figure 7 illustrates the effect of this interference and shows a planform with

high velocity exhausts in the center, either from jets or fans. At the low forward speeds during the transition the exhaust interferes with the free-stream flow, causes it to speed up to get around the exhaust, and also separates in some regions behind the exhaust; as a result negative pressures occur over large areas of the lower surface. The negative pressures are represented here by the shaded portions, the darker shades meaning lower pressures. If it is not taken into consideration in designs that have flat areas beside and behind high velocity exhaust, this low-pressure region could result in large losses in lift, large pitching moments, and stability problems during the transition between hovering and forward flight. The fan-in-wing or fan-in-fuselage types might find military application where high subsonic or supersonic speeds are needed, but there are problems that will have to be carefully resolved before the system is ready for operational use.

The third and most successful ducted-fan VTOL to date is the tilting-duct type shown in figure 8. The wing-tip-mounted ducts rotate through 90° for hovering and forward flight. The technical feasibility of this type has been demonstrated and its state of the art is approximately the same as those for the tilt-rotor and tilt-wing configurations although, at this time, not quite as well supported by wind tunnel and flight-test experience. This type could have merit for certain military applications where compactness is desired at the expense of some hovering efficiency and short take-off and landing capability.

A number of turbojet VTOL configurations have received attention, such as ones using tilting jets, deflected jets, and small lightweight lifting jets. Although these types have been demonstrated to be technically feasible with varying amounts of research and several jet research aircraft have been successfully tested, no operational aircraft have been flown. There is one small operational jet, however that is expected to fly in the near future. It is the Hawker P.1127 transonic strike aircraft shown in figure 9.

With a VTOL weight of about 12,000 pounds the Hawker is powered with a Bristol BE-53 turbofan engine with swivelling nozzles, two on each side of the fuselage. In hovering, the four nozzles are pointed downward and the transition is performed by rotating the nozzles rearward.

In this country most of the interest of the military has been in VTOL supersonic fighters but their development is expected to follow well behind that of other VTOL types. The operational experience to be gained with this subsonic configuration should provide some of the information needed for proceeding to the supersonic applications.

[redacted]

The plot of hovering time against cruising speed (fig. 10) is again shown to indicate the four most promising types at the present state of the art in their respective areas. Now that the feasibility of these types has been established, the VTOL aircraft field is now ready for the next step, that is to build some of these higher performance machines so that the operational experience needed to determine their potential can be obtained and to define more clearly the service requirements in the various areas. It is expected that this experience will be gained in the near future with the machines on each end of the chart (fig. 10), the compound helicopter and the turbojet fighter. It appears highly desirable, therefore, to obtain as soon as possible an operational tilt-wing machine which fills in the middle of the chart and seems particularly well suited for transport missions that require long range and where higher speed is advantageous.

By indicating that operationally useful machines can and should be obtained at the present state of the art, it is not meant that a great deal of research is not still needed in this field. On the contrary, before the full potential of VTOL systems is realized, there is a vast amount of research, development, and experience needed.

Problem areas common to all of the VTOL types and needing additional research and development are: cost and weight of airframe and propulsion system, handling qualities, all-weather capability, and ground erosion and recirculation. Cost and weight both must be reduced for the airframes and, much emphasis must be placed on propulsion systems, including gearing, rotors, and propellers. Continued research is needed on handling qualities and all-weather capability is something that must be achieved to utilize these machines fully. In addition ground erosion and recirculation needs evaluation, particularly for the higher performance types.

Even the helicopter, which is being obtained in increasing numbers, is far from an optimum system. Besides needing a drag reduction program to improve its range and endurance, the helicopter has many other areas still needing attention. The cyclic loads, particularly in the cruising range and vibration are problems. All-weather capability should again be emphasized for the helicopter and the need for improved behavior when operating in or near severe turbulence.

The compound helicopter will also have some of these problems plus a few of its own such as rotor instabilities at the higher forward speeds. Reduction of hub, pylon, and interference drag will be even more important at these higher speeds. If tip-driven rotors are used, the noise level is a big problem and, in this connection the question of whether a tip-driven or gear-driven rotor is best for the compound helicopter is not clear at this time. There are proponents for each method both here and in England; therefore, their relative merits are in need of evaluation.

[redacted]

The tilt-wing configuration needs detailed research on loads and stresses leading to the development of lightweight propellers, research on gearing and turbine engines leading to lighter weight and especially lower cost and greater freedom from maintenance, and continued structural research; all of these lead to a higher percentage of useful load to gross weight.

In addition continual aerodynamic and flight research on improved performance and handling qualities and operational evaluation of compromise factors such as VTOL and STOL capability, speed as opposed to range, and the seriousness of ground erosion problems are needed.

Some of the more important research needs of turbojet configurations are discussed next. The need for the development of lightweight engines cannot be stressed too greatly. Noise and ground erosion and ingestion problems will have to be evaluated and reduced. And finally, operating problems could be especially severe with turbojet configurations.

Research is being carried on in many of these areas at the present time and others will undoubtedly be studied in the near future. Some, such as the development of really lightweight, inexpensive gas turbines, will need concerted effort, time, and ingenuity to solve, and many are such that only experience with useful machines can effectively show the way.

CONCLUDING REMARKS

Although a great deal of research and development will be required before operational VTOL aircraft will be obtained, the state of the art in this field has advanced to the point where operationally useful machines of some VTOL types can be designed and built. There is a great need now for experience with such aircraft to determine their capabilities under conditions of field operation. Efforts should be made as soon as possible to obtain operational machines to provide this experience.

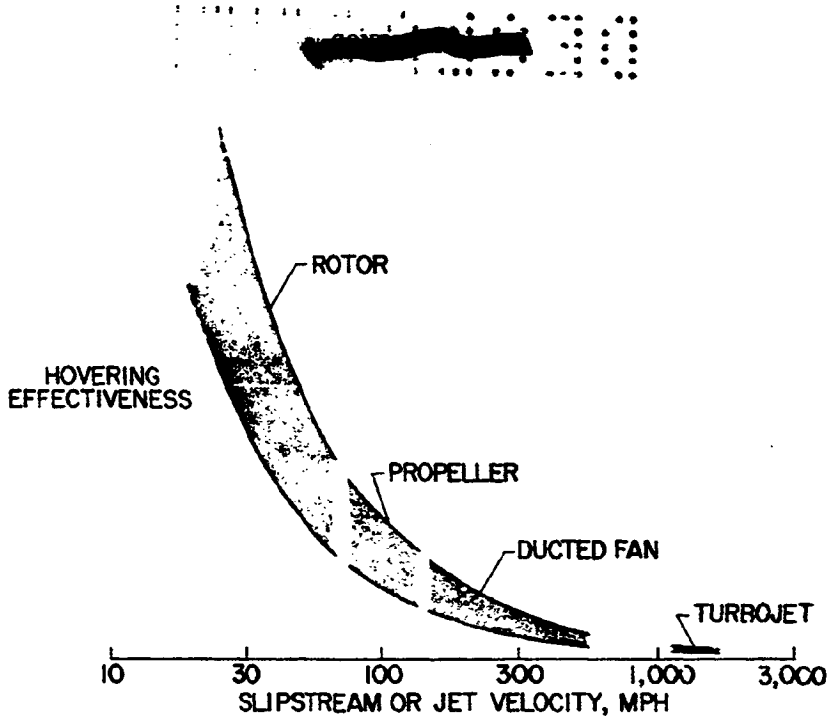

Figure 1.- Variation of hovering effectiveness with slipstream or jet velocity for various propulsion types.

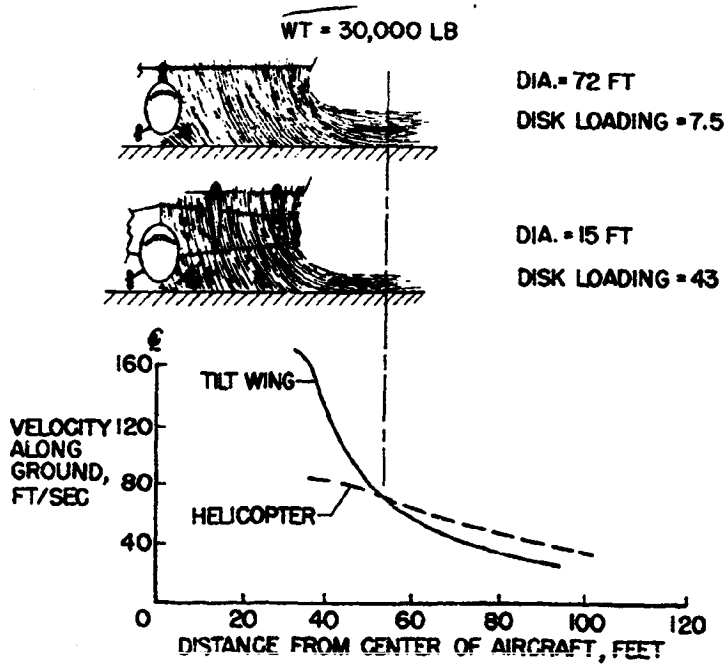

Figure 2.- Comparison of slipstream velocity along the ground for a helicopter and a typical four-propeller tilt-wing configuration.

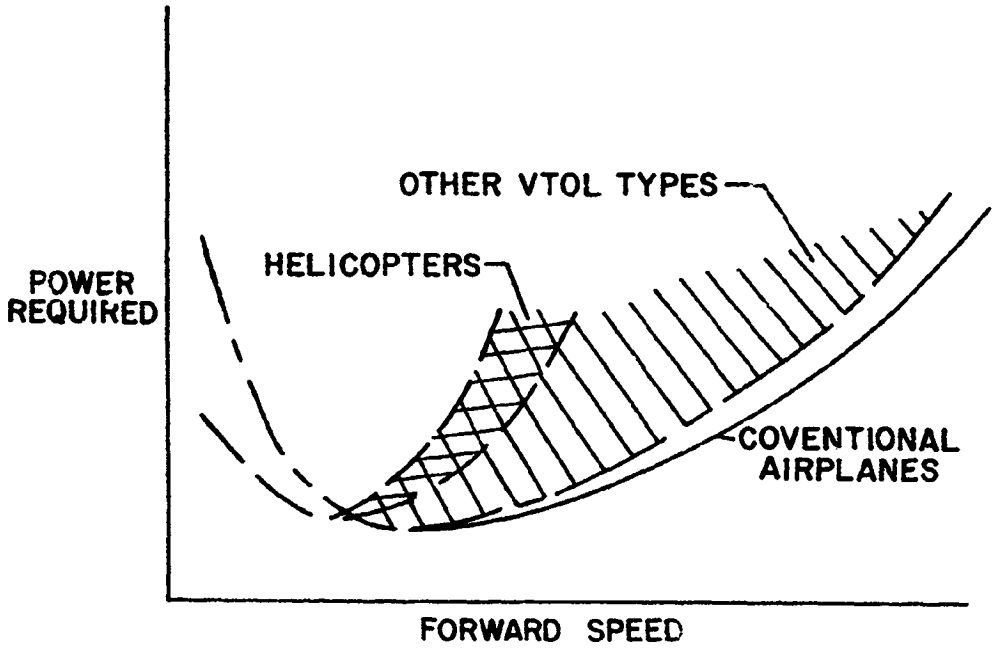

Figure 3.- Typical variation of power required with forward speed for various VTOL types.

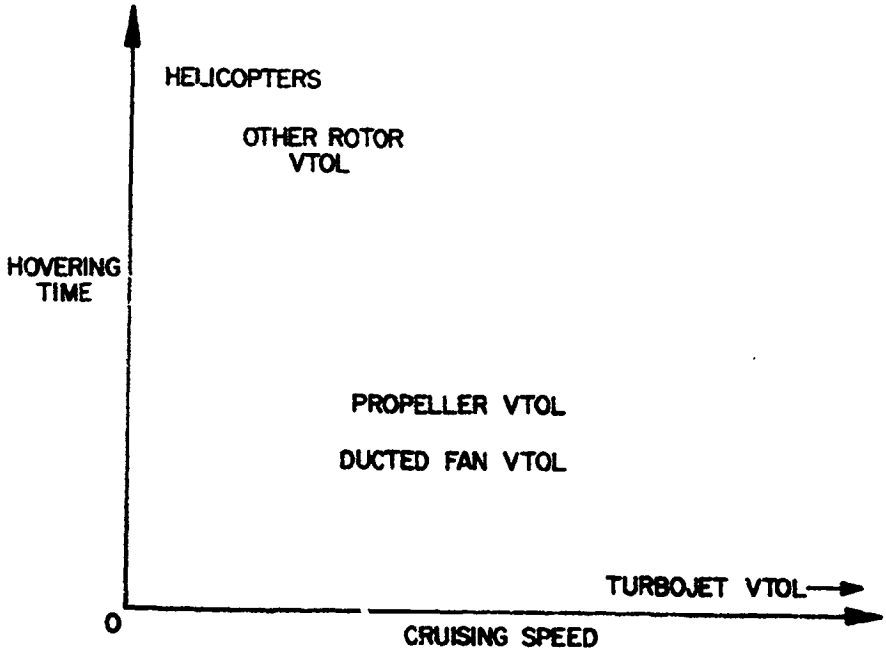

Figure 4.- Logical areas of applications for various VTOL types.

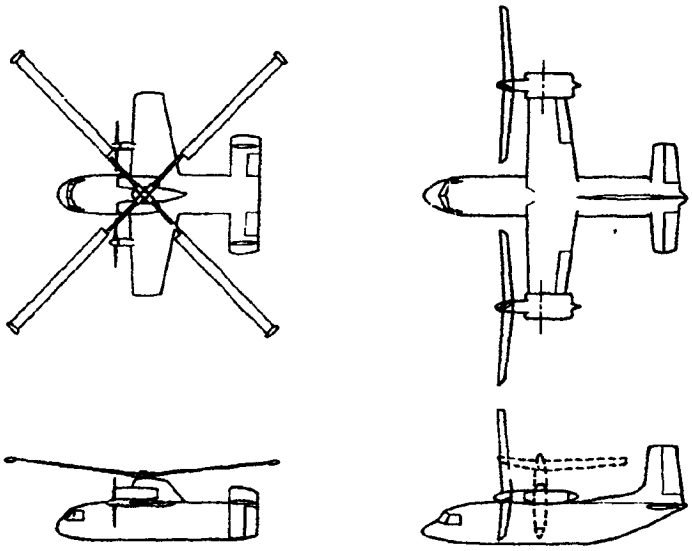

(a) Compound helicopter. (b) Tilt-rotor configuration.

Figure 5.- Rotor types.

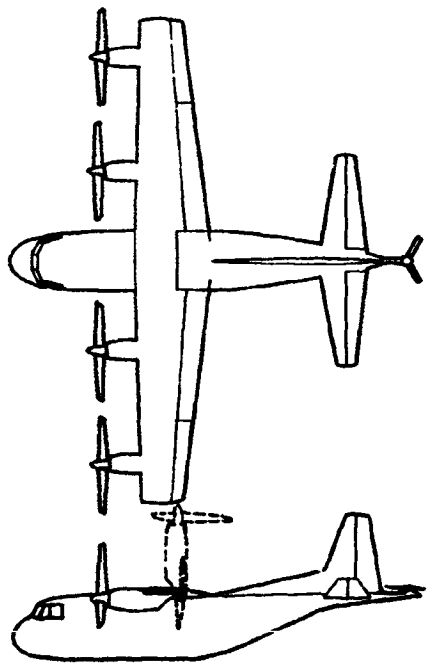

Figure 6.- Tilting-wing configuration.

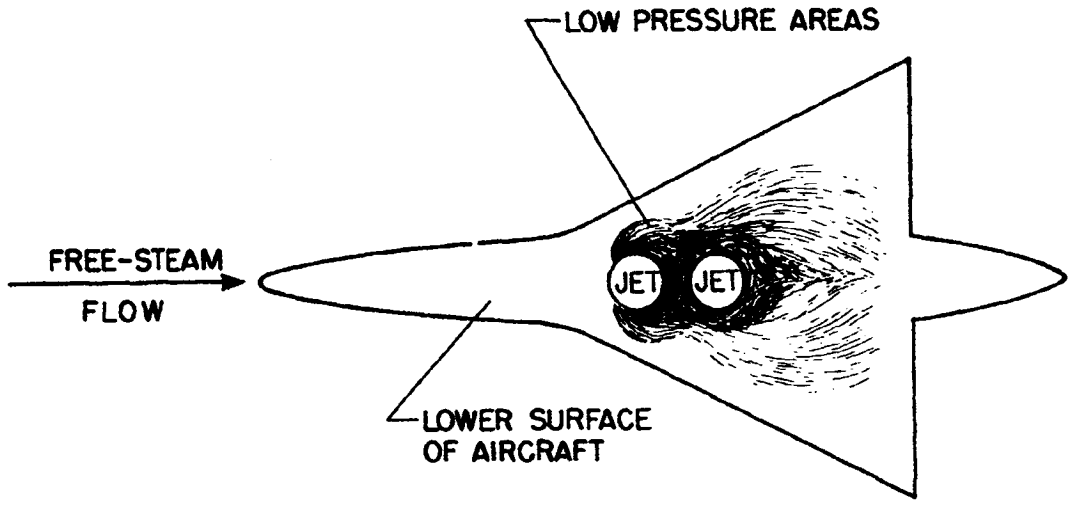

Figure 7.- Effect of interference between exhaust and free-stream flow.

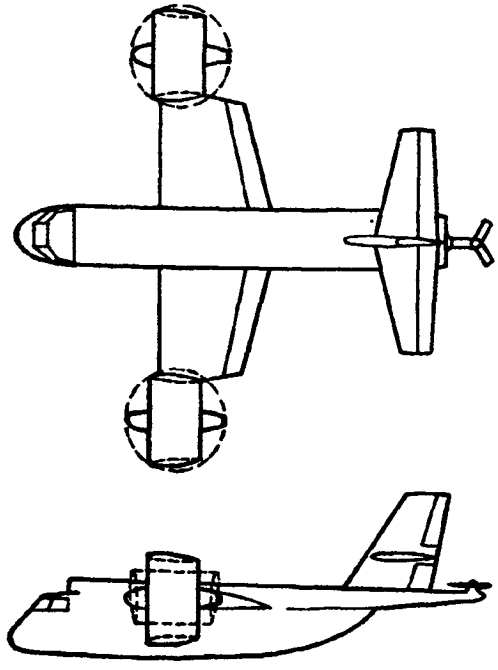

Figure 8.- Tilting-duct configuration.

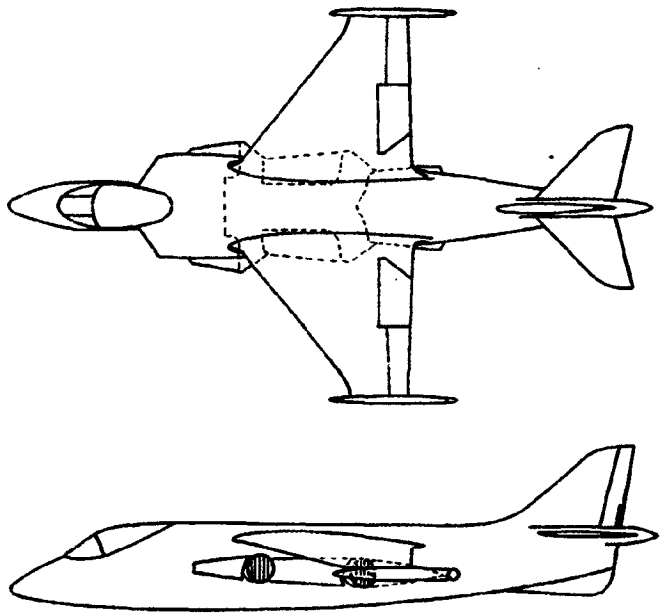

Figure 9.- Hawker P.1127 turbofan configuration.

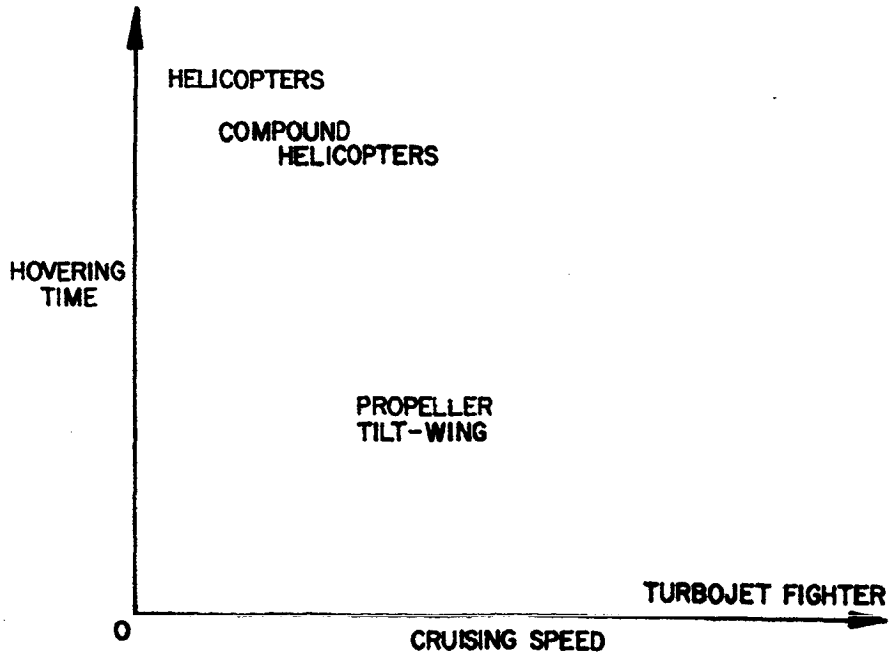

Figure 10.- The four most promising types at the present state of the art in their respective areas of application.

II. AERODYNAMIC RESEARCH RELATIVE TO VARIABLE-SWEEP MULTIMISSION AIRCRAFT

By Edward C. Polhamus and Alexander D. Hammond

Langley Research Center

INTRODUCTION

The development of a multimission military aircraft would be highly desirable both from the standpoint of easing the strain on the national budget by reducing the number of aircraft types and of providing versatility which would increase the effectiveness of the aircraft in the performance of a given mission. Some of the capabilities which might be required of such an aircraft are shown in figure 1 along with their respective aerodynamic and configuration requirements. The first three capabilities are grouped together since they all require good subsonic characteristics. The first, a long loiter capability for combat air patrol and the second, a long ferry range for efficient aircraft deployment both require a high subsonic lift-drag ratio. The third capability, STOL, is desirable for carrier and short-field operation and requires the development of high lift. All three of these capabilities can best be obtained with a high-aspect-ratio wing having a large span and a low-sweep angle. The fourth capability is that of a high-altitude supersonic attack or intercept and requires a high lift-drag ratio at supersonic speeds which dictates a rather slender configuration with a moderate-span wing which is either very thin or highly swept. The fifth capability listed in figure 1 is that of a low-altitude high-speed attack that would increase the probability of long-range penetration of antiaircraft defenses. The high dynamic pressures encountered on the deck at high speeds require a low-lift-curve slope to reduce the gust-induced normal accelerations, and low friction and wave drag (drag due to lift is insignificant at high dynamic pressures) to assure sufficient speed and range. In order to best satisfy these requirements, a slender aircraft having little or no wing is required. It is apparent from figure 1 that these five capabilities are highly incompatible and that an efficient multimission aircraft will require a means of varying its aerodynamic characteristics. This can be best accomplished with some type of variable-wing geometry. There are, of course, several types of variable-wing geometry. However, in view of the extremely large variations in wing span desired, variable wing sweep, as indicated in the lower right sketch of figure 1, appears to provide the best method. The Langley Research Center of the National Aeronautics and Space Administration has therefore initiated a research program to provide the aerodynamic information needed for the development of a variable-sweep multimission military

aircraft, and it is the purpose of this paper to briefly describe some of the results of this program.

SYMBOLS

C_L	lift coefficient
C_{L_α}	lift-curve slope
C_l	rolling-moment coefficient
C_m	pitching-moment coefficient
$C_{m_{C_L}}$	longitudinal-stability parameter
C_n	yawing-moment coefficient
c	wing chord
D_i	induced drag
g	acceleration due to gravity
L/D	lift-drag ratio
$(L/D)_{max}$	maximum lift-drag ratio
M	Mach number
Δn	normal-acceleration increment
pb/2V	nondimensional rolling velocity
W	weight of aircraft
α	angle of attack
Γ_t	tail dihedral
δ_{HT}	horizontal-tail deflection

δ_s spoiler-control projection

Λ wing sweep angle

WING DEVELOPMENT

Variable wing sweep, of course, is not a new concept and the feasibility of in-flight-sweep variations has been demonstrated with the Bell X-5 and the Grumman XF10F. Application to a modern multimission military aircraft, however, requires additional considerations. First, current military requirements are such that considerably higher sweep angles must be considered, and second, a method of eliminating the need for the fore and aft wing translation used in the X-5 and F10F would be highly desirable. This translation was used to control the stability of the aircraft and consisted of a forward shift of the wing as the sweep increased; thereby, a relatively constant stability margin is provided. This translation, however, causes additional mechanical complexity, drag penalties, and a reduction in usable fuselage volume, each of which will be further compounded by the higher wing sweep angles currently needed. The first study, therefore, was directed toward the use of large sweep variations and the development of a method of controlling the longitudinal-stability variation with sweep that would not require the fore and aft wing translation used in the previous aircraft. Four of the aircraft arrangements studied are shown in figure 2 with the high-sweep condition shown by the solid outline and the low sweep, by the dashed outline. A complete description of this study can be found in reference 1. The configuration shown in the upper left was an all-wing design utilizing an 80° arrow planform and pylon-mounted engines on the outer wing panel which were used in an attempt to control stability by means of center-of-gravity shifts. The arrangement in the upper right was a more conventional engine-in-fuselage configuration utilizing a canard surface for longitudinal control and aft folding tails as an aid in the control of stability variations with wing sweep. This wing had a leading-edge sweep of 75° for the highly swept condition and had a wing pivot located in close proximity to the fuselage. The design shown in the lower left utilized the same wing; however, a larger aft tail was used, the canard was removed, and longitudinal control was obtained with elevons for the highly swept conditions and with the aft tail for the unswept condition. All three arrangements exhibited undesirable stability characteristics which are described in reference 1. The design shown in the lower right of figure 2 consisted of a fairly conventional arrangement having a fixed aft tail; however, the wing planform was modified to incorporate improvements with regard to stability that were indicated from the results on the previous configurations. This wing had an outboard pivot and a fairly large and effective fixed portion of the wing. With this arrangement the lift of the outboard

panel, which increases with decreasing sweep, and the lift of the fixed portion combine in such a manner as to keep the stability relatively constant. For this configuration essentially the same stability was obtained in both the high- and low-sweep positions with only minor variations in the intermediate-sweep range. It appears therefore that with this type of variable-sweep wing the need for wing translation can be eliminated. The aerodynamic characteristics of this configuration throughout a large Mach number range can be found in references 1 to 6.

In order to illustrate the importance of the pivot location and the amount of fixed area, wind-tunnel tests were made of the two variable-sweep wing arrangements shown in figure 3. The horizontal tail has been omitted in the interest of clarity since the purpose of the drawing is to compare the two wings. However, the same horizontal tail was used in conjunction with both wings. The type of variable-sweep wing just described is shown in both the 25° and 75° sweep conditions by the solid lines. The distinguishing features of this wing are the large fixed area ahead of the pivot and an outboard-pivot location. The large fixed portion provides the aerodynamic solution to the stability variations with sweep mentioned previously while the outboard pivot provides the large span variations desired. Shown by dashed lines is a variable-sweep wing having essentially the same area and sweep conditions, but having an inboard pivot and a small fixed area similar to that of the X-5 wing. While the geometry of the two configurations is quite similar in both sweep conditions, extremely large differences in longitudinal stability exist, as shown in figure 4 where the pitching-moment coefficient is presented as a function of lift coefficient for the two configurations at low speed. On the left the results obtained for the inboard pivot are presented while on the right the results obtained with the outboard-pivot configuration are presented. In the top portion of figure 4 the characteristics of the configuration without the horizontal tail are shown for two wing-sweep positions. For the inboard pivot the results indicate a large stability shift, in the stable direction, as the sweep is increased from 30° to 70°. It is, of course, this type of variation in longitudinal stability which dictated the use of fore and aft wing translation on the X-5. However, for the outboard-pivot configuration which, as it will be recalled, provides approximately the same variations in wing span as the inboard-pivot configuration, the results indicate an actual reduction in stability as the wing was swept from 25° to 75°. This unusual situation illustrates the powerful effect of the fixed portion of the wing in controlling the stability variation with sweep and indicates the possibility of actually counteracting the Mach number effect on stability. Because of the reduction in lift-curve slope with sweep the tail contribution to stability increases with increasing wing sweep. The tail-on results are presented in the bottom portion of figure 4 and an extremely large increase in stability is indicated for the inboard-pivot wing. This increase when combined with the increase due to Mach number would result in excessive stability

and trim drag at supersonic speeds. For the outboard-pivot wing, however, only a very slight increase in stability occurred with increasing sweep. It should be noted that an additional 10° of sweep variation was utilized with the outboard-pivot configuration. These results indicate that by properly proportioning the areas of the fixed and rotating portions of the wing the stability variation with sweep can be controlled without the need for translation. Complete aerodynamic characteristics of these configurations at subsonic, transonic, and supersonic speeds are presented in references 7 to 9, respectively.

AIRCRAFT CONFIGURATIONS STUDIED

Since the preliminary study just described indicated that by careful wing design longitudinal stability could be handled throughout a rather large sweep range, a program was initiated to investigate the aerodynamic characteristics of variable-sweep aircraft designed specifically to meet the multimission requirements listed in figure 1. A large number of configurations were considered and eight wind-tunnel models were constructed and tested at subsonic, transonic, and supersonic speeds. Two of these configurations, which illustrate the major configuration considerations, are shown in figures 5 and 6.

These configurations differed somewhat from those described previously in that the wings could be completely folded which, as previously mentioned, is desirable from both performance and gust-acceleration considerations in the low-level high-speed-attack phase of the multimission. With regard to performance the fully folded wing, in addition to reducing the friction drag, should allow complete area-ruling benefits on transonic wave drag to be more nearly realized. The method described in reference 10 was utilized in area ruling the configurations. In connection with the gust-induced normal accelerations the fully folded wing provides relief through both a reduction in lift-curve slope and an increase in wing loading.

The configurations were designed around two turbofan engines and their volumes were compatible with those of aircraft in the 60,000-pound class. The configuration (7) shown in figure 5 is characterized by a wing-pivot location within the fuselage (see section A-A) and a relatively small fixed portion of the wing. While this arrangement exhibits fairly large increases in longitudinal stability with increasing sweep, it allows a large portion of the wing to be hidden for the low-altitude attack and may afford some structural advantage over configurations having the pivot located within the wing. The results are therefore valuable in assessing structural, performance, and longitudinal-stability

trade-offs. Configuration 8 (see fig. 6) was quite similar to configuration 7 with the main difference being associated with the outboard-pivot location and the relatively large fixed-wing area. This configuration, while possibly having larger structural penalties because of the pivot location, exhibits more desirable longitudinal stability characteristics than configuration 7, and would be expected to have lower trim drag at supersonic speeds.

Since the most complete data available at the present are that for configuration 8 and since it exhibits desirable longitudinal-stability characteristics, it will be used throughout the remainder of this paper to illustrate some of the aerodynamic characteristics of variable-sweep multimission aircraft. The wind-tunnel models were 1/24 scale and a photograph of configuration 8 with the wings extended is shown in figure 7. The jet-engine inlets were designed and constructed so as to provide the proper mass flow for a Mach number of 1.2.

PERFORMANCE

The effect of wing sweep on the maximum lift-drag ratios at subsonic and supersonic speeds is shown in figure 8. The wing had a streamwise thickness of 6 percent when swept 25° and had a rounded leading edge. The subsonic results are presented for a Mach number of 0.6 and have been corrected to full-scale turbulent skin-friction conditions corresponding to an altitude of 30,000 feet. The supersonic results are presented for a Mach number of 2.2 at an altitude of 60,000 feet. For the supersonic-attack mission it will be noted that a wing-sweep position of approximately 75° would be desirable. It will be noted, however, that at subsonic speeds the maximum lift-drag ratio for this sweep would be somewhat less than 10 and a fixed-wing aircraft would therefore have relatively limited loiter and ferry capability. However, for the variable-sweep aircraft with the wings rotated forward to 25° sweep, the large increase in wing span increases the maximum lift-drag ratio to slightly in excess of 18 at subsonic speeds. This, of course, would nearly double the endurance time for the loiter mission and would result in a large increase in the ferry range.

In addition to loiter, ferry, and high-altitude supersonic-attack capability, a high-speed low-altitude-attack capability is highly desirable. Because of the high dynamic pressure encountered during this mission, the drag due to lift, even for a wingless configuration, is a small portion of the total drag, and the maximum lift-drag ratios become rather meaningless with the minimum drag in pounds becoming of prime importance. Therefore, in order to illustrate the role that variable sweep plays in connection with the drag in the low-altitude-attack mission, figure 9 has been prepared. Here the total drag associated with a

60,000-pound airplane in level flight at sea level is presented as a function of wing sweep for various Mach numbers. The results indicate that for a supersonic low-altitude attack at a Mach number of 1.2 a considerable reduction in level-flight drag is obtained as the wings are rotated back because of the reduction in wetted area and wave drag. It is interesting to note that even at a Mach number of 0.9 the benefit of the fully folded wing is still realized. At a Mach number of 0.6, however, the angles of attack required for level flight become large enough so that the drag due to lift becomes significant and the low wing sweep provides the lower drag. The drag due to lift at $M = 1.2$ is shown by the hatched area, and the low value indicates that if additional drag improvements are to be realized for the supersonic mission, reductions in friction and wave drag through reductions in wetted and maximum cross-sectional areas must be resorted to.

EFFECTS OF LIFT-CURVE SLOPE

Figure 10 shows the variation of the lift-curve slope (based on a common full-scale area of 600 sq ft) with Mach number for the 25°, 75°, and fully folded wing-sweep positions. The main point of interest is the fact that in the fully folded condition the lift-curve slope is reduced to 25 or 30 percent of that associated with the fully extended (25°) wing. This large variation in lift-curve slope is of interest mainly in connection with gust and pull-up response (both of which are important for the low-altitude attack), and its effect on these are illustrated in figure 11.

The conditions represented are for an aircraft weighing 60,000 pounds (corresponding to a wing loading, for the extended case, of about 90) and flying at sea level. Presented on the left of figure 11 is the response to a 50 fps sharp-edged gust as a function of Mach number for several wing-sweep positions - 25°, 75°, and 109°. The results indicate rather large reductions in the gust response as the wing sweep is increased. At a Mach number of 1.2 with the wings fully folded, the gust response is slightly less than that encountered with the 75° wing position at a Mach number of 0.90 and considerably less than that for the 25° wing position at a Mach number of 0.6. It should be pointed out that inasmuch as a common reference area was used for the lift-curve slopes there is no effect of wing loading on the gust response. It should be noted that in the fully folded condition the wing outer panel is locked to the fuselage; therefore, aeroelastic effects would be expected to be small for both the model and the airplane. For the 75° sweep position, however, aeroelastic effects would be somewhat greater on the airplane than on the model (aluminum with streamwise thickness of 6 percent in 25° position and a dynamic pressure of 333 lb/sq ft at $M = 1.2$), and some reduction in gust accelerations would be expected.

The low-lift-curve slopes which make possible the reductions in gust accelerations raise a question as to the effect of lags (due to the larger rotations required) in pull-up response in connection with terrain clearance during the low-level-attack mission. This effect is shown on the right-hand portion of figure 11 where the longitudinal distance traveled while gaining an altitude of 50 feet following a pull-up from level flight at a Mach number of 1.2 at sea level is shown as a function of the steady-state normal-acceleration increment achieved in the pull-up. Results are presented for the ideal no-lag condition $C_{L_\alpha} = \infty$ in which the required rotation is obtained instantaneously and for three wing-sweep positions. If a steady-state normal-acceleration increment Δn of 3g is assumed, it will be noted that even for the ideal case a distance of 1,400 feet would be traveled before 50 feet of altitude were gained. The lag associated with the low-lift-curve slope of the fully folded wing at 3g increases the distance traveled to approximately 2,400 feet, but it will be noted that this is only about 100 feet or about 1/10 second greater than that experienced with the wing in the 75° sweep position and only about 400 feet greater than that with the wing in the fully extended position ($\Lambda = 25°$). It therefore appears that large reductions in vertical-gust response can be obtained with the fully folded wing without seriously reducing the pull-up response.

L 1 2 7 9

LONGITUDINAL STABILITY

The effect of Mach number on the longitudinal-stability parameter $C_{m_{C_L}}$ is presented in figure 12 for the various wing positions. Shown are the subsonic data with the wings extended, the transonic data with the wings fully folded, and the supersonic data with the wings in the 75° position. There are several items of interest. First, it will be noted that the shift in static margin from $M = 0.6$ with the wings extended to $M = 2.0$ with the wings in the 75° position is only about 8 percent of the mean aerodynamic chord of the extended wing. It appears, therefore, that by careful wing design large sweep variations can be combined with large Mach number increases without encountering stability increases greater than those associated with fixed-wing aircraft. In fact, it appears possible to actually reduce the stability changes.

Secondly, while a considerable reduction in stability occurs at transonic speeds with the wings fully folded, a rather large increase can be produced by the use of 20° of negative dihedral in the horizontal tail as indicated by the filled-in circular symbol. This is due mainly to the favorable effect of the sidewash component of the trailing vortex induced velocity at offcenter positions. There is an additional benefit from the negative tail dihedral in that it reduces the stability at $M = 2.0$ (no favorable sidewash component), thereby, a reduction in the

supersonic stability shift results. It appears from these results that reasonable stability characteristics can be obtained despite the large Mach number and sweep range that may be required for multimission military aircraft.

LATERAL STABILITY AND CONTROL

With regard to static lateral and directional stability it is sufficient to point out that the only problem encountered was the usual one of directional instability at the higher angles of attack at supersonic speeds. It appears, however, that the 20° negative dihedral in the horizontal tail suggested in connection with the longitudinal stability would be sufficient to take care of the directional problem.

Figure 13 shows the lateral-control characteristics. For wing sweeps up to 75° or 80° the lateral control can be obtained by the deflection of a spoiler-slot-deflector control on the movable outboard wing. The control would be located just ahead of a trailing-edge high-lift flap having a full span (needed for STOL) and would span the outboard wing. The data on the left of figure 13 were obtained at a Mach number of 0.13 for a spoiler projection of 10 percent of the wing chord. The deflector projection was 3/4 of the spoiler projection. The variation of the rolling-effectiveness parameter $pb/2V$ with angle of attack is shown for the wing swept 25° (solid curve) and 75° (dashed curve). The spoiler-slot-deflector control has more effectiveness at low angles of attack when the wing is at 25° sweep than for the 75° swept wing. However, the rolling effectiveness is approximately the same at high angles of attack for both wing sweeps. The magnitude of $pb/2V$ required for fighter-type aircraft at subsonic speeds is in the order of 0.06 to 0.07, and it will be useful to note that with the 25° wing position the requirement can be met with a 10-percent projection.

When the wing is fully sweptback for the low-altitude-attack mission the spoilers, of course, cannot be used but lateral control can be obtained by differential deflection of the horizontal-tail surfaces. Data for differential tail deflection have been obtained at a Mach number of 1.2. The rolling effectiveness is shown for $\pm 2\frac{1}{2}^\circ$ differential tail deflection on the right of figure 13 and the level of control effectiveness for the angles of attack shown are comparable to those obtained at subsonic speed for the spoiler-slot deflector. For this Mach number, however, the roll-rate requirement is greatly exceeded and a control sensitivity problem may be encountered. Another problem is indicated on the lower part of figure 13 where the variation of the ratio of yawing-moment coefficient to rolling-moment coefficient is shown for the differentially deflected horizontal tail on the right and the spoiler-slot

deflector on the left. The magnitude of the yawing moment due to rolling moment is considerably higher for the differential-tail control than for the spoiler control. This is due to the large induced side-force load on the vertical tail resulting from differential deflection of the horizontal tail. For this reason it is felt that an effort should be made to develop a lateral control on the wing for this maximum-sweep case. The most obvious possibility is the use of the leading-edge droop-nose flap as a trailing-edge flap-type control when the wing is fully swept as indicated in the sketch by the shaded area, or the use of a split flap-type control as shown by the dashed lines. Data are currently being obtained at transonic speeds on both of these lateral-control devices.

OTHER AERODYNAMIC CONSIDERATIONS

The wind-tunnel studies described previously and in references 11 to 14 indicate that with proper design, no extreme static aerodynamic problem areas appear to be associated with the variable-sweep multi-mission aircraft. However, for dynamic conditions, further analyses will be necessary in order to evaluate fully the multimission capabilities of the variable-sweep aircraft. These analyses should include studies of the results of wind-tunnel investigations already underway including flutter and buffet tests, oscillation tests in pitch and yaw, and tests under conditions of steady rolling, as well as simulator studies of possible roll-coupled divergence, roll-to-sideslip ratio, and control sensitivity.

MULTIMISSION PERFORMANCE ESTIMATES

So far the discussion has dealt with the aerodynamic characteristics of variable-sweep multimission aircraft; however, by way of conclusion some preliminary calculations of the performance capabilities of a possible multimission military airplane are given. It should be pointed out that, while these calculations were based on rather rough weight and engine-performance assumptions, it is felt that they are illustrative of the possible multimission capabilities. The design was based on configuration 8, had a take-off gross weight of 63,000 pounds, had 28,000 pounds of internal fuel, and was powered by two turbofan engines. The calculations indicated that with the wings extended take-off and landing distances, over a 50-foot obstacle, of less than 3,000 feet were possible with relatively simple high-lift devices. A low-level strike radius of approximately 800 nautical miles appears possible with half of the outbound leg being accomplished at a Mach number of 1.2 with the wings folded. A strike or intercept radius of

900 nautical miles could be obtained at a high altitude and a Mach number of 2.3 with the wings in the 75° position. By adding 3,500 pounds of fuel in the bomb bay and 8,000 pounds of external fuel, with the wings extended, a ferry distance of approximately 6,000 nautical miles appears feasible. From these performance estimates it appears that a variable-sweep aircraft can provide for a great deal of versatility and that one aircraft can actually perform several missions efficiently. In addition, the wind-tunnel studies described indicate that with proper design no extreme static aerodynamic problem areas appear to be asscciated with this type of aircraft.

REFERENCES

1. Alford, William J., Jr., and Henderson, William P.: An Exploratory Investigation of the Low-Speed Aerodynamic Characteristics of Variable-Wing-Sweep Airplane Configurations. NASA TM X-142, 1959.

2. Alford, William J., Jr., Luoma, Arvo A., and Henderson, William P.: Wind-Tunnel Studies at Subsonic and Transonic Speeds of a Multiple-Mission Variable-Wing-Sweep Airplane Configuration. NASA TM X-206, 1959.

3. Spearman, M. Leroy, and Foster, Gerald V.: Stability and Control Characteristics at a Mach Number of 2.01 of a Variable-Wing-Sweep Configuration With Outboard Wing Panels Swept Back 75°. NASA TM X-32, 1959.

4. Spearman, M. Leroy, and Foster, Gerald V.: Effects of Various Modifications on the Supersonic Stability Characteristics of a Variable-Wing-Sweep Configuration at a Mach Number of 2.01. NASA TM X-260, 1960.

5. Foster, Gerald V.: Stability and Control Characteristics at Mach Numbers of 2.50, 3.00, and 3.71 of a Variable-Wing-Sweep Configuration With Outboard Wing Panels Swept Back 75°. NASA TM X-267, 1960.

6. Foster, Gerald V.: Effects of Spoiler-Slot-Deflector Control on the Aerodynamic Characteristics at a Mach Number of 2.01 of a Variable-Wing-Sweep Configuration With the Outer Wing Panels Swept Back 75°. NASA TM X-273, 1960.

7. Spencer, Bernard, Jr.: Stability and Control Characteristics at Low Subsonic Speeds of an Airplane Configuration Having Two Types of Variable-Sweep Wings. NASA TM X-303, 1960.

8. Luoma, Arvo A.: Stability and Control Characteristics at Transonic Speeds of a Variable-Wing-Sweep Airplane Configuration With Wing Outboard Panels Swept 113.24° and 75°. NASA TM X-342, 1960.

9. Foster, Gerald V., and Morris, Odell A.: Stability and Control Characteristics at a Mach Number of 1.97 of an Airplane Configuration Having Two Types of Variable-Sweep Wings. NASA TM X-323, 1960.

10. Whitcomb, Richard T.: A Study of the Zero-Lift Drag-Rise Characteristics of Wing-Body Combinations Near the Speed of Sound. NACA Rep. 1273, 1956. (Supersedes NACA RM L52H08.)

11. Bielat, Ralph P., Robins, A. Warner, and Alford, William J., Jr.: The Transonic Aerodynamic Characteristics of Two Variable-Sweep Airplane Configurations Capable of Low-Level Supersonic Attack. NASA TM X-304, 1960.

12. Spearman, M. Leroy, and Robinson, Ross B.: Stability and Control Characteristics at a Mach Number of 2.01 of a Variable-Sweep Airplane Configuration Capable of Low-Level Supersonic Attack - Outer Wing Swept 75°. NASA TM X-310, 1960.

13. Robinson, Ross B., and Howard, Paul W.: Stability and Control Characteristics at a Mach Number of 1.41 of a Variable-Sweep Airplane Configuration Capable of Low-Level Supersonic Attack - Outer Wing Swept 75° and 108°. NASA TM X-320, 1960.

14. Robinson, Ross B., and Spearman, M. Leroy: Stability and Control Characteristics at a Mach Number of 2.2 of a Variable-Sweep Airplane Configuration Capable of Low-Level Supersonic Attack - Outer Wing Swept 75°. NASA TM X-330, 1960.

MULTIMISSION CONSIDERATIONS

CAPABILITY	(1) LOITER (2) FERRY (3) STOL	+	(4) HIGH-ALT. SUPERSONIC ATTACK	+	(5) LOW-ALT. HIGH-SPEED ATTACK	= MULTIMISSION CAPABILITY
MAJOR AERODYNAMIC CONSIDERATIONS	HIGH SUBSONIC L/D AND C_L	+	HIGH SUPERSONIC L/D	+	LOW C_{L_α} AND LOW MIN. DRAG	= VARIABLE AERODYNAMICS
DESIRABLE WING GEOMETRY	LARGE SPAN LOW SWEEP	+	MODERATE SPAN HIGH SWEEP	+	LITTLE OR NO WING	= VARIABLE-WING GEOMETRY
TYPICAL CONFIG.	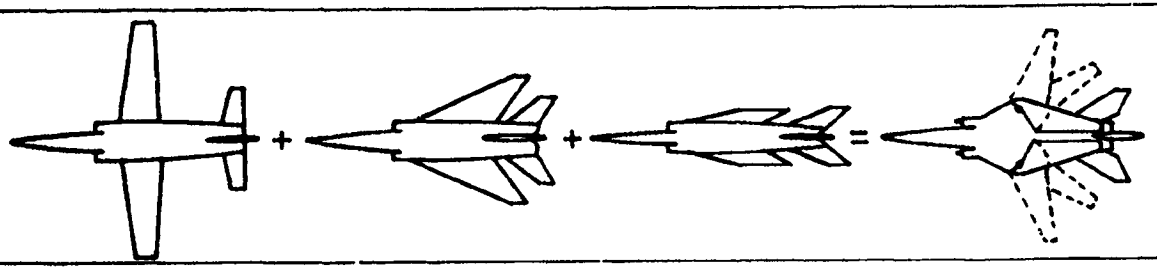					

Figure 1

VARIABLE-SWEEP-CONFIGURATION STUDY

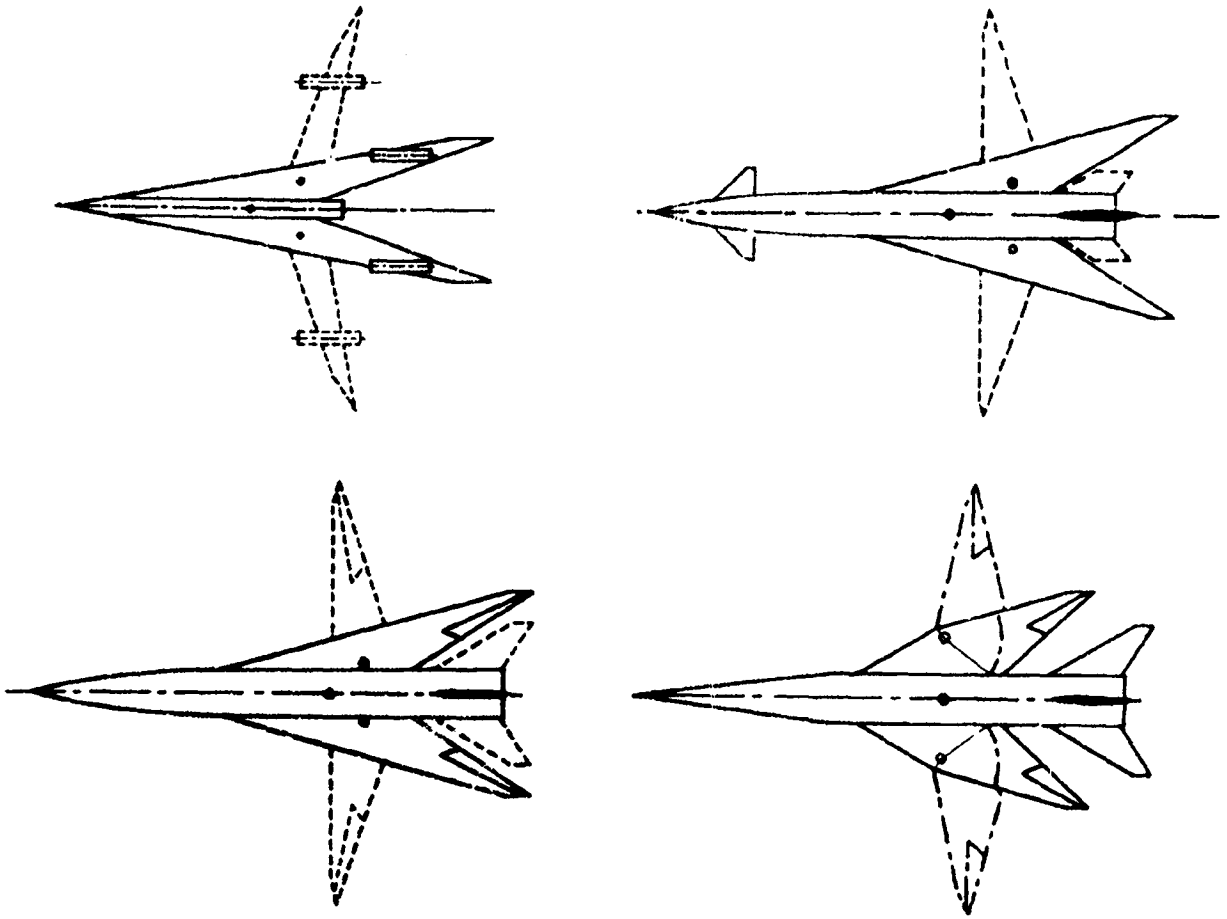

Figure 2

COMPARISON OF VARIABLE-SWEEP WINGS

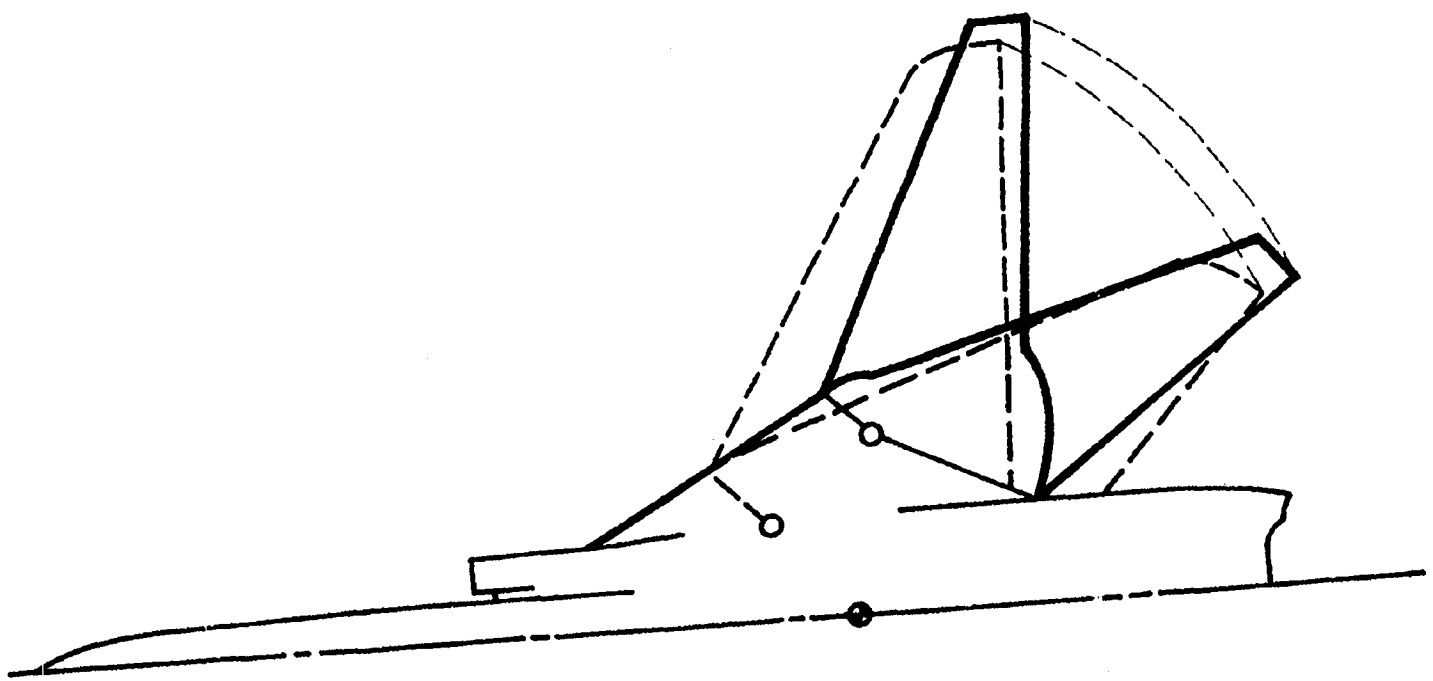

Figure 3

EFFECT OF PIVOT LOCATION ON LONGITUDINAL STABILITY

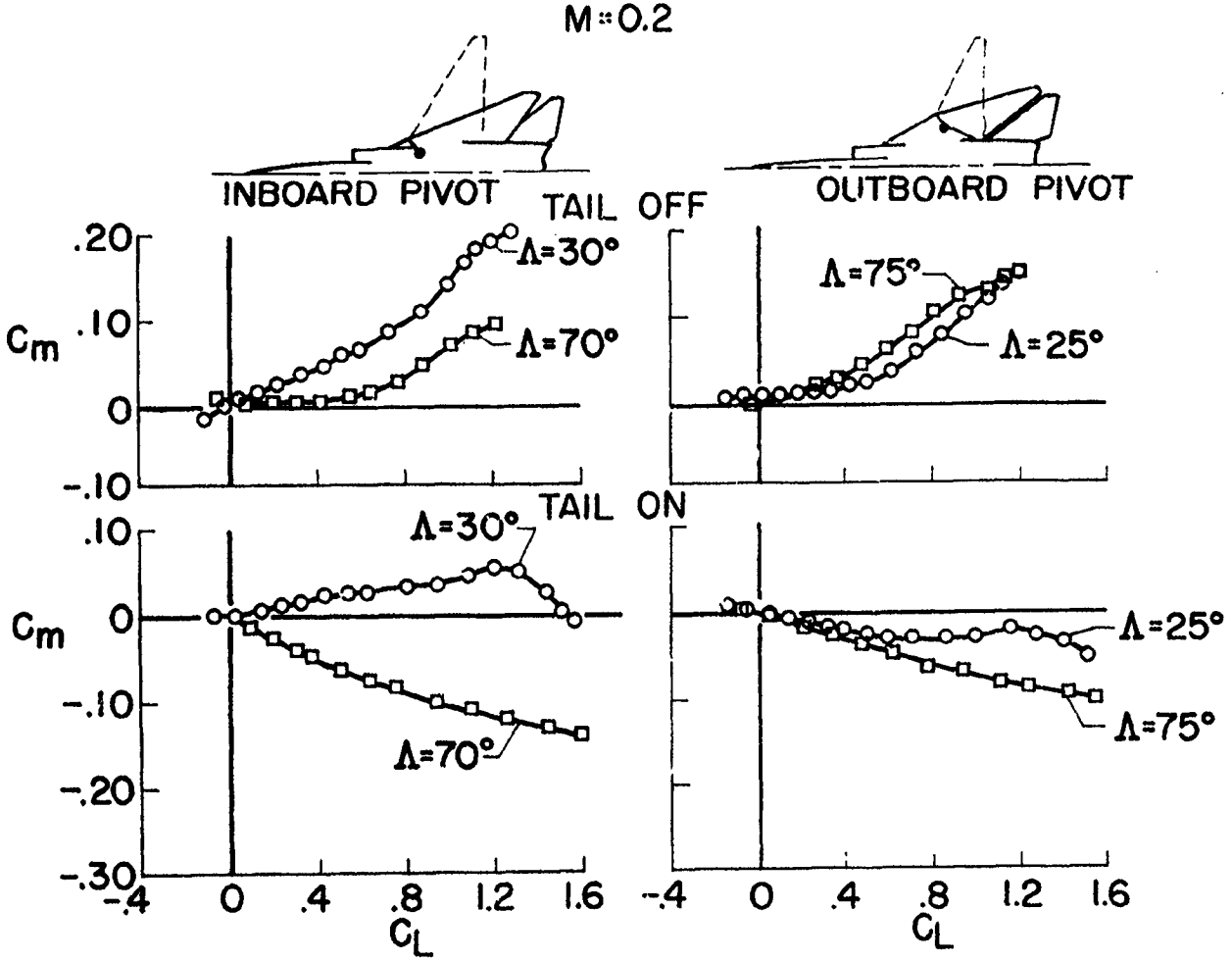

Figure 4

CONFIGURATION 7

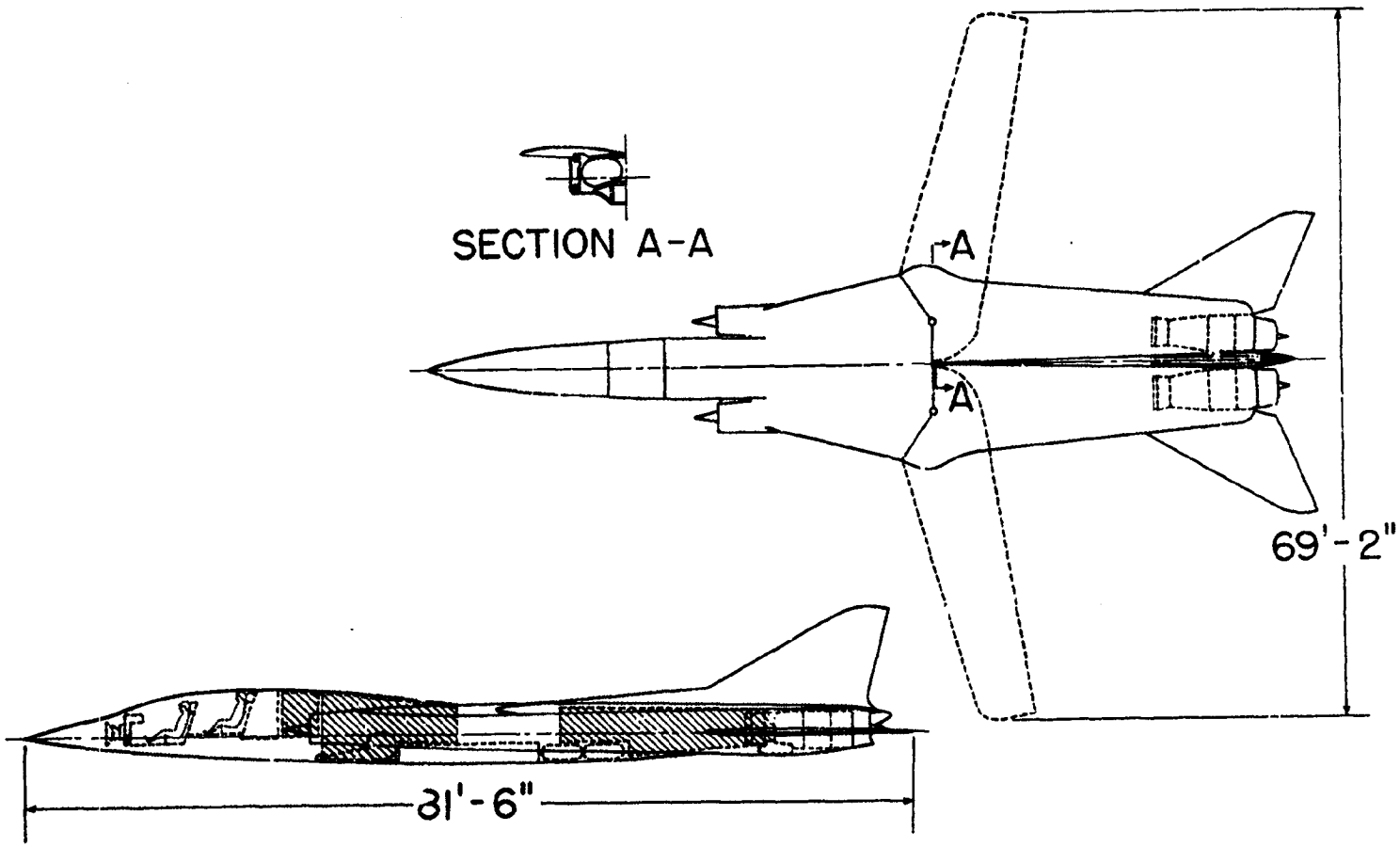

Figure 5

CONFIGURATION 8

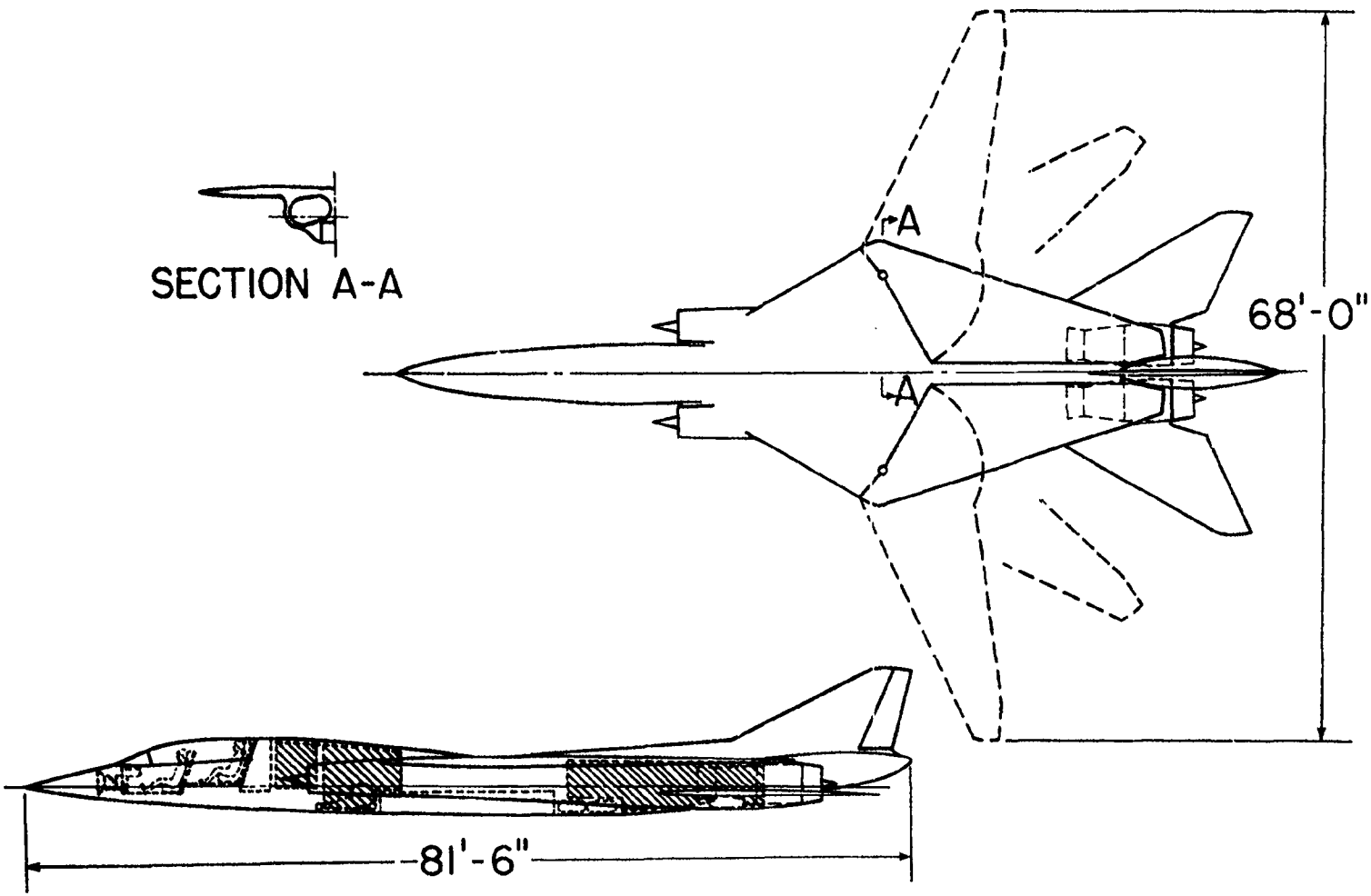

Figure 6

PHOTOGRAPH CF CONFIGURATION 8

Figure 7

L-60-2014.1

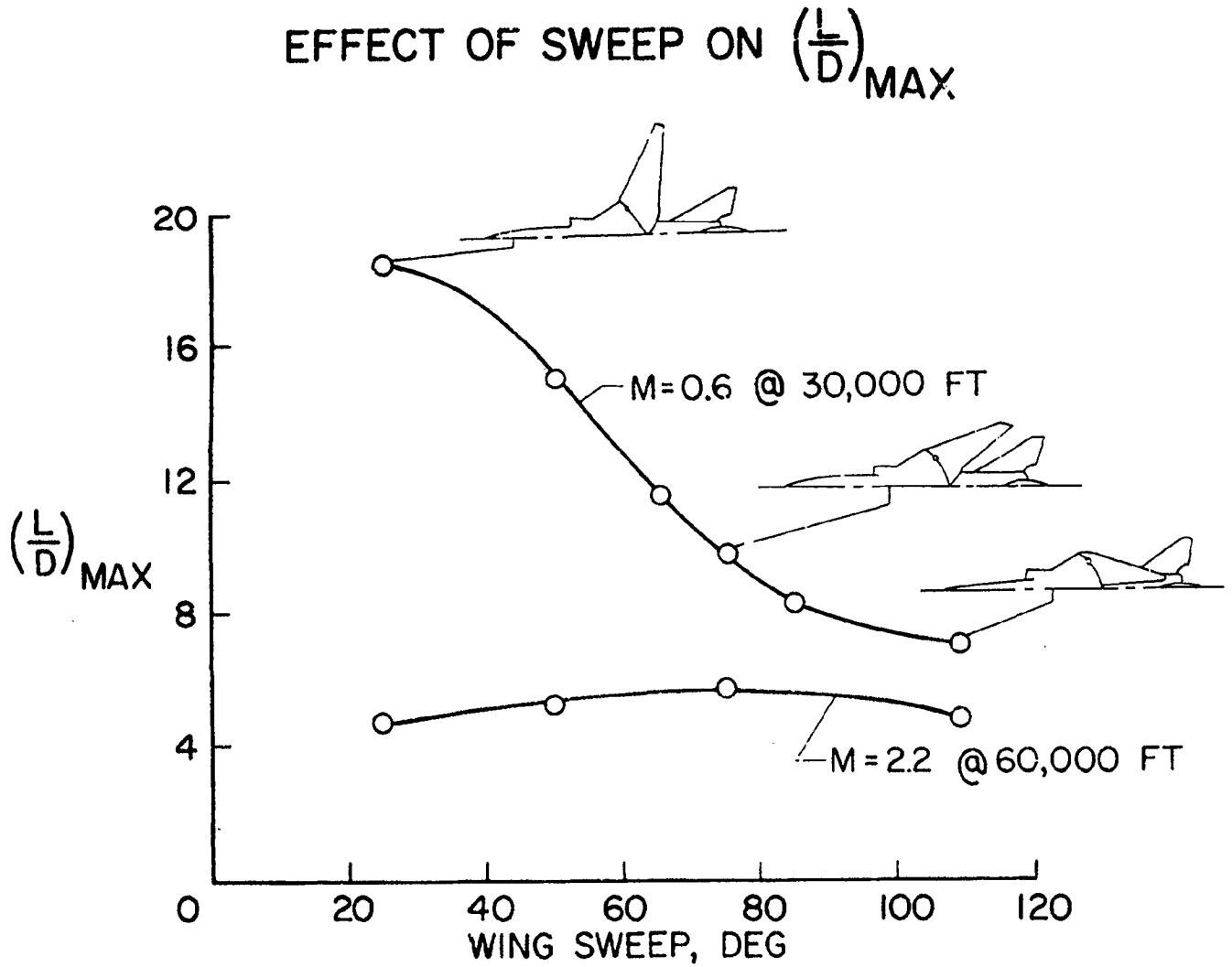
EFFECT OF SWEEP ON $(\frac{L}{D})_{MAX}$
$(\frac{L}{D})_{MAX}$
20
16
12
8
4
0
20
40
60
80
100
120
WING SWEEP, DEG
M=0.6 @ 30,000 FT
M=2.2 @60,000 FT

Figure 8

EFFECT OF SWEEP ON SEA-LEVEL DRAG

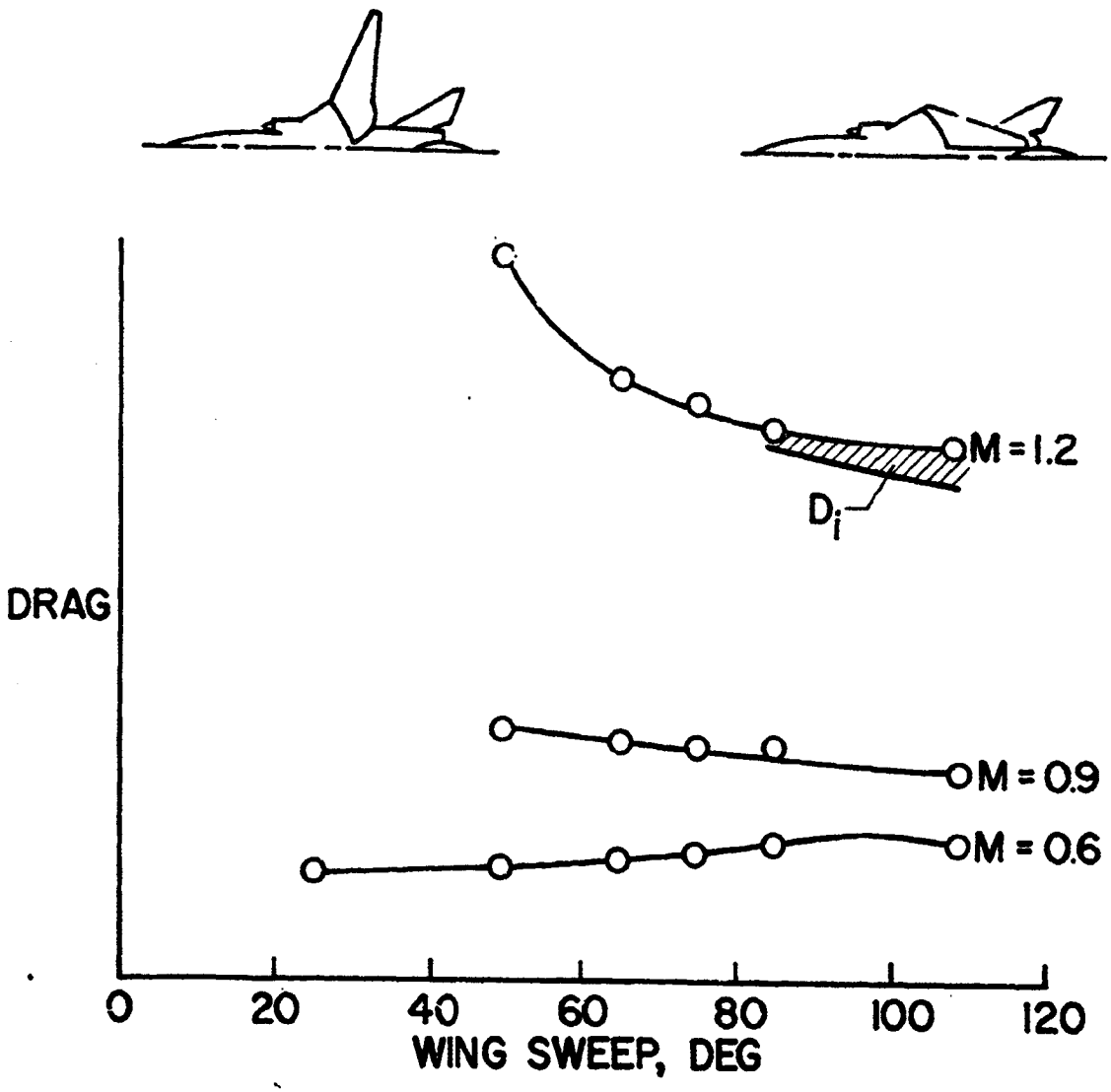

Figure 9

EFFECT OF SWEEP ON C_{L_α}

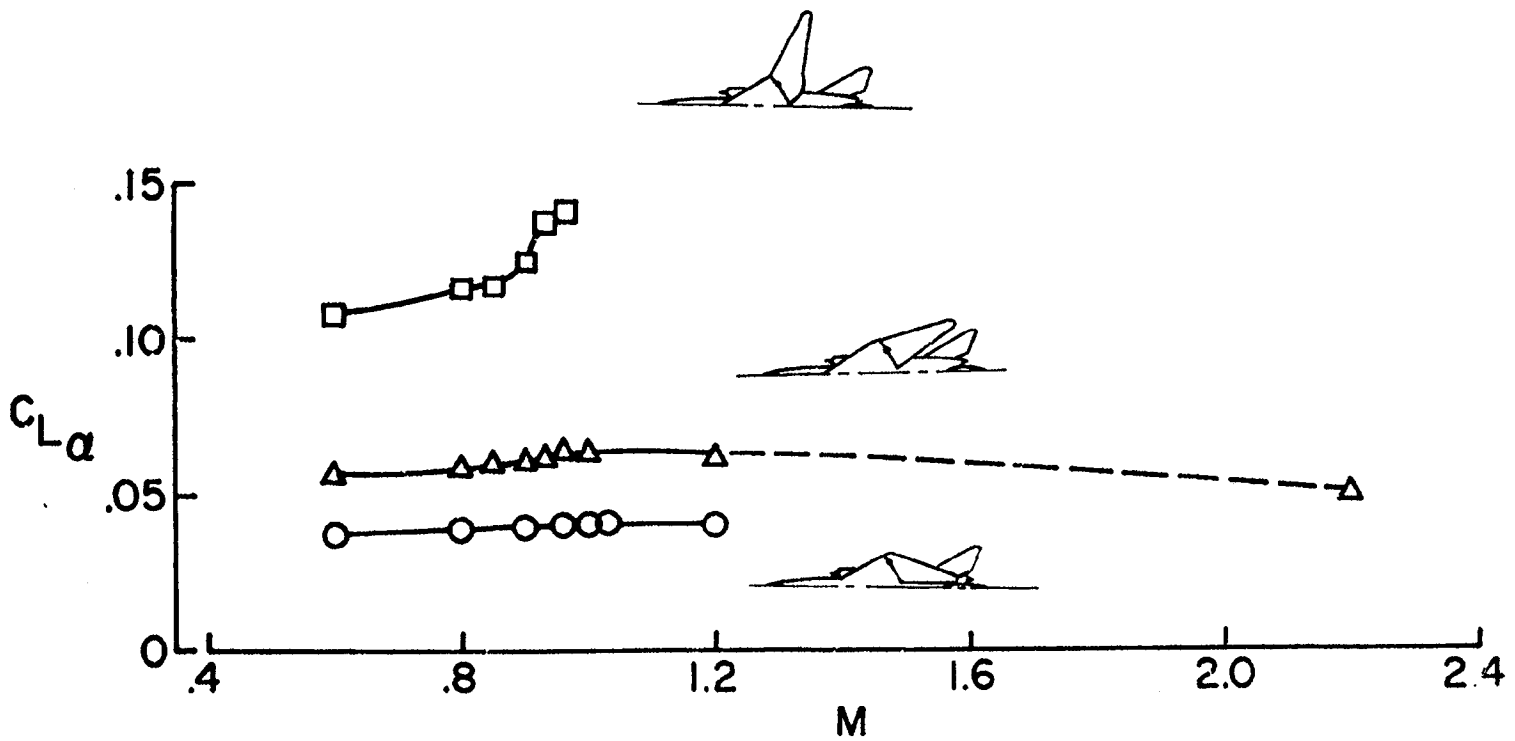

Figure 10

EFFECT OF SWEEP ON GUST AND PULL-UP RESPONSE

W = 60,000 LB; SEA LEVEL

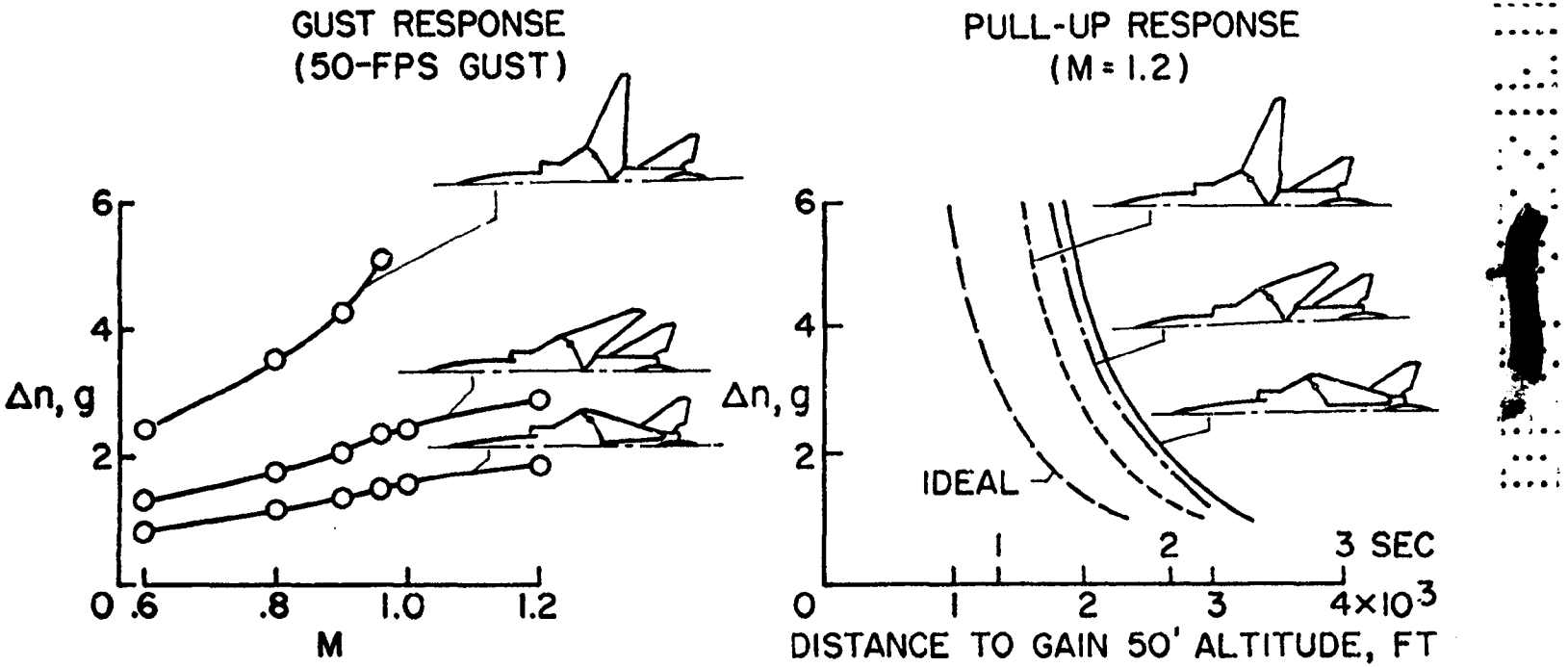

Figure 11

LONGITUDINAL-STABILITY CHARACTERISTICS

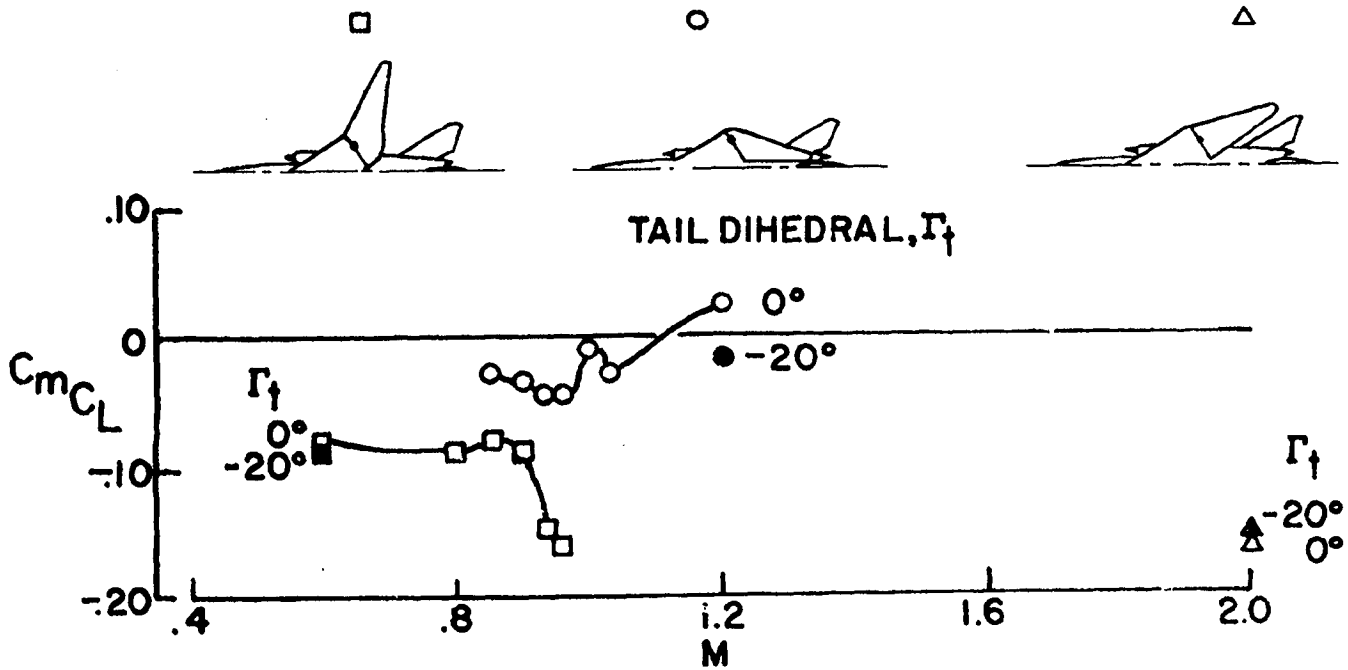

Figure 12

LATERAL CONTROL

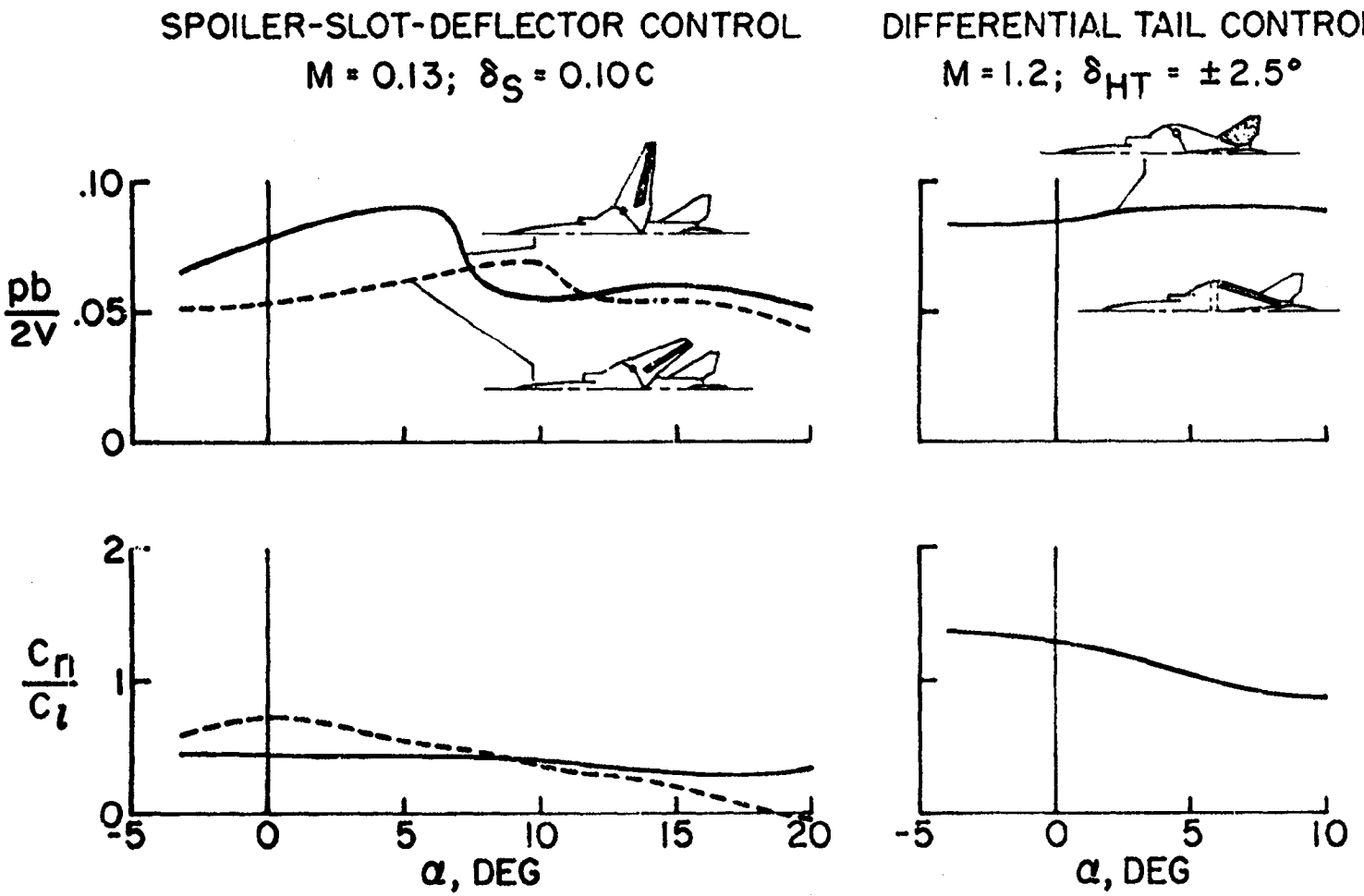

Figure 13

III. SUPERSONIC CRUISE AIRCRAFT

By Donald D. Baals, Cornelius Driver,
and Owen G. Morris

Langley Research Center

INTRODUCTION

The aviation world is on the threshold of sustained supersonic flight at a level of efficiency approaching the best of our subsonic aircraft. This potential has been recognized in the concept of the B-70. Now the supersonic transport is on the horizon.

The supersonic transport represents a great technical challenge. Not only must this vehicle have the aerodynamic efficiency of the supersonic bomber, but it must also embrace: (a) the overriding element of passenger safety, (b) the problem of community acceptance (noise), and (c) economy of operation.

This paper will be devoted primarily to the aerodynamic problems of large supersonic aircraft as related to performance. Smaller vehicles have been considered in part II of this compilation. The stability and control problems are of equal importance but are not discussed herein.

SYMBOLS

A	aspect ratio
A_{max}	maximum cross-sectional area
A_{Wet}	wetted area
ΔC_D	incremental drag coefficient
C_{D_o}	minimum drag coefficient
C_{D_w}	wave-drag coefficient
C_f	mean skin-friction coefficient
C_L	lift coefficient

C_{L_α}	lift-curve slope
c	chord
K	proportionality factor for wave drag
L/D	lift-drag coefficient
l	length
M	Mach number
m	mass flow through slot
m_0	mass flow through a stream tube having the same cross-sectional area as the wing area
n	fineness ratio
R	Reynolds number
S	wing area
SFC	specific fuel consumption
t	thickness
V	volume
W	weight
$\beta = \sqrt{M^2 - 1}$	
δ	wedge angle
Λ	angle of sweep

L 1 2 1 1

DISCUSSION

For long-range supersonic aircraft the cruise efficiency is the primary design factor. From the Breguet range equation, which relates the elements determining cruise efficiency, the controlling aerodynamic term is the lift-drag ratio L/D. This ratio is determined by two basic factors - the minimum drag (mainly wave and friction drag at supersonic

speeds) and the drag due to lift. In figure 1 the relative drag breakdown for two representative bomber configurations in the 400,000 pound-class is shown. For the subsonic configuration, the skin-friction drag and the drag due to lift are about equal, and the trim drag is small. For a Mach number 3 configuration, the total drag is about three times that of the subsonic airplane. Note that a new drag element, shock-wave drag, has been introduced. Even for the efficient configuration assumed, this element is about one-half the entire subsonic drag. Supersonic friction drag alone is equal to the entire subsonic drag.

Figure 2 points up the importance of aircraft geometric characteristics relative to the supersonic wave and friction drags. Shown here is the volume coefficient $V^{2/3}/S$ as a function of gross weight for various categories of aircraft. The volume coefficient is a measure of aircraft fineness ratio and is an indication of wave drag. Note that the volume coefficient for a bomber configuration with its high payload density is less than that for a cargo aircraft which has a much lower payload density. Note also that, as the gross weight of the aircraft decreases, the volume coefficient characteristically increases because the configuration is thickened to meet fuel and payload volume requirements. This condition places a wave-drag penalty on the small aircraft.

The wetted-area ratio characteristics shown on the upper half of figure 2 necessarily follow the same general pattern. Since the friction drag is a direct function of the wetted area, the parameter shown is a measure of the friction drag for a given skin-friction coefficient.

Figure 3 shows the variation of skin-friction coefficient for adiabatic conditions as a function of Reynolds number and Mach number for both laminar and turbulent flow over an aerodynamically smooth surface. The turbulent curves have been experimentally verified for incompressible flow to a Reynolds number of $1,000 \times 10^6$. At higher Mach numbers the skin-friction coefficient is still in the process of evaluation. Note that there is little effect of Mach number on the laminar friction coefficient, but there is a pronounced effect on the turbulent values. Shown on this figure are typical Reynolds number ranges for a Mach number 2 fighter, a Mach number 3 bomber-transport configuration wing at $R \approx 90 \times 10^6$, and a fuselage at $R \approx 300 \times 10^6$.

Under laboratory conditions, the maximum Reynolds number for which laminar flow has been maintained without some form of boundary-layer control is about 5×10^6 to 10×10^6. A maximum value of Reynolds number of 28×10^6 at a Mach number of 1.6 has been attained (ref. 1) for a

cooled body of revolution, but the flow was very sensitive to the slightest surface irregularities, even fingerprints. For a wing, the effects of leading-edge sweep also have been shown to be adverse relative to attainment of laminar flow.

There does appear to be a realm for application of boundary-layer control at subsonic speeds; however, supersonically, there appears to be little potential for attaining extensive laminar runs - especially when the problem of traversing the pressure rise across a shock wave is considered.

The real problem of skin friction at supersonic speeds i primarily that of attaining the turbulent values for a smooth flat plate. Three-dimensional roughness, surface waves, gaps, and so forth will tend to increase the drag level as noted on the figure. The experimental data of reference 2 has shown the roughness effects to be less critical at the higher Mach numbers. Current research is now leading to rational procedures for estimating the pressure and friction drag for arbitrary types of roughness under turbulent conditions.

L
1
2
1
1

One interesting approach to reducing the turbulent skin-friction values is illustrated in figure 4. This figure shows the unpublished results of tests obtained by John R. Sevier in the Langley 4- by 4-foot supersonic pressure tunnel on a two-dimensional airfoil at a Mach number of 2 wherein air was injected into the boundary layer to reduce the local-velocity gradients and therefore the skin friction. A substantial reduction in turbulent skin friction is noted, even if the initial drag penalty for the addition of the slots is considered.

Because of the momentum drag penalty, it is nct feasible to take air aboard to provide the injection flow; however, if low-energy air were already available, as from inlet bleed air, then this air might be efficiently utilized. Even bypass air may have appreciable energy; thus its momentum loss would have to be subtracted from the values shown here. The approximate amount of inlet bleed air available is noted in figure 4 and this amount is shown to lead to a substantial reduction in skin friction. Whether this approach is practicable cannot be firmly stated at the moment, but further research and application studies are indicated. Certainly, the effect of Reynolds number on friction-drag reduction must be determined along with the effect of full-chord injection.

Drag due to lift, as previously indicated, may be the largest single element of the total drag during unaccelerated flight. As the cruise speed is increased into the supersonic speed range, the lifting efficiency - that is, the drag due to lift - progressively deteriorates.

Theories have been developed which indicate that large improvements are obtainable through the proper selection of planform and loading distribution.

Figure 5 is taken from reference 3 and summarizes the present state of theoretical knowledge. The ordinate, the drag due to lift parameter $\frac{\Delta C_D}{\beta C_L^2}$, is shown as a function of β times aspect ratio for several wing planforms. If this plot is considered to be for a fixed Mach number, the β term may be neglected, and all planforms will still have the same relative standings. These values are the minimum values of wave plus vortex drag as predicted by linear theory. The two-dimensional flat-plate value of 0.25 and the minimum subsonic value of $\frac{1}{\pi A}$ are shown for reference. The point to be made here is that large reductions in drag due to lift are indicated for the swept and the arrow wings, those for the arrow wings approaching the minimum subsonic value at low Mach numbers. Considerable experimental work has been performed in the Mach number range from 2 to 3 for geometric aspect ratios of about 2 or for an adjusted aspect ratio of about 5 on this figure.

Figure 6 taken from an unpublished paper by C. E. Brown, F. E. McLean, and E. B. Klunker summarizes recent work of the Langley Research Center on a family of arrow wings. (See refs. 4 and 5.) The drag-rise factor $\frac{1}{\beta}\frac{\Delta C_D}{C_L^2}$ is plotted against the parameter β cot Λ, which specifies the position of the Mach line relative to the leading edge. For values less than 1, the Mach line is ahead of the leading edge; at a value of 1, it lies along the leading edge.

The solid line (fig. 6) represents the theoretical drag-rise factor for an uncambered surface. The experimental agreement (shown by the square symbols) is good for a wide range of values of β cot Λ. Shown by the dashed line is the theoretical variation of the drag-rise factor for a restricted camber loading. Here the best experimental values show only about one-half the anticipated theoretical gain. Subsequent analysis indicated that thickness effects of the $2\frac{1}{2}$-percent-thick biconvex airfoil could lead to local supersonic flow, and shock-induced separation would be anticipated. Although oil-flow studies did not appear to indicate flow breakdown, there is hope that a revised wing employing double-wedge sections in an attempt to eliminate supercritical flow might show substantial reductions in drag due to lift.

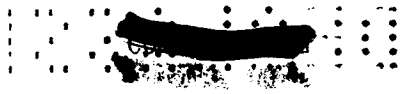

Another approach to improving the lift-drag ratio is the utilization of favorable interference. Although theoretical gains have been computed for many unconventional approaches, most applications run into practical problems associated with real flows, poor off-design characteristics, or large increases in wetted or base area.

Figure 7 shows the results of a simple experiment at a Mach number of 3.11 to see whether the lift-drag ratio of a 60° delta wing could be improved by the addition of a compression wedge to the under surface. (See ref. 6.) Pressures were integrated over the body and the lower surface of the wing for a wide range of angle of attack, wedge angle, and height-to-chord ratio. The resulting pressure drag is plotted against lift. The base drag was not included in these integrations.

These results show no significant gain in lift-drag ratio, since most of the points fall above the experimental wing-alone curve. It should be noted, however, that, if a body or protuberance must be there in the first place, consideration of the interference flow fields can reduce the drag penalty. If base drag could be eliminated by some form of base bleed or by filling the base with engine exhaust, then the added volume may actually have a zero drag penalty.

Up to this point, the elements of wave drag, skin friction, and drag due to lift, which comprise the lift-drag ratio, have been considered. Now the levels of L/D currently attainable are considered.

Figure 8 shows the variation of lift-drag ratios with Mach number for a range of configurations. The level of the subsonic bomber and transport for full-scale flight conditions is shown on the left. For comparison, a marked decrease in the L/D level for current operational supersonic aircraft is shown. This reduction is the direct result of the effect of the addition of wave drag and the increased drag due to lift characteristic of supersonic flight.

The experimental symbols shown (fig. 8) are for wind-tunnel results at a Reynolds number of 4×10^6 for various research configurations representative of bomber types. (See refs. 7 to 10.) The exception is the swept-wing configuration denoted by the diamond symbols, which has a volume coefficient representative of transport-type configurations. The solid symbols are for complete configurations under trimmed flight conditions. The open symbols are incomplete configurations such as wing-body combinations. Note that there is a decided change in type of configuration being considered as a function of M. The highly swept, high-panel-aspect-ratio configuration tends to be optimum for a Mach number of 2 or less, whereas the low-aspect-ratio delta or trapezoidal planform predominates in the Mach number range from 2 to 4. Correction to full-scale Reynolds number of 100×10^6 has been made by assuming the boundary layers to be turbulent. A lift-drag ratio of about 8.5 is

indicated at a Mach number of 3 for bomber-type configurations. A decrement in lift-drag ratio of from 0.5 to 1.0 might be anticipated for conversion to transport configurations.

An estimate of future capability for bomber-type configurations has also been attempted as shown. The assumptions used are: (1) zero-lift wave-drag coefficient, $C_{D_W} = 0.0018$, (2) friction coefficient 10 percent less than the turbulent value for a smooth flat plate, (3) wetted-area-to-wing-area ratio of 2.8, and (4) drag-due-to-lift parameter $\frac{\Delta C_D}{\beta C_L^2}$ from 0.14 at $M = 1.5$ to 0.18 at $M = 4.0$. These estimates result in a level of potential lift-drag ratio of the order of 10 at a Mach number of 3. With such a gain, the level of cruise efficiency $\frac{M \frac{L}{D}}{SFC}$ would be equal to or better than that obtained by the best of the current subsonic bomber and transports. With the other great advantages of flight at a Mach number of 3, the long-range subsonic aircraft would become technically obsolete.

Thus far, the on-design problems of supersonic flight, which are primary considerations in the design of a long-range bomber, have been discussed. However, there are a whole host of off-design problems applicable to the commercial supersonic transport which may dictate the design.

Part IV of this compilation shows that a typical commercial supersonic transport may consume only one-half of its fuel under supersonic cruise conditions. The remainder is consumed in take-off, acceleration and climb, letdown, and in fuel reserves. These off-design areas along with other problems associated with passenger safety, jet noise, and the sonic boom must be solved without seriously compromising cruise performance.

Figure 9 illustrates one of the off-design areas which is critical for the supersonic transport - the landing and take-off problem. Plotted here is the variation of the velocity in knots with wing loading for a range of lift coefficients, that is, a simple plot of the lift-coefficient equation. Shown for reference are the landing and take-off speeds for the present subsonic jet transports - landing at about 125 knots and take-off in the range of 165 knots. For the wing loadings shown, these speeds represent a usable C_L of approximately 1.2 to 1.4. Shown for comparison are some estimated values for a so-called "conventional" supersonic transport with an aspect ratio of about 2.5. Even though the wing loadings are substantially reduced over those of the present subsonic jet, the low aspect ratio and resulting low usable lift coefficient result in take-off speeds of the order of 200 knots with landing speeds of about 150 knots. Also noted on this figure is an effective-aspect-ratio scale. This is

possible, since the effective aspect ratio defines the lift-curve slope C_{L_α} and therefore the usable C_L for a given ground clearance angle. Flap effects are not included.

If present jet transport speeds are to be considered a maximum from the landing and take-off speed standpoint, it is evident that a practicable supersonic transport configuration must attain higher trimmed lift coefficients. This condition can only be provided through higher effective aspect ratio or a considerable advance in the trimmed flap effectiveness over that currently attainable. A variable-geometry wing has great potential in this respect.

Another off-design problem is that of transonic acceleration. The propulsion studies presented in part IV of this compilation show that the airframe-engine combination tends to be thrust marginal for the high-altitude transonic accelerations dictated by the sonic boom. (The boom problem will be discussed in part VIII of this compilation.)

One aerodynamic element of this problem is the transonic wave drag. Figure 10 is a summary of the transonic-wave-drag characteristics plotted against equivalent-body fineness ratio for a wide range of aircraft configurations, ranging all the way from the century series fighters at the low-fineness-ratio end to idealized research configurations at the high-fineness-ratio end. Theoretically, the wave drag is a function of the reciprocal of the fineness ratio squared. The ideal Sears-Haack length-volume body is shown to have a K-value of 11.1. Most of the airplane-type configurations settle out closer to a K-value of about 15. Detail refinement may be able to reduce this number, but it appears to represent a reasonable value for preliminary analysis.

With a minimum of assumptions as to aircraft size and geometry, it is possible to compute the variation of the general drag characteristics with altitude for a range of key variables. Figure 11 shows the drag in pounds for a transport-type configuration at $M \approx 1$. The plot on the left is shown for constant values of aspect ratio and fineness ratio for a range of values of maximum equivalent-body cross-sectional area to wing area. Note that the drag reaches a minimum at an altitude of about 35,000 feet and then increases rapidly. At the higher altitudes the drag due to lift predominates and wave and friction drags become secondary.

On the right-hand plot, the effective aspect ratio (or more exactly, the drag due to lift) is varied. Aspect ratio is shown to be a powerful parameter in reducing drag - especially at the higher altitudes.

Dashed lines represent the general range of thrust available for various jet-propulsion systems which have been sized for cruise at a

Mach number of 3. An accelerative force of 22,000 pounds, which would produce an acceleration of 2 feet per second per second, has been subtracted from the engine thrust so that the values shown here indicate the net thrust available to overcome drag.

There is a critical transonic thrust-drag problem in the altitude range of 40,000 to 50,000 feet. This altitude may be the altitude dictated by sonic-boom considerations. The dropoff in engine thrust with altitude is so abrupt that the type of propulsion system and how it is matched to the airframe will be the primary factors determining acceleration altitude. At the extreme altitudes both the airframe aerodynamics and the propulsion system must be made optimum to attain the altitude levels desired.

Figure 12 presents some of the representative research configurations under study which illustrate certain aerodynamic approaches applicable to the supersonic transport problems. Configuration A is a low-minimum-drag, low-wetted-area configuration made optimum for supersonic cruise. A double-bubble fuselage with the major axis in the horizontal plane improves the supersonic L/D. Landing C_L will be increased through the use of a variable-incidence wing. Configuration B employs the lifting area rule. Its wing is twisted and cambered. Fuselage contouring and bodies located on the wing upper surface provide favorable interference fields for the lifting condition. The wing may employ variable sweep to increase the landing C_L. Configuration C employs outboard tails to improve the supersonic trim drag. The horizontal tails riding in the wing upwash improve the supersonic drag due to lift characteristics. Configuration D is a variable-sweep approach to the minimum drag supersonic configuration. A variable-dihedral horizontal tail controls the transonic aerodynamic-center shift and change in directional stability. Configuration E employs a blended wing-body approach with rapid thickness taper to reduce minimum drag. Twist and camber are incorporated. Relatively thick outboard wing panels of variable sweep are provided. Configuration F considers a modification of the so-called "conventional" supersonic transport to improve low-speed and transonic characteristics through variable geometry. The extensible tips shown provide about a 20-percent increase in area for subsonic flight. Alternate approaches employing variable sweep at the tip or substantial tip droop are also considered.

These configuration studies are merely illustrative of several aerodynamic approaches under consideration for possible application to the supersonic transport. However, they do serve to illustrate the aerodynamic tools available to the designer to meet the extremely difficult requirements of the supersonic transport.

SUMMARY

There has been a gradual improvement in supersonic cruise efficiency to a level approaching that of the best of the present subsonic aircraft. There is still room for further gains in supersonic lift-drag ratio by fundamental research on wave drag, skin friction, and drag due to lift. However, intensive research effort is required.

The most obvious problems are in the off-design areas of landing, take-off, transonic acceleration, and subsonic hold. These problems must be met without appreciable degradation of supersonic performance. The most difficult problem, however, is the recognition that a problem exists in the first place. Consider that the total hours of supersonic flight on all the B-58 airplanes number but a few hundred, whereas the supersonic life of a successful transport may total as much as 25,000 hours. The technical problems inherent in such an advance are truly awe-inspiring.

Although the problems discussed in this paper are broad and complex, there do not appear to be any obstacles which cannot be solved by a vigorous and effective research effort.

REFERENCES

1. Czarnecki, K. R., and Sinclair, Archibald R.: An Investigation of the Effects of Heat Transfer on Boundary-Layer Transition on a Parabolic Body of Revolution (NACA RM-10) at a Mach number of 1.61. NACA Rep. 1240, 1955. (Supersedes NACA TN's 3165 and 3166.)

2. Czarnecki, K. R., Sevier, John R., Jr., and Carmel, Melvin M.: Effects of Fabrication-Type Roughness on Turbulent Skin Friction at Supersonic Speeds. NACA TN 4299, 1958.

3. Beane, B. J.: Curves of Minimum Wave Plus Vortex Drag Coefficient for Several Wing Planforms. Rep. No. SM-22989, Douglas Aircraft Co., Inc., Nov. 1957.

4. Hasson, Dennis F., and Wong, Norman D.: Aerodynamic Characteristics at Mach Numbers From 2.29 to 4.65 of 80° Swept Arrow Wings With and Without Camber and Twist. NASA TM X-175, 1960.

5. Carlson, Harry W.: Aerodynamic Characteristics at Mach Number 2.05 of a Series of Highly Swept Arrow Wings Employing Various Degrees of Twist and Camber. NASA TM X-332, 1960.

6. Hasel, Lowell E.: An Experimental Pressure-Distribution Investigation of Interference Effects Produced at a Mach Number of 3.11 by Wedge-Shaped Bodies Located Under a Triangular Wing. NASA TM X-76, 1959.

7. Hill, William A., Jr.: Lift-Drag Ratios for Arrow Wings Alone and in Combination With a Body, Nacelles, and Vertical Tails at Mach Number 3. NASA TM X-371, 1960.

8. Hallissy, Joseph M., Jr., and Hasson, Dennis F.: Aerodynamic Characteristics at Mach Numbers 2.36 and 2.87 of an Airplane Configuration Having a Cambered Arrow Wing With a 75° Swept Leading Edge. NACA RM L58E21, 1958.

9. Church, James D., Hayes, William C., Jr., and Sleeman, William C., Jr.: Investigation of Aerodynamic Characteristics of an Airplane Configuration Having Tail Surfaces Outboard of the Wing Tips at Mach Numbers of 2.30, 2.97, and 3.51. NACA RM L58C25, 1958.

10. Grant, Frederick C., and Sevier, John R., Jr.: Transonic and Supersonic Wind-Tunnel Tests of Wing-Body Combinations Designed for High Efficiency at a Mach Number of 1.41. NASA TN D-435, 1960.

[redacted]

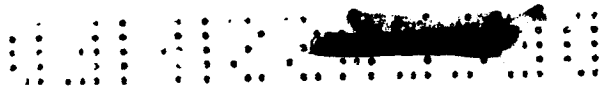

CRUISE DRAG BREAKDOWN

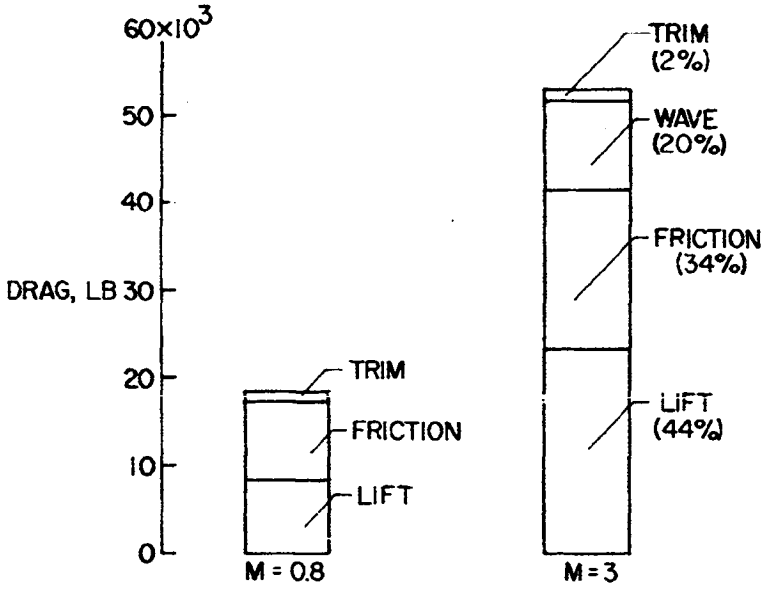

Figure 1

EFFECT OF AIRPLANE SIZE

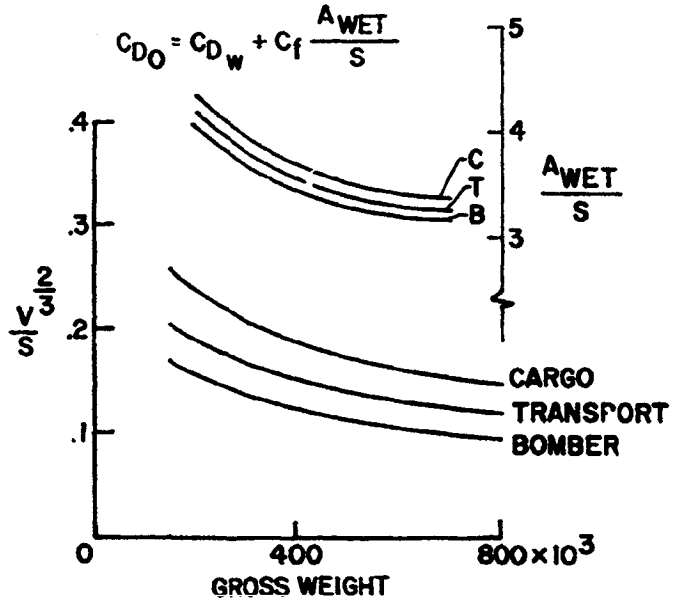

Figure 2

SKIN-FRICTION CHARACTERISTICS

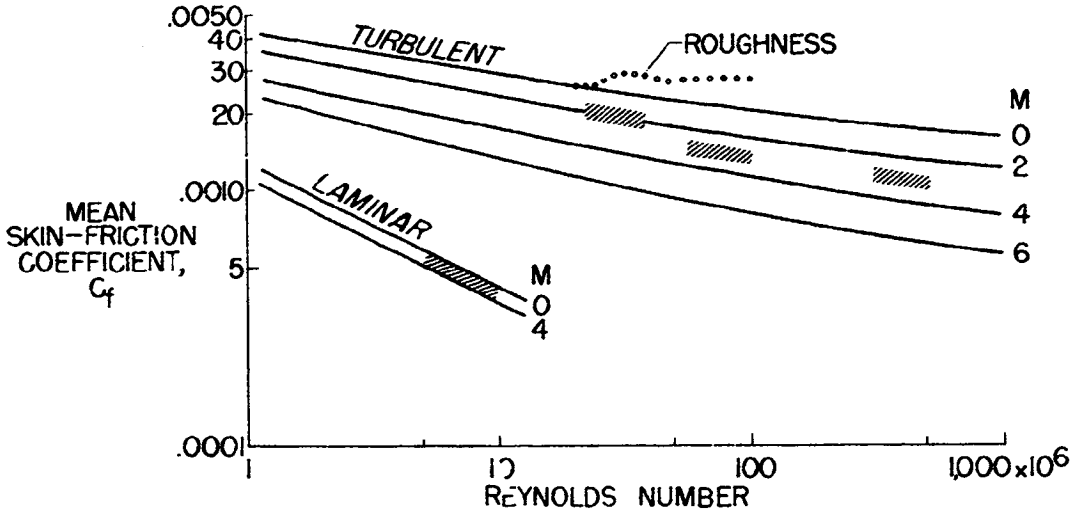

Figure 3

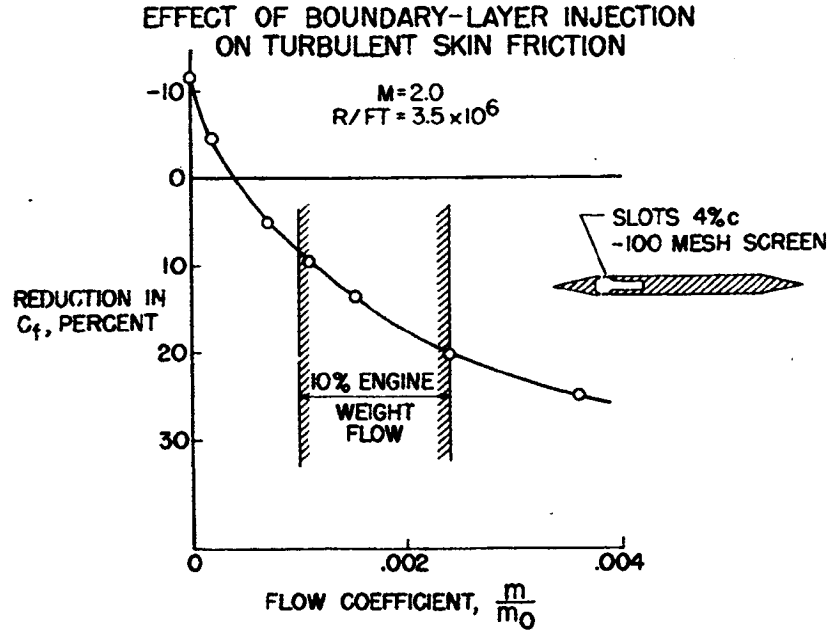

Figure 4

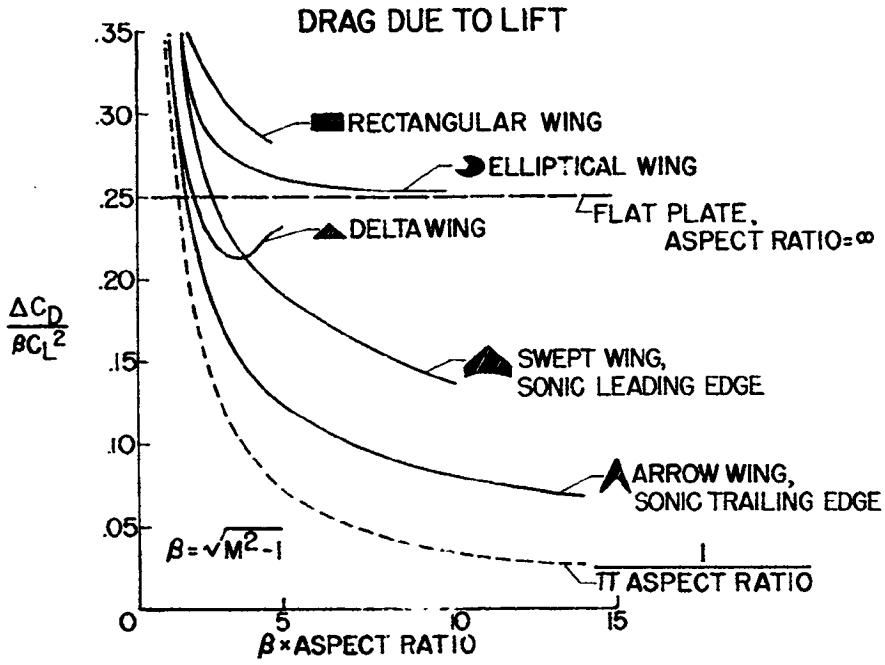

Figure 5

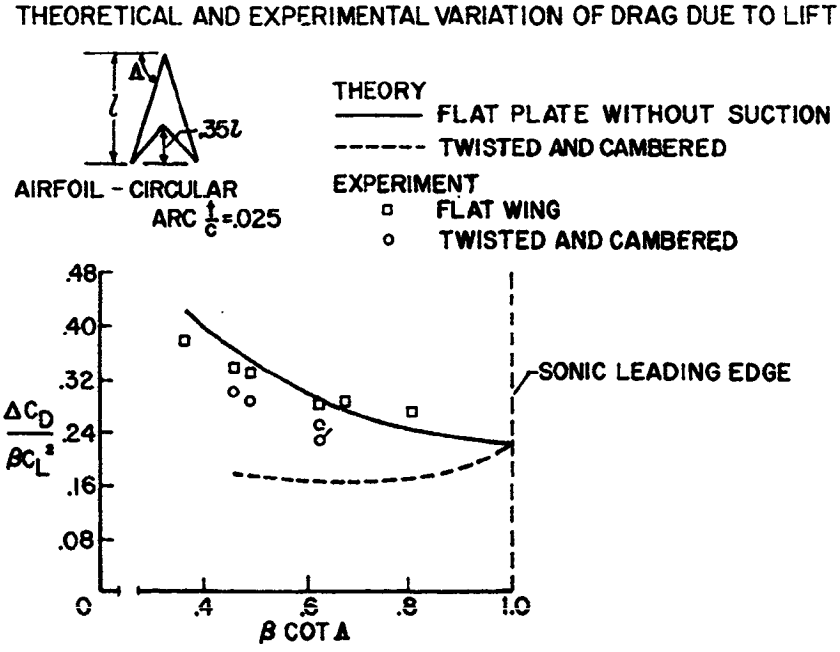

Figure 6

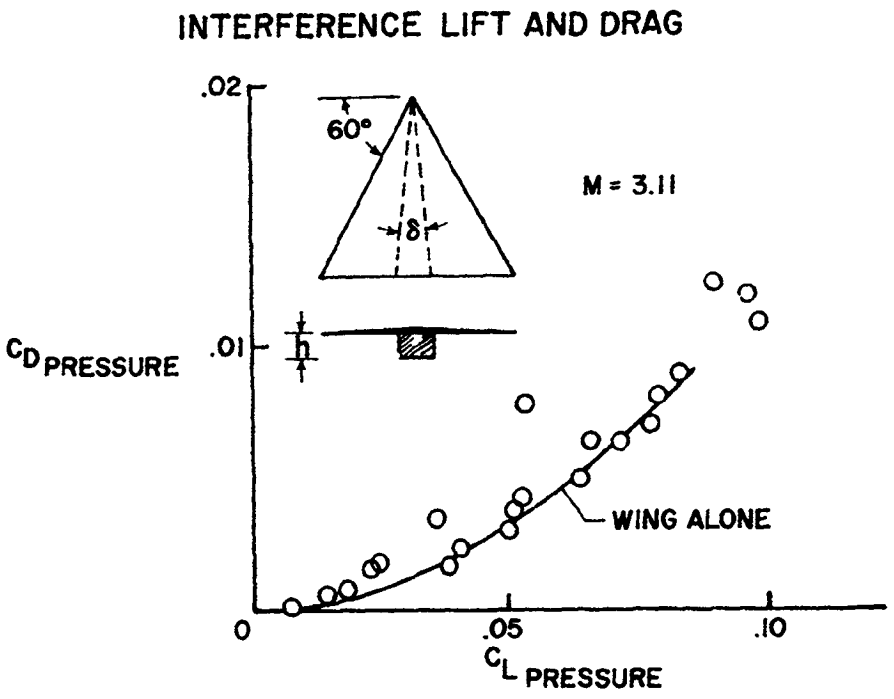

Figure 7

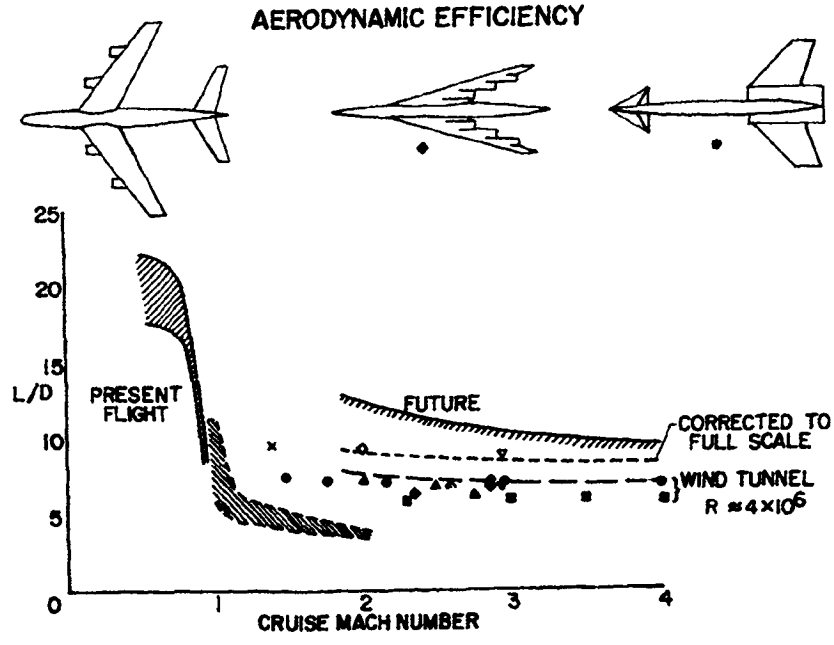

Figure 8

[redacted]

CONFIGURATION EFFECTS ON LANDING AND TAKE-OFF SPEEDS

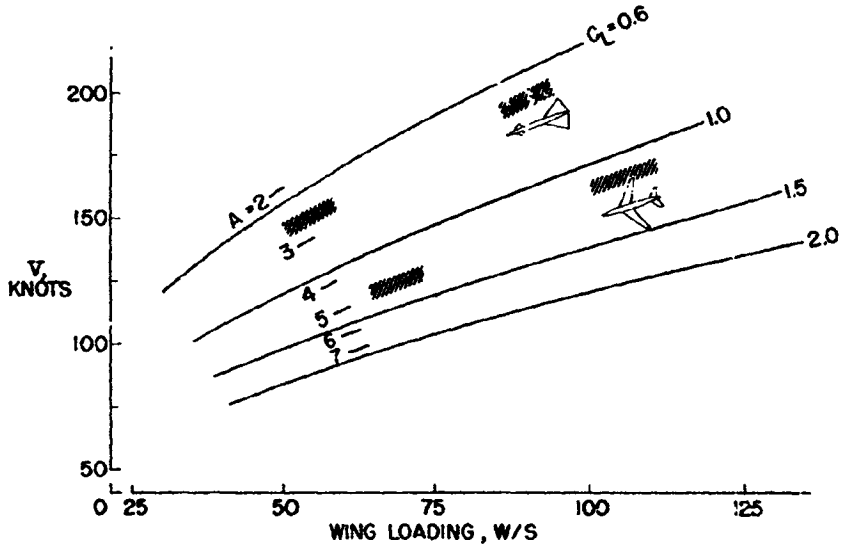

Figure 9

EFFECT OF FINENESS RATIO ON TRANSONIC WAVE DRAG

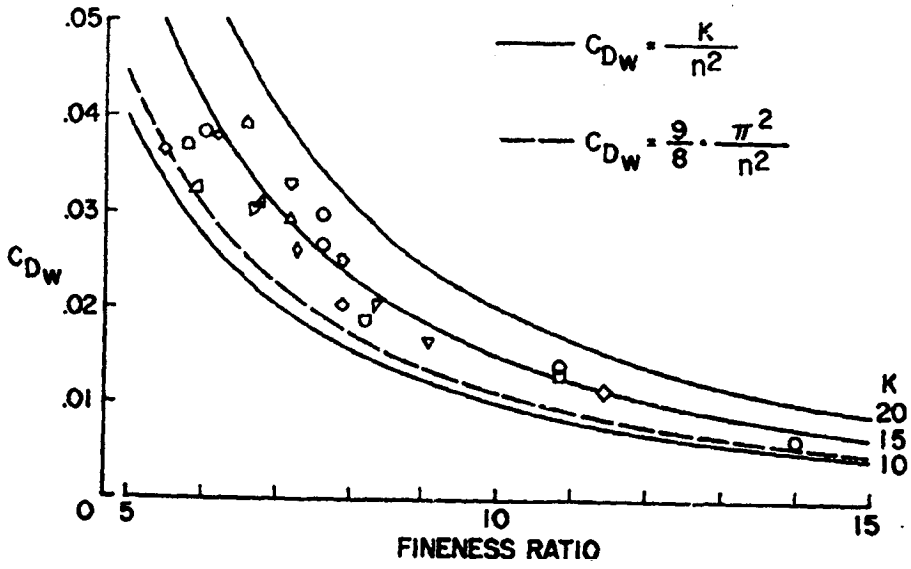

Figure 10

[redacted]

TRANSONIC DRAG CHARACTERISTICS (M≈1)

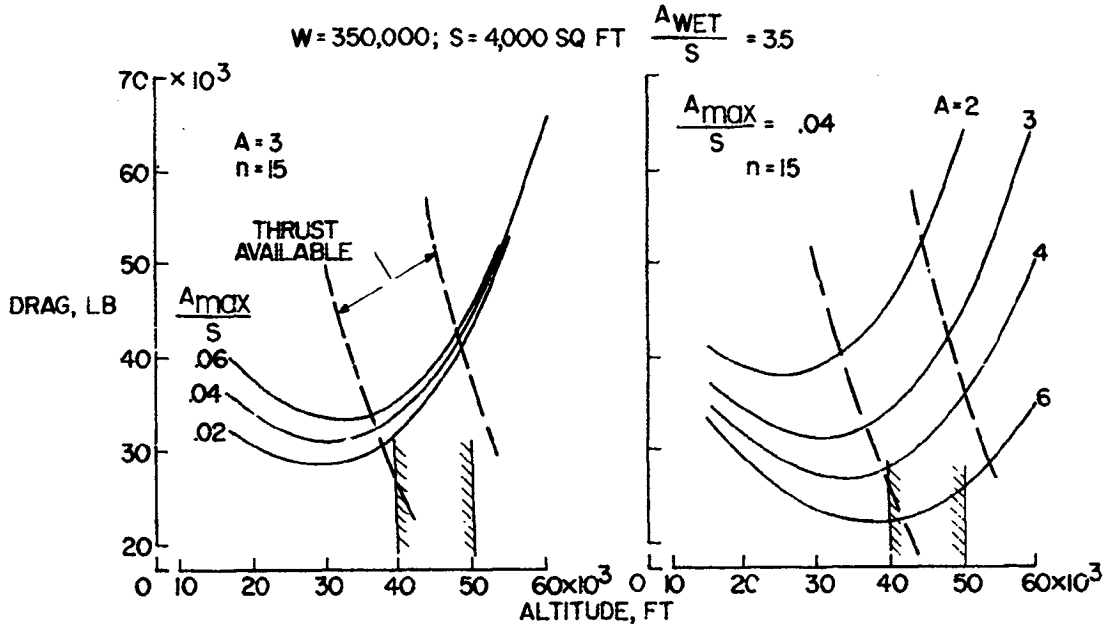

Figure 11

TRANSPORT RESEARCH CONFIGURATIONS

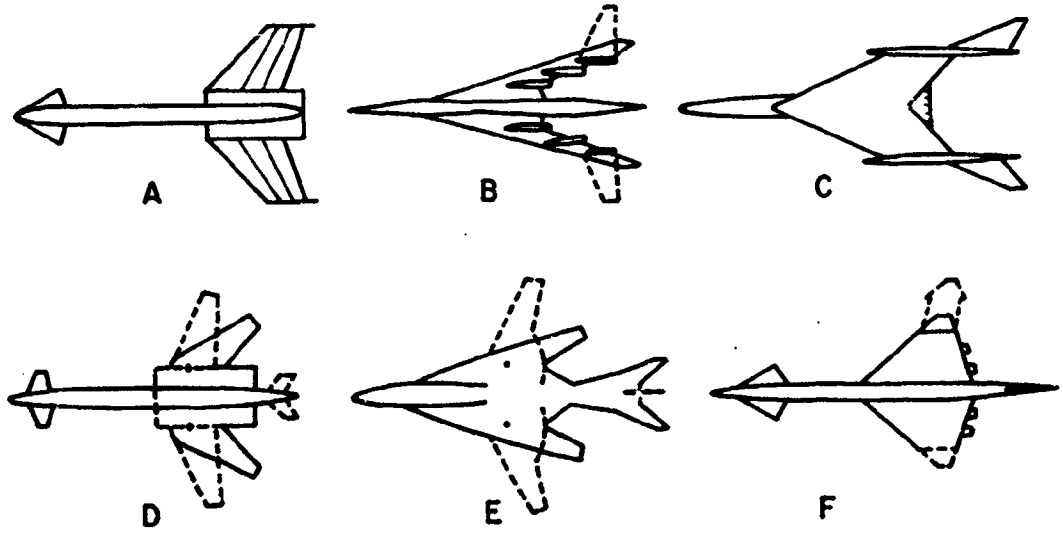

Figure 12

IV. AIR-BREATHING PROPULSION SYSTEMS FOR SUPERSONIC AIRCRAFT

By Lowell E. Hasel, Willard E. Foss, Jr.
Langley Research Center

and David N. Bowditch
Lewis Research Center

INTRODUCTION

In this part, the state of the art for several propulsion system components is reviewed, and some of the important factors which must be considered during the design of a supersonic propulsion system are pointed out. The discussion will be centered around the Mach number 3 cruise airplane of part III and the multimission airplane of part II.

SYMBOLS

$\frac{A}{A_{M=3}}$	ratio of free-stream tube area required by engine at any Mach number to corresponding area at design point of M = 3
h	altitude
M	Mach number
$\left(\frac{m}{m_o}\right)_{BLEED}$	mass-flow ratio, boundary-layer bleed
p	static pressure
p_t	total pressure
$\frac{p}{p_t}$	inlet control parameter
α	angle of attack

DISCUSSION

The pressure recovery characteristics of supersonic inlets have an important effect on propulsion-system performance because for every percentage of loss in recovery there is a greater percentage of loss in net thrust. The recoveries which have been obtained at zero angle of attack from several types of supersonic inlets are shown in figure 1. The inlets include two-dimensional and long axisymmetric types with large amounts of internal compression and a short axisymmetric type with equal amounts of external and internal compression. The off-design spillage drag of the long axisymmetric inlet is considerably less than that of the short axisymmetric inlet. These inlets were designed for $M = 3$ and all have variable geometry provisions - either as variable ramps or as translating center bodies. The inlets, as sketched, have equal capture areas, and the sketches therefore indicate the relative lengths of the supersonic diffusers. The two-dimensional inlet has the highest recovery, varying from 0.89 at $M = 3$ to 0.94 at $M = 2$. These values are quite high and further significant increases of recovery will not be easily attainable with any inlet design. There is no fundamental reason why the recovery of the long axisymmetric inlet should be less than that of the two-dimensional design. The difference shown in figure 1 merely indicates that additional development time must be spent on the long axisymmetric inlet. All of the inlets incorporated some form of boundary-layer bleed. The amount of bleed at $M = 3$ was from 7 to 12 percent of the inlet flow. Additional boundary-layer removal through the existing bleed system did not significantly improve the performance of the long axisymmetric design at $M = 3$. Because of the drag penalty associated with the bleed air, the optimum recovery - that is, the recovery at which the maximum value of thrust minus bleed drag is obtained - may be less than the maximum recovery. Our present knowledge of the behavior of the turbulent boundary layer in the presence of adverse pressure gradients is not sufficient to be able to predict exactly the effect which boundary-layer bleed will have on the increase of pressure recovery. Therefore, a detailed experimental tailoring of the bleed system will be necessary for each inlet to develop the optimum design.

These inlets, in addition to having a high pressure recovery, must be able to supply the required engine airflow. The airflow characteristics of several turbojet and turbofan engines are presented in figure 2. These engine airflows, as presented, are a function of pressure recovery and are based on the recoveries of the two-dimensional inlet. The recoveries have been extrapolated to a value of 0.96 at $M = 1.0$ (fig. 1).

In figure 2 the airflow variation is expressed as the ratio of the free-stream tube area required by the engine at any Mach number to the corresponding area at the design point of $M = 3$ and is plotted as a

function of Mach number. The shaded area indicates the envelope of the airflow characteristics of a series of turbojet engines and the cross-hatched area represents the corresponding envelope for turbofan engines. The differences of the airflow characteristics of the turbojet engines are small throughout the Mach number range, but a large difference exists between the turbofan engines. The airflow characteristics of the two-dimensional and short axisymmetric inlets shown in figure 1 have been included here to indicate that the inlet and engine airflow characteristics have similar trends with Mach number. These inlet airflows can, of course, be controlled to varying degrees during the inlet design to match the airflow of a specific engine. It should be mentioned that the comparison between the engine and short axisymmetric inlet airflows is not strictly correct because of the lower recovery of this inlet. Accounting for this effect would increase slightly the stream tube area ratios of the engines at off-design Mach numbers.

All of the engines require a significantly smaller stream tube of air at low Mach numbers than at the design speed of $M = 3$. This excess air must be diverted from the engine, either by spillage ahead of the inlet or by bypass ducts located behind the inlet. Regardless of how the air is diverted, a drag penalty will be incurred.

The magnitude of this matching drag penalty is now examined. The discussion will be based on a turbofan airflow characteristic defined by the top of the cross-hatched area in figure 2. At any off-design Mach number the distance between the top of the cross-hatched area and the design value of 1 represents the amount of air which must be spilled or bypassed. At $M = 1.2$ this amounts to 41 percent of the design stream-tube area.

The matching drags created by four typical methods of diverting the excess air are presented in figure 3. These drags have been divided by the thrust of a typical turbofan engine and are presented as a function of Mach number. The sketches on the left side of the figure depict two typical ways of spilling the air ahead of the inlet - behind the shock wave of a 5° translating wedge and by means of the flow field of a 10° half-angle translating cone. On an inlet these shapes would be the initial compression surfaces. The excess air may also be bypassed from the subsonic diffuser by means of sonic nozzles which are parallel to the airplane axis or are inclined at some angle, such as 10°. It has been assumed in these drag calculations that the total pressure recovery at the exit of the sonic nozzles was equal to the inlet recovery.

The spillage drag is generally largest at transonic speeds, and it is also most critical at these speeds because the value of the acceleration force - that is, thrust minus drag - is small, as will be shown subsequently.

The least drag at transonic speeds is incurred by the use of the sonic nozzle, exiting axially, and the drag penalty is about $1\frac{1}{2}$ percent of the engine thrust. A word of caution is in order here. An increase in frontal area may be necessary to bypass the large amount of excess air at transonic speeds and exhaust it in an axial direction. The drag penalty associated with this increase in frontal area is not accounted for in this comparison. The highest drag is created by the 5° wedge and is about 10 percent of the engine thrust. Spillage ahead of the inlet can be accomplished more efficiently with the 10° cone than with the 5° wedge. It is also apparent that bypassing the air through a sonic nozzle inclined to the axis results in an appreciable rise in the bypass drag. At Mach numbers from 2 to 3 the matching drag is smaller when the air is spilled ahead of the inlet instead of being bypassed from the subsonic diffuser by a sonic nozzle. Use of a supersonic bypass nozzle would result in bypass drags which were less than those of the 10° cone at supersonic speeds but would not result in drags which were lower than those of the sonic nozzle at transonic speeds. It is of interest to note that the matching drag of the short axisymmetric inlet is quite high. For example, at $M = 1.6$ the calculated value would be about 0.094 for the airflow spillage considered in figure 3. The magnitude of these matching drags in terms of engine thrust is a function not only of the airflow being diverted but also of the engine thrust per pound of airflow. For an afterburning turbojet, the percentage loss of thrust per pound of air diverted would be about half the corresponding value for turbofan engines.

In figure 4 the percent of change in the zero-angle-of-attack recovery has been plotted as a function of angle of attack. These data indicate that at a Mach number of 3, the pressure recovery may be reduced by 6 to 18 percent by an angle of attack of only 4°. These percentage reductions become smaller as the Mach number is reduced. With a two-dimensional inlet, the angle-of-attack or angle-of-yaw effects may be reduced by use of a horizontal or vertical compression surface, respectively. Such an arrangement is not possible with a three-dimensional design. It appears highly desirable that the supersonic inlet, regardless of its type, should be shielded from flow-angularity effects as much as possible by placing the inlet in a flow field generated by the airplane wing or fuselage. Such an arrangement may also reduce the inlet size, reduce the amount of supersonic compression which the inlet must accomplish, and simplify the inlet-control system.

The controls for supersonic inlets form a very vital part of the propulsion system. Generally, both contraction and bypass controls are required. The functions of these controls are to obtain high-pressure recovery and to prevent shock regurgitation which results in large decreases in pressure recovery, inlet buzz, and the attending engine surge. Shock regurgitation should be prevented for a number of reasons.

A combination of the discontinuous drop in recovery from perhaps 0.05 to 0.55 and the buzz that usually follows shock regurgitation will cause the engine to surge at Mach numbers near 3. This means that most if not all of the thrust of the unstarted system will be lost and inlet drag incurred until the inlet can be restarted and the engine returned to normal operation, which may require a complete shut down and restart. In addition to the destabilizing force associated with this thrust loss, the inlet will spill large amounts of flow which could affect operation of nearby inlets or cause a high pressure region under a nearby wing or on the body. Further, a structural problem is caused by the engine surge. Duct static pressures in excess of free-stream total pressure have been measured during engine surge in a turbojet-engine-inlet configuration. These pressures are much higher than normally exist in the inlet and require a considerable increase in the structural weight over that required for normal operation.

The contraction control is required to vary the inlet throat for changes in airplane Mach number and angle of attack or yaw. Because the effect of Mach number and angle of attack on optimum contraction differs for the various inlet types and with position on the airplane, a particular control will probably have to be developed for each specific application. Attempts to measure a throat supersonic Mach number for use as a control parameter have been frustrated by the terminal shock affecting the static pressure throughout the throat region. Therefore, since no contraction-control parameters with general application have been observed, it may be necessary to schedule the inlet contraction as a function of one or more parameters that are indicative of airplane Mach number and angle of attack or yaw. The problem of sensing flow angle can be simplified by sheltering the inlet under a wing or near the body, thereby restricting major flow-angle changes to either yaw and cross flow or angle of attack.

The contraction control is required to be fast acting to prevent shock regurgitation during airplane maneuvers and gusts. These external disturbances cause temporary errors between the desired and actual contraction; therefore, the desired contraction must be less than the optimum value by a margin equal to the maximum expected error to prevent shock regurgitation. Since these errors can be reduced by increasing the complexity of the control, a compromise must be made between the control complexity and the performance margin required for stable inlet operation.

The bypass control positions the normal shock near the inlet throat to obtain high recovery and at the same time matches the inlet and engine airflows by spillage ahead of the inlet or by a bypass in the subsonic diffuser. For this type of control, the problem is to position the terminal shock as far upstream in the throat as possible, without allowing airplane maneuvers or engine transients to force it forward of the throat. The entire bypass control loop, which includes the sensor,

control, bypass actuators, and the response of throat conditions to bypass movement, must be analyzed to determine the decrement in recovery required for stable inlet operation. The response of throat conditions to bypass movement, or duct dynamics, has been measured for a number of inlet-cold-pipe and inlet-engine configurations. Good agreement has been obtained between these measured duct dynamics and a simple prediction based on a dead time equal to the acoustic travel time from the bypass to the throat, in series with a first order system based on the ability of the diffuser to store mass. In order to keep the recovery decrement required for a stable, controlled inlet operation small, the throat flow conditions must respond quickly to bypass movement. In order to obtain this fast response, the prediction shows that the bypass must be placed near the throat to minimize the dead time and the diffuser volume must be small to reduce its storage capacity.

In order to illustrate possible bypass control signals, static pressure distributions on the centerbody of an axially symmetric inlet with flush slot bleed are shown in figure 5. In the plot on the left side of the figure for a Mach number of 2.88, the shock moves up to and is compressed on the flush slots as recovery is increased. Just as recovery is increased from 0.851 to the peak value of 0.854, the shock begins to move ahead of the bleed and appears to furnish a control signal with large gain. However, at a Mach number of 2.48, the terminal shock does not travel ahead of the slots as peak recovery is reached so that no static pressure rise as large as that across the terminal shock is available for control purposes. Therefore, when the problems of off-design operation and the need for a supercritical margin to obtain stable inlet operation are considered, it appears that in this inlet it is not possible to place a sensor where the terminal shock will consistantly pass it at conditions near peak recovery. This was also found to be true for the two-dimensional inlet (fig. 1) with porous bleed because although the axial position of the geometric throat was constant, the peak recovery shock position was found to be a function of contraction, Mach number, and angle of attack. The throat bleed and boundary layer, thus, seem to distort the throat flow so that direct shock-position sensing does not seem feasible. However, for this axially symmetric inlet, the static pressure downstream of the slots appears to vary continuously as recovery is changed at both Mach numbers of 2.88 and 2.48. A control, which sensed a constant ratio between the static-pressure sensor just downstream of the slot and a throat total pressure, set recovery within 2 percent of its peak value from Mach numbers of 2.0 to 2.88 at zero angle of attack. A constant ratio of throat-exit static pressure to throat total pressure was also found to be a very satisfactory control parameter for the two-dimensional inlet just mentioned. The parameter is, therefore, believed to be of general use and is equivalent to setting a constant throat-exit Mach number. Summarizing the inlet control situation, it appears that considerable development effort will be required for each different inlet installation.

L 1 2 1 3

Regarding the exhaust system, reasonable performance can be obtained from a conventional sonic exhaust nozzle at subsonic speeds. For the engine which must operate at supersonic speeds, however, variable-geometry ejector nozzles are required. The performance of such a nozzle is shown in figure 6. Here the ratio of the net thrust minus boattail drag divided by the ideal net thrust is plotted as a function of Mach number. The performance is shown for a design which has primary and secondary nozzles of variable area and a variable external shape. The net thrust ratio reaches a minimum value of 0.82 at transonic speeds and gradually increases to 0.91 at the design Mach number of 3. Inasmuch as the ideal variable-geometry ejector has a thrust ratio of about 0.97, it is believed that considerable improvements in ejector performance, particularly at transonic speeds, may be realized with further research.

All of the propulsion-system components which have been discussed result in losses in the thrust which is available from an engine. The magnitude of these losses is shown in figure 7 in which the ratio of net thrust to ideal net thrust is plotted as a function of Mach number. This breakdown includes the losses due to the two-dimensional inlet pressure recovery, inlet control margin, boundary-layer bleed, spillage, and the variable-geometry ejector just discussed. The largest individual losses are due to the inlet recovery and variable-geometry ejector. The losses due to control margin, boundary-layer bleed, and spillage drag are each small, but the sum is significant, and such losses are inherent in any propulsion system. As a result of all these losses the available thrust is from 70 to 75 percent of the ideal thrust. Increases in the available thrust ratio above these values will depend principally upon future improvements in inlet and exit performance.

Turning to the engines themselves, both turbojet and turbofan engines are being considered for use in the multimission and supersonic cruise airplanes. As is known, the basic gas generator for these two types of engines is essentially the same. In the fan engine, however, extra power is extracted from the main gas stream by a turbine to compress additional air, which does not pass through the gas generator, so that for a given gas generator the total airflow of the turbofan is greater than that of the turbojet.

When the power plants are considered, the thrust characteristics of the engine must be compared with the drag characteristics of the airplane. This comparison has been made in figure 8 for the supersonic transport. (The comparison would be somewhat different for the supersonic bomber.) The airplane was assumed to accelerate to $M = 0.9$ at low altitude, climb to 40,000 feet at $M = 0.9$, and then climb gradually while accelerating with augmented power to $M = 3.0$.

The line labeled drag represents the level of drag encountered during the climb and acceleration, and the symbols represent the loiter,

subsonic-cruise, and supersonic-cruise drag values. The two shaded regions represent the levels of thrust obtainable by typical turbojet and turbofan engines matched to this airplane with a nonaugmented take-off thrust-to-weight ratio of 0.31. The band on the left is for unaugmented operation; the other band is for full augmentation. The downward jog between the two bands is, of course, associated with the climb to altitude.

The most significant thing shown in figure 8 is the fact that the thrust-minus-drag margin is a minimum at transonic speeds and is much smaller than the margin which exists at either subsonic or supersonic speeds. This characteristic may well determine the required engine size. Other problem areas are take-off noise (which is rather high for the turbojet even without augmentation), the fact that sea-level loiter and subsonic cruise are performed at extremely low percentages of the available unaugmented thrust, and the necessity for the attainment of low specific fuel consumption at supersonic cruise conditions. L 1 2 1 3

A large percentage of the fuel usage of the supersonic transport occurs in off-design flight. This is illustrated in figure 9 where the fuel rate for such an airplane is plotted against flight time. The mission segments considered are climb and acceleration, cruise, let-down, loiter, and reserves. Only about half of the fuel is used during design-point operation. This fact stresses the great need for obtaining efficient propulsion system performance in off-design operation as well as at the design point.

The same situation exists in connection with the multimission airplane. In figure 10 the percentage of fuel used by such an airplane during the various phases of three important missions is shown. The three missions are: a $M = 1.2$ sea-level-dash mission, a supersonic-cruise mission, and a subsonic-ferry mission. In each case the mission is broken down into take-off, climb, and acceleration, the dash or cruise part of the mission, and the loiter and landing. It is apparent that the major part of the fuel usage for the three missions occurs at quite different operating conditions: $M = 1.2$ at sea level, $M = 2.2$ at altitude, and $M = 0.85$ at altitude. Here again an extremely versatile engine is required for this airplane. In other words, the engine should have a low specific fuel consumption for a wide range of operating conditions.

The basic characteristics of turbojet and turbofan engines are compared in a qualitative sense in figure 11, where specific fuel consumption is plotted against thrust for several operating conditions. The turbojet engine data selected are representative of current $M = 3.0$ designs, whereas the turbofan data have been obtained from industry and NASA estimations of the probable characteristics of such engines. The two curves on the left are for $M = 0.9$ flight at 35,000 feet with no

[redacted]

augmentation, and the other two curves are for M = 3.0 flight at 65,000 feet with augmentation. The two engines have been sized arbitrarily to give the same thrust at take-off conditions.

At subsonic speeds it can be seen that the turbofan potentially offers lower specific fuel consumption and thus more efficient operation over a much broader range of thrust than the turbojet. This characteristic, which is obtained with little if any penalty in specific fuel consumption in the supersonic-cruise condition, obviously is of great benefit at off-design operation such as subsonic cruise and loiter. In addition, because of the greatly increased airflow the turbofan potentially offers advantages of lower noise during take-off, greater thrust augmentation at transonic speeds, and lower operating temperatures during both acceleration and supersonic cruise.

L 1 2 1 3

One disadvantage of the turbofan is that it might require a greater frontal area for a given thrust and will have greater air inlet and ducting weights. Obviously, therefore, there is the problem of trade-offs - that is, the optimum engine for a given airplane or mission can be determined only by a step-by-step consideration of all the factors involved. Nevertheless, the potential advantages of the turbofan appear great enough for both the supersonic and the multimission airplanes that its development should be pursued vigorously.

In summary, the state of the art with regard to air-breathing propulsion systems for supersonic airplanes may be expressed as follows. Sufficient research and development has been conducted in the fields of air inlets and jet exits to enable a reasonably high level of on-design performance to be obtained. A great deal of detailed tailoring will be required, however, to match components so that optimum performance will be obtained over a wide range of operating conditions, and satisfactory control arrangements worked out. In connection with the engines themselves, the turbofan appears to offer a number of significant advantages which appear to make its future development highly desirable.

[redacted]

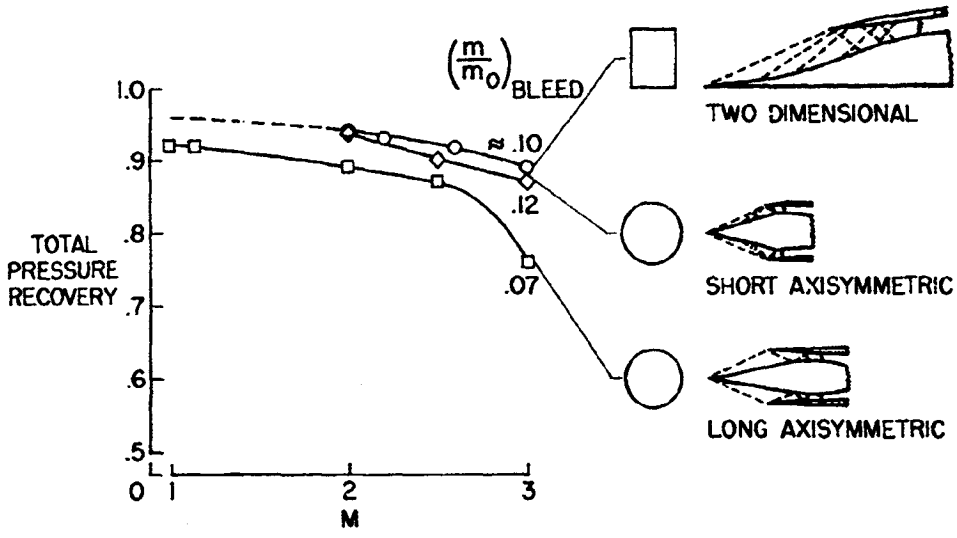

Figure 1

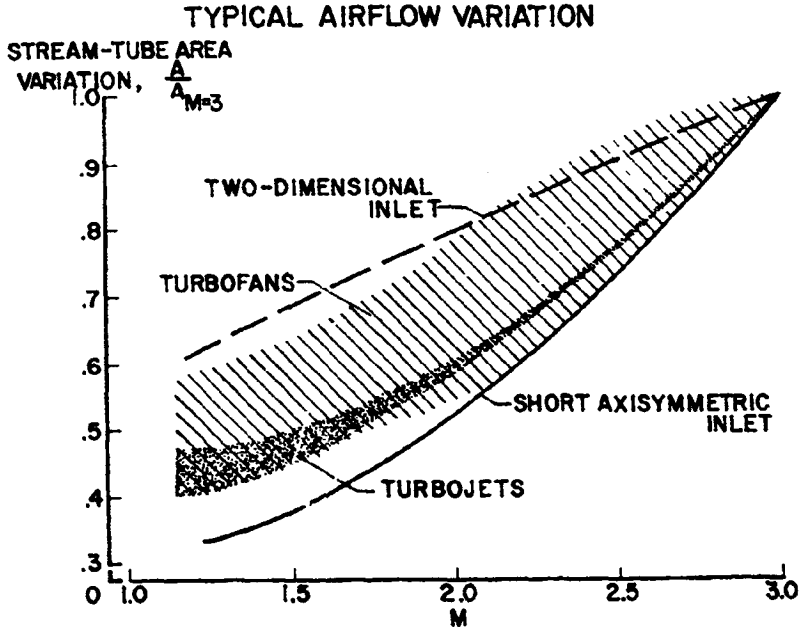

Figure 2

MATCHING DRAG FOR TURBOFAN ENGINE

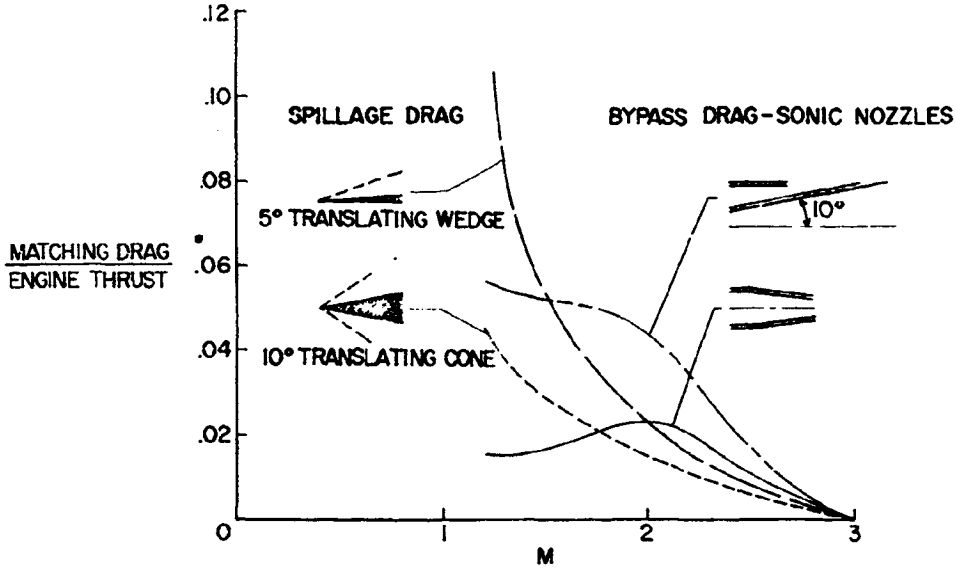

Figure 3

EFFECT OF ANGLE OF ATTACK ON PRESSURE RECOVERY
M=3

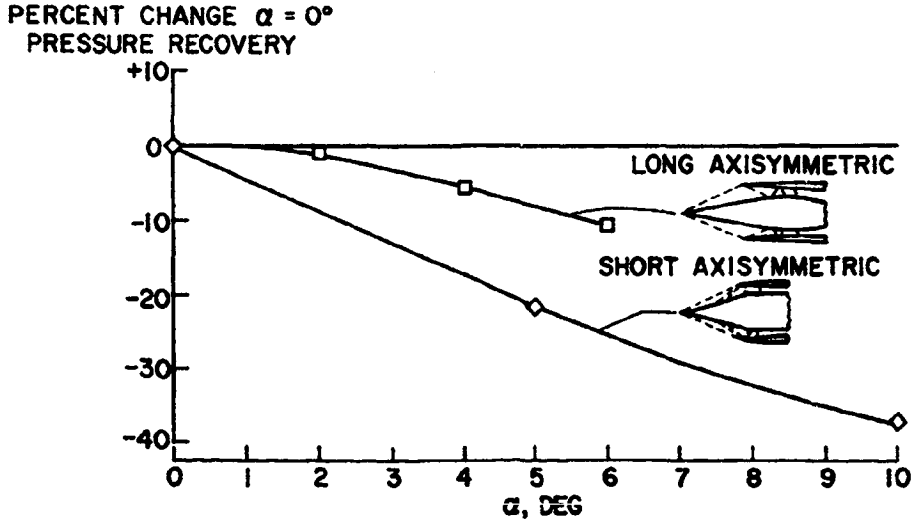

Figure 4

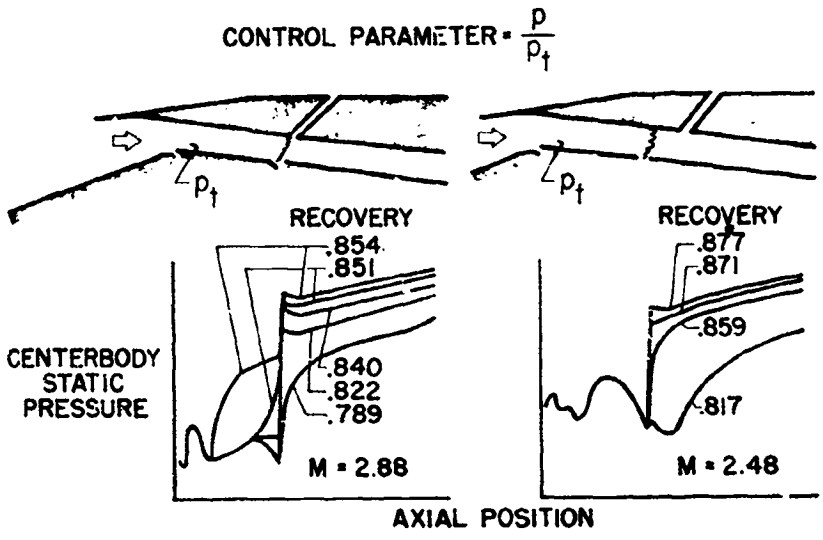

Figure 5

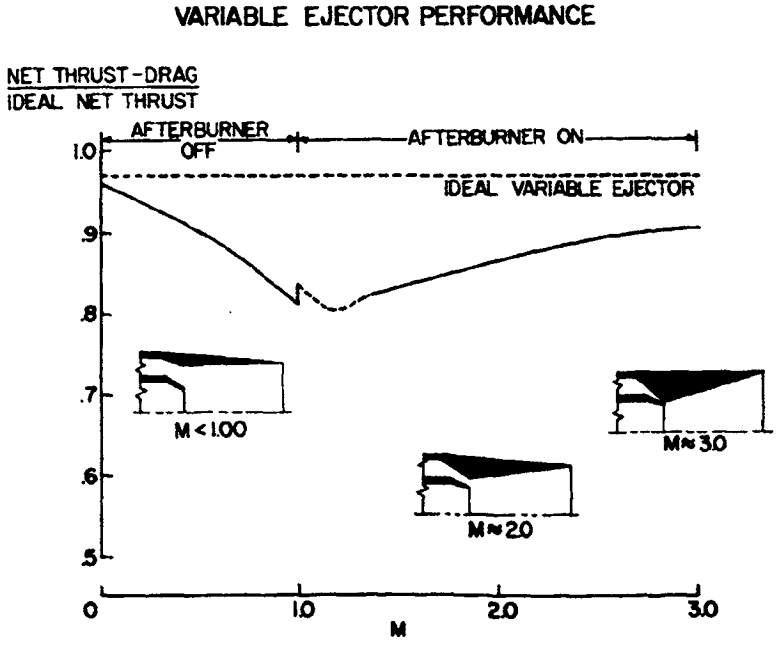

Figure 6

THRUST LOSS BREAKDOWN

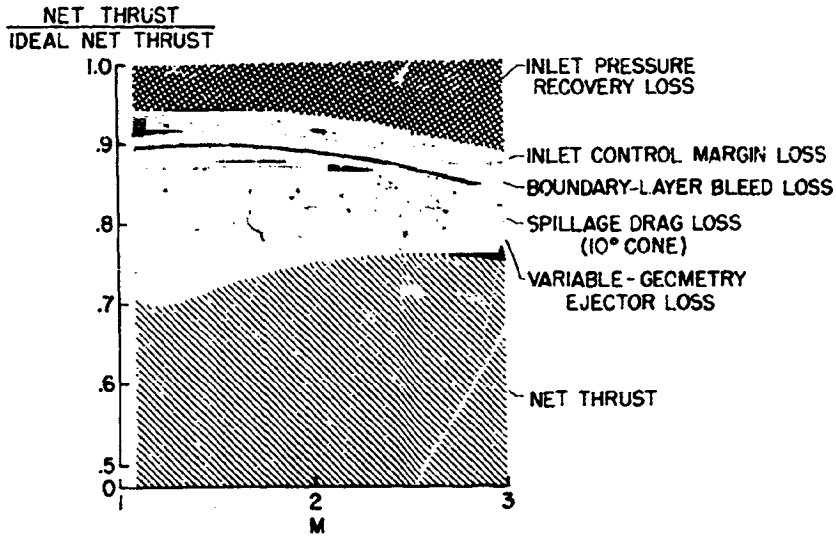

Figure 7

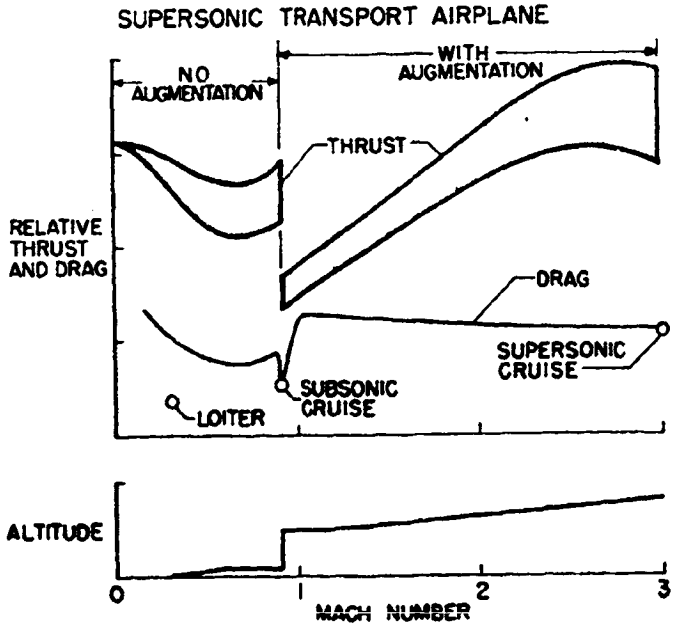

Figure 8

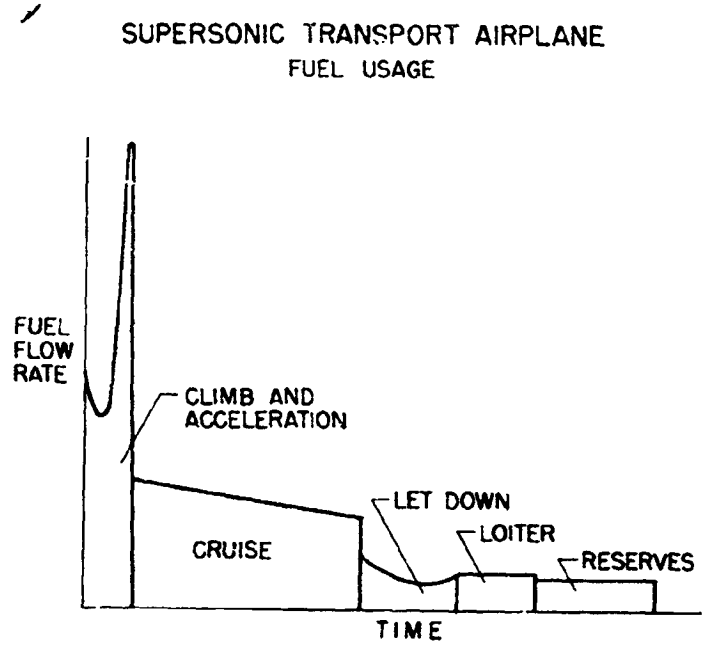

Figure 9

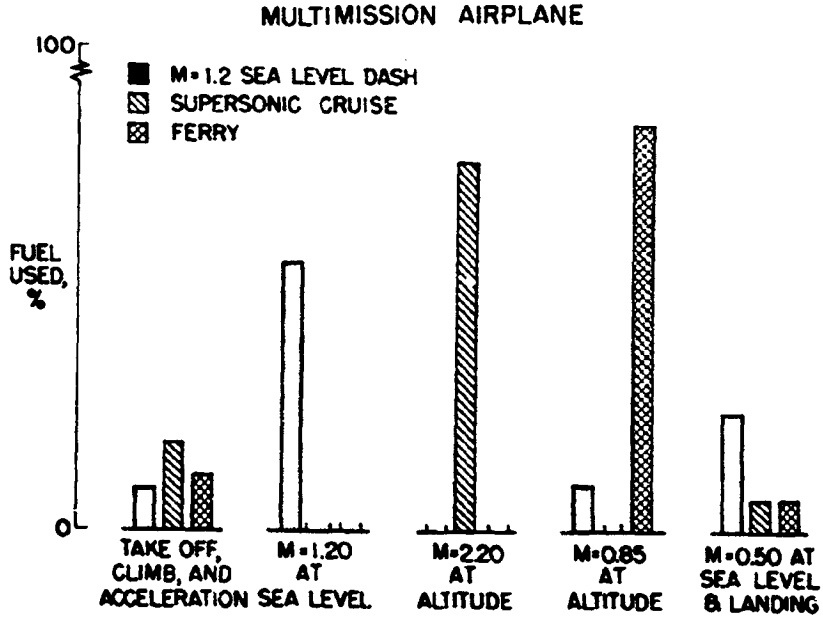

Figure 10

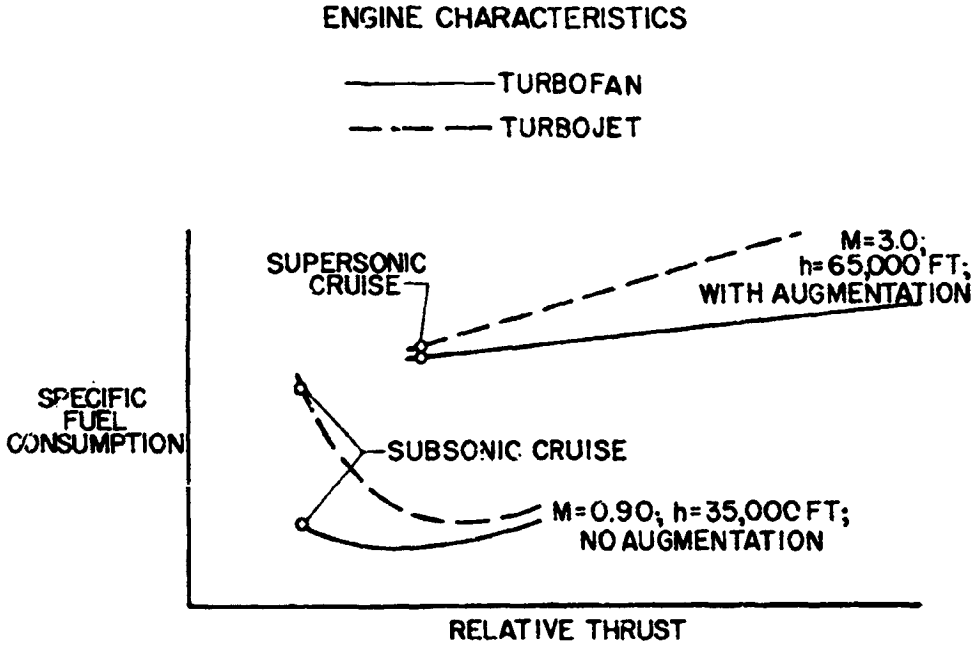
ENGINE CHARACTERISTICS
TURBOFAN
TURBOJET
SUPERSONIC CRUISE
M=3.0; h=65,000 FT; WITH AUGMENTATION
SPECIFIC FUEL CONSUMPTION
SUBSONIC CRUISE
M=0.90; h=35,000 FT; NO AUGMENTATION
RELATIVE THRUST

Figure 11

V. THE X-15 FLIGHT RESEARCH PROGRAM IN RELATION TO THE DEVELOPMENT OF ADVANCED MILITARY AIRCRAFT

By Jack Fischel

Flight Research Center

INTRODUCTION

H 182

The design, construction, and development of advanced military aircraft undoubtedly will involve the utilization of many relatively new concepts in several different, but related, areas. In many cases, these new concepts will require new flight techniques or involve development problems inherent in the use of relatively unproven methods, materials, structures, systems, and configurations. Moreover, flight verification will be required of aircraft aerodynamics and flight behavior because of the usual uncertainties associated with predicted data. Solutions to these problems obviously would require flight testing involving extensive time and effort before the aircraft could become operationally acceptable.

Upon the inception of the X-15 research airplane project, many new and far-reaching techniques and principles were studied and applied in the aircraft design and are currently being demonstrated and investigated. Because similar concepts are likely to be used in advanced military aircraft, the X-15 flight program will provide significant information, over a broad flight environment, pertinent to the development of these vehicles. This paper discusses the research objectives of the X-15 flight program, some of the flight aerodynamic characteristics currently being obtained, some development problems encountered, and the experience obtained with the advanced systems investigated.

SYMBOLS

C_D drag coefficient

C_L lift coefficient

C_l rolling-moment coefficient

$C_{l_\beta} = \frac{\partial C_l}{\partial \beta}$

$C_{l_{\delta_a}} = \frac{\partial C_l}{\partial \delta_a}$

C_m pitching-moment coefficient

$C_{m_\alpha} = \frac{\partial C_m}{\partial \alpha}$

$C_{m_{\delta_h}} = \frac{\partial C_m}{\partial \delta_h}$

C_N normal-force coefficient

$C_{N_\alpha} = \frac{\partial C_N}{\partial \alpha}$

C_n yawing-moment coefficient

$C_{n_\beta} = \frac{\partial C_n}{\partial \beta}$

$C_{n_{\delta_v}} = \frac{\partial C_n}{\partial \delta_v}$

M Mach number

q dynamic pressure

α angle of attack

β angle of sideslip

δ_a aileron deflection

δ_h horizontal-tail deflection

δ_v vertical-tail deflection

[redacted]

OUTLINE OF FLIGHT PROGRAM

Research Objectives

In order to provide some understanding of the contributions forthcoming from the X-15 flight program, a listing of the flight research objectives is presented as follows: (1) aerodynamic and structural heating, (2) aerodynamic loads and structural research, (3) aerodynamic derivatives, (4) flight control, (5) lift and drag characteristics, (6) recovery and landing, (7) aeromedical studies, and (8) operational evaluation. These items are discussed individually in the following paragraphs.

In regard to the item (1), aerodynamic and structural heating, one of the primary objectives of the X-15 flight test program is to make heat-transfer studies on a full-scale flight vehicle in the true environment. In order to accomplish this objective, temperature gradients in the structure will be obtained as well as the isolated skin temperatures from which heat-transfer coefficients could be determined. During the flight tests, primary emphasis will be placed on studies of the aerodynamic heat transfer to the vehicle, particularly in the areas where interfering flows are experienced and where available analytical methods might be expected to give less satisfactory predictions. The flight results will be nondimensionalized wherever possible so as to be of most general applicability. Detailed studies of boundary layer and local flow conditions will be made in selected areas on the airplane in order to accomplish this nondimensionalizing.

In the area of aerodynamic loads and structural research, aerodynamic and structural loads data are being obtained on the wing, control surfaces, and various structural components of the X-15 airplane during flights and also during landings. This information is of interest to structural designers and aerodynamicists in proving the integrity of structures and predicted loads characteristics and the efficiency of control surfaces under varying environments.

Determination of aerodynamic derivatives in flight over the operating envelope is of obvious significance for verification of wind-tunnel and estimated derivatives and for flight-planning purposes.

The flight control research areas are manifold and include investigation of control problems in supersonic and hypersonic flight; control problems in trajectory flight, including exit, control at low dynamic pressure and near zero g, and reentry; advanced flight control systems, and control in the Dyna-Soar research areas. Among the significant objectives included are: determination of the adequacy of the display, of the console stick, and of the stability augmentation system;

the use of reaction controls; simulation requirements; handling qualities in the hypersonic regime, in a high-dynamic-pressure high-temperature environment, and in a low-dynamic-pressure high-angle-of-attack regime; and a study of a type of adaptive control system for effective operation in an extreme control environment.

Research on lift and drag characteristics involves determination of scale effects on lift and drag. These effects, of course, aid in the verification or interpretation of wind-tunnel results and extend the knowledge of Reynolds number effects. Also, base-drag characteristics are being determined.

The recovery and landing research performed is applicable not merely to the safe landing of the X-15 but to the proper determination of suitable recovery techniques for use on vehicles having low lift-drag ratios, and, certainly, is applicable to the Dyna-Soar.

Aeromedical studies involve determination of physiological aspects in a varied g environment or in near-critical regimes. Another important aspect is the flight evaluation of a pressure suit made to withstand the range in temperature and pressure and the blast effects anticipated for normal and emergency operation.

Operational evaluation is applicable to the various systems, materials, and structure utilized in the aircraft and will provide information pertinent to these items in a varied flight environment.

Performance Envelope

The extent of the flight regimes available to the X-15 is shown in figure 1 in terms of altitude and Mach number. The flight envelope obtainable with the XLR11 interim engines extends to a peak altitude of 135,000 feet and a Mach number of 3.4. The design altitude with the XLR99 final engine is 250,000 feet. The design speed is a Mach number of about 6.5. Higher altitudes at lower airspeeds, as shown by the dashed curve, can be achieved in acute semiballistic or ballistic flight trajectories. For flights to extremely high altitudes, however, recovery is uncertain because of the reentry problem.

Until now, the X-15 has achieved a peak Mach number of 3.2 and a peak altitude of 107,000 feet by using the interim rocket engines. Further expansion and exploration of the flight envelope available with the XLR11 engines will continue in the next few months, with special emphasis on several of the research areas discussed, such as heating, flight control, and aerodynamic derivatives. Meanwhile, an XLR99 final rocket engine is currently being installed in one of the X-15 airplanes and will be used in the near future to expand the flight envelope to the

airplane design limits. Exploration of the research areas discussed will be pursued simultaneously within this flight envelope after all the airplanes have had the larger engine installed.

RESULTS OBTAINED TO DATE

As is well known, a substantial amount of theoretical and laboratory research, as well as simulation, was performed in support of the X-15 project. Therefore, verification is required of these predicted characteristics under full-scale flight conditions. The operational experience with systems, techniques, and materials, also requires evaluation.

Stability Derivatives and Flight Control

The current status of the flight evaluation of some of the principal stability derivatives is shown in figure 2 as a function of Mach number for a limited angle-of-attack range ($4^\circ < \alpha < 10^\circ$). Shown are the lift-curve slope and the longitudinal-, directional-, and lateral-stability parameters. For comparison, wind-tunnel data for a similar angle-of-attack range are also shown, by the faired curves, and indicate fairly good agreement. The pitch, yaw, and roll control derivatives evaluated in flight are compared with predicted results in figure 3. Good agreement is also indicated. Although good agreement between flight and wind-tunnel derivatives is apparent in the range below a Mach number of approximately 3, particular interest is centered in the flight-derivative evaluation at Mach numbers in excess of 3, where no previous flight evaluations have been made. Verification of wind-tunnel derivatives at these higher speeds will provide information pertinent to the development of other advanced vehicles.

It is of some significance to note that various flight motions have been reasonably well predicted in simulator studies thus far by using wind-tunnel derivatives. This agreement has provided a degree of assurance in expanding the flight envelope. Although the stability augmentation system has been used in most of the flight studies performed, further research is planned with and without the use of various damper modes to evaluate the augmentation system and to determine any control limitations resulting during normal operation or from damper-out conditions. In specific flight regimes, such as at high dynamic pressure or during reentry, control limitations may be critical; therefore, the X-15 should provide information applicable to minimum control requirements of other advanced vehicles.

Lift-Drag Characteristics

A comparison of flight and wind-tunnel drag polars at three speeds is shown in figure 4. Presented are the variations of lift coefficient with drag coefficient for Mach numbers of 0.9, 1.1, and 2.0. Agreement is reasonably good at the subsonic and higher supersonic speeds, but the flight-determined drag coefficient is somewhat higher at the lower supersonic speed. Brief base-pressure data indicate that this disagreement in the low supersonic range is due largely to a discrepancy between the base-drag measurements obtained from wind-tunnel and flight tests. This is yet to be resolved. Nevertheless, the drag-due-to-lift characteristics measured in flight agree reasonably well with predicted characteristics.

Extension of the lift-drag evaluation under full-scale conditions to determine scale effects and base-drag contributions will provide a better understanding of wind-tunnel results and allow interpretation of wind-tunnel tests of other advanced vehicles to full-scale conditions.

Heating

In the research area of aerodynamic heating, a potential high-speed problem area, the highest temperatures recorded have been in the neighborhood of 400° F, obtained during a speed-buildup mission which resulted in a maximum Mach number of 3.2.

Figure 5 presents only a brief sample of the type of temperature measurements being obtained. A sectional sketch is shown of the midspan station on the wing with the chordwise distribution of skin temperature at the time peak temperature was realized. This distribution occurred after the peak Mach number of 3.2 for this flight was attained. The lower skin temperatures are higher than those of the upper skin mainly because of angle-of-attack effects and partly because of the thinner skin on the lower surface. The lower temperatures near the leading edge are attributed to the heavy leading-edge heat sink designed to handle the large heating rates to be encountered during the design missions. An example of the internal variation in temperature is also shown in the plot in the upper right corner of this figure. The rapid rise in skin temperature produces a considerable lag and, consequently, differences in temperature between the free skin areas, spar caps, and internal webs. For example, at the 50-percent chord there is a difference of about 300° F between the lower skin and the center of the web. Present indications are that predicted and measured full-scale temperatures are in fair agreement, and, therefore, a degree of assurance for extending the flight program has been provided.

As mentioned, the data shown constitute only a brief sample of the temperatures measured, for there are 650 thermocouples located on the X-15 to provide a rather complete coverage of skin and internal temperatures. Future flights are planned with more nearly stabilized flight conditions to provide nondimensional heat-transfer coefficients which will be useful for applying results to other airplanes. Although plans have been made to obtain data on the X-15 in the speed range up to $M > 6$, it might be added that this full-scale heating information is sorely needed for development of even the $M = 3$ to $M = 4$ airplane.

Dynamic-Loads Problems

H
1
8
2

One of the problem areas which became evident early in the X-15 flight program is panel flutter. A review of the X-15 structural design shows that the type of structure and the materials utilized in the construction of the X-15 were governed by the heat environment anticipated during various hypersonic flight missions. The X-15 side-fairing panels were constructed of a flat sheet stiffened by a corrugated backing, and no adequate analytical methods were, or are, available to predict flutter of a flat-sheet panel, much less the complex panels used on the X-15. Moreover, prior to flight testing, no wind-tunnel tests had been performed to investigate panel flutter on these specific panels. During flight tests, panel flutter of the side-fairing panels was experienced. Subsequent wind-tunnel and flight tests provided a simple fix that appears adequate to avoid this phenomenon, at least for the present.

Figure 6 shows an example of the relative panel response measured during flight for the original panels and for the stiffened panels as a function of dynamic pressure. The upper curve represents response of the unstiffened panel, and the lower curve shows response of the stiffened panel. The abrupt increase in panel response for the unstiffened panel represents the start of panel flutter. The beneficial effect of the modification is illustrated by the general reduction of panel response and the absence of panel flutter. Flutter of the vertical-tail panels has also been detected during wind-tunnel tests, and modifications to the vertical-tail structure have been incorporated. Further wind-tunnel tests are planned to clear the airplane flight envelope to the design dynamic pressure, and continued monitoring by means of flight measurements and inspection during the flight program, particularly in a high-temperature and high-dynamic-pressure environment, will provide additional background for future advanced designs.

Inasmuch as recent general studies and experiences have indicated that panel flutter is the type most likely to be encountered in advanced designs and in a higher speed environment, it appears that additional studies are required to establish design procedures for avoiding this phenomenon.

Recovery and Landing

Another problem encountered in the X-15 flight research program pertains to the recovery and landing. The increasingly critical nature of the approach and landing maneuver as lift-drag ratios have decreased has caused a general focusing of attention and research effort on these problems as related to more advanced high-speed aircraft and also to hypervelocity and reentry vehicles. For these advanced vehicles, it was thought that a lower limit of lift-drag ratio existed beyond which it was not possible to effect a safe landing. Landing of the X-15 was even considered questionable.

During the past few years, the Flight Research Center has devoted much effort to evaluation of suitable approach and landing techniques for vehicles having peak lift-drag ratios approaching values as low as 3. As a result of these studies, which included flight simulation with aircraft such as the F-102 and F-104A, the approach and landing technique for the X-15 was evolved. A summary of the flight touchdown conditions experienced thus far is shown in figure 7 which presents the variation of vertical velocity with angle of attack. The touchdown vertical velocities and angles of attack have generally been well within the design envelope shown, and the technique utilized is deemed satisfactory. As expected, with this technique a high level of pilot proficiency is required for landing, and increased pilot experience generally provides improved approach and touchdown conditions. Inasmuch as future advanced military vehicles probably will utilize power and hence will have peak lift-drag ratios for landing which are greater than that of the X-15, no significant landing problems are foreseen. However, in the emergency power-off condition, where lift-drag ratio may be quite low, these advanced vehicles may benefit from the landing techniques developed with the X-15. In addition, the X-15 has provided, and will continue to provide, some significant advances to the state of the art for skid landing-gear systems.

Systems Evaluation

In addition to the research performed in the areas discussed, information and experience are being obtained in preflight and flight evaluation of the major systems listed as follows: (1) stability augmentation system, (2) reaction controls, (3) adaptive controls, (4) controllers, (5) display, (6) inertial platform, (7) physiological, (8) operational, (9) hot nose, (10) rocket engine, and (11) energy management. Although most of these systems are being independently developed in various ground-based environments, it is only in a flight environment, in combination with other systems, that a realistic demonstration can be effected. In contrast to the agreement found between flight and predicted aerodynamic characteristics thus far, the systems

experience in flight has not always been satisfactory. This is more or less anticipated when a system is in the development or checkout stage. In some instances, component reliability or integration problems have been encountered, and in others component or system development is required. Also, some of these systems have never been flight evaluated and are being developed in laboratory or mockup studies for future flight use. In all cases, continuous product-improvement effort is, and will be, necessary to provide satisfactory flight operation and reliability. It is relatively certain that many of these systems or modifications of these systems will have future application to the various flight areas covered by the X-15, as well as to other flight regions. Therefore, it is safe to say that these systems are, and will be, developed to the satisfactory stage and should be available for application to other advanced vehicles.

CONCLUDING REMARKS

A discussion has been presented of the flight-research objectives and some of the results obtained to date in the X-15 flight-research program which are pertinent to the development of advanced military aircraft. Flight studies performed thus far, up to a Mach number of approximately 3, indicate that the aerodynamic force and heating data obtained agree reasonably well with wind-tunnel predicted data. More significant data, having an influence on other advanced vehicles, will be obtained in a number of research areas when the speed range is extended to Mach numbers between 3 and 6.

Some aerodynamic problems, dynamic structural problems, and systems operational problems were encountered, and probably will continue to be encountered, as a result of the use of new configurations, materials, structure, and systems concerning which little or no practical knowledge is available or which require full-scale verification. These are some of the same problems which will be encountered in the development of any advanced aircraft and can be evaluated and finally solved only by a realistic study in a flight environment. Therefore, the current flight studies being performed with the X-15 will provide information which will benefit the development of advanced military aircraft.

X-15 PERFORMANCE ENVELOPE

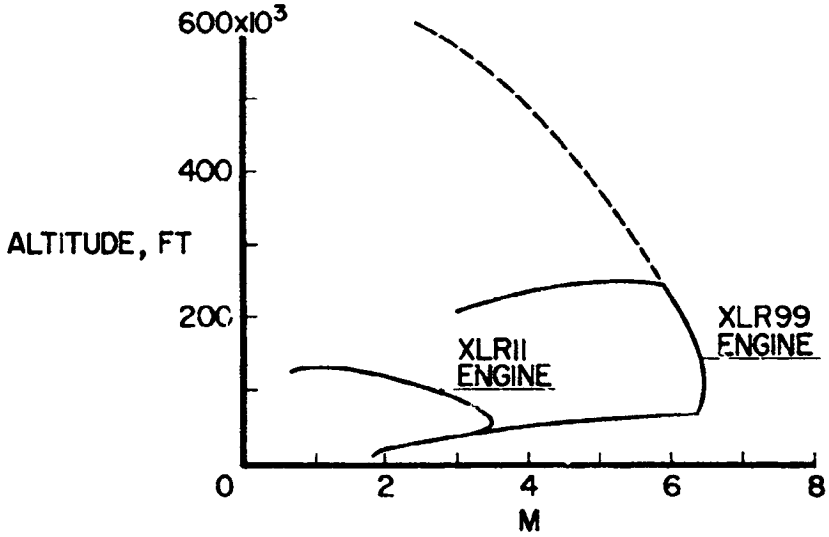

Figure 1

X-15 STABILITY DERIVATIVES

$\alpha \approx 4°-10°$

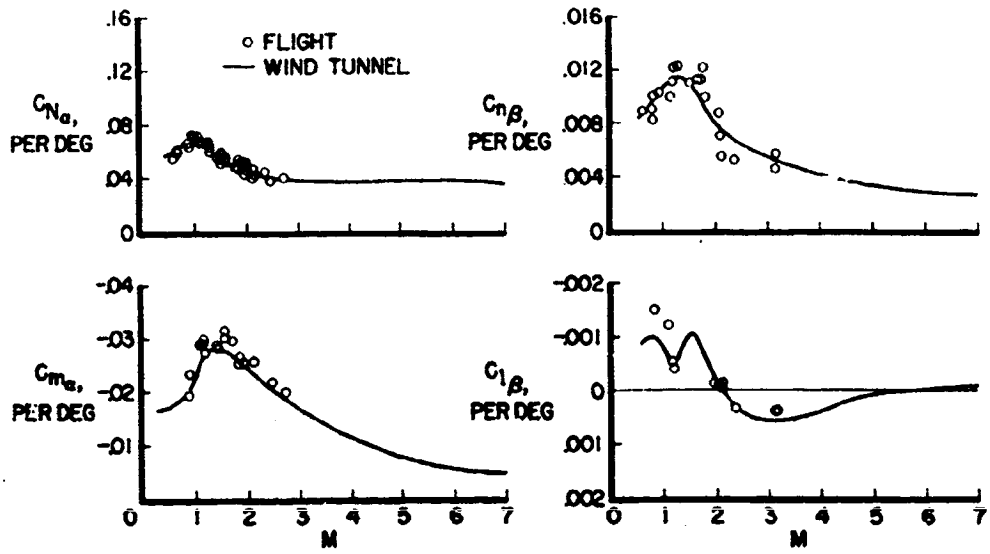

Figure 2

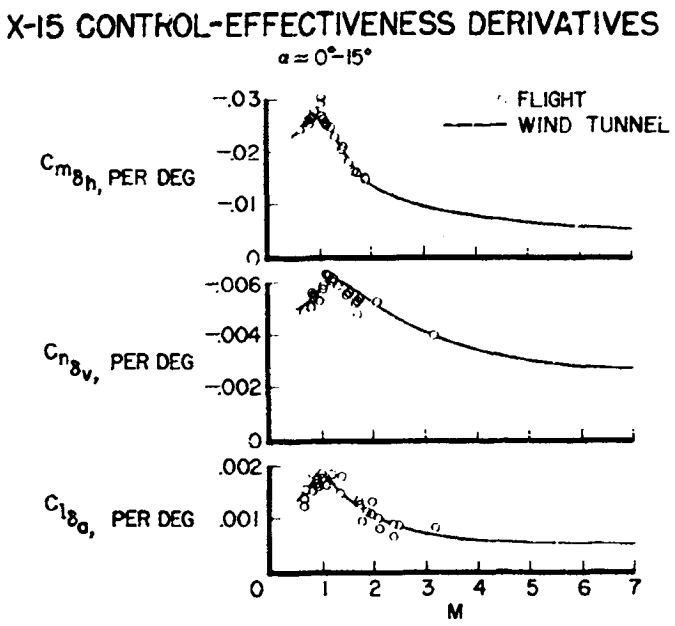

Figure 3

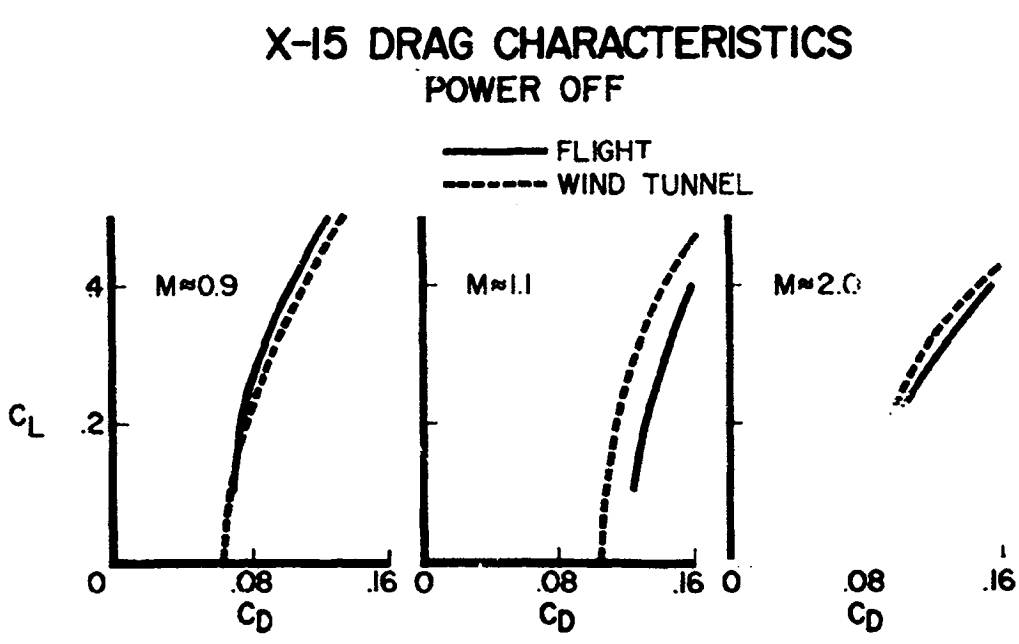

Figure 4

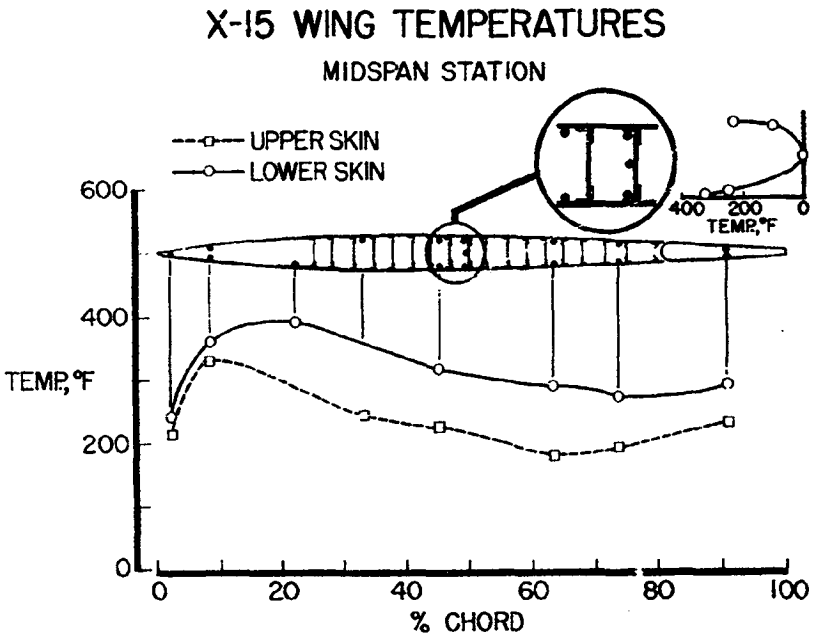

Figure 5

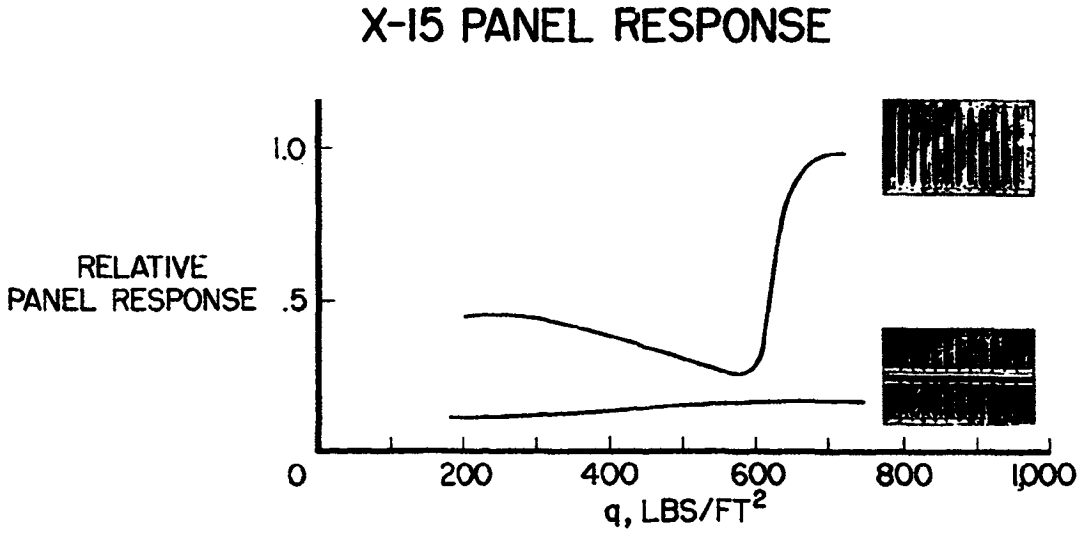

Figure 6

X-15 TOUCHDOWN CONDITIONS

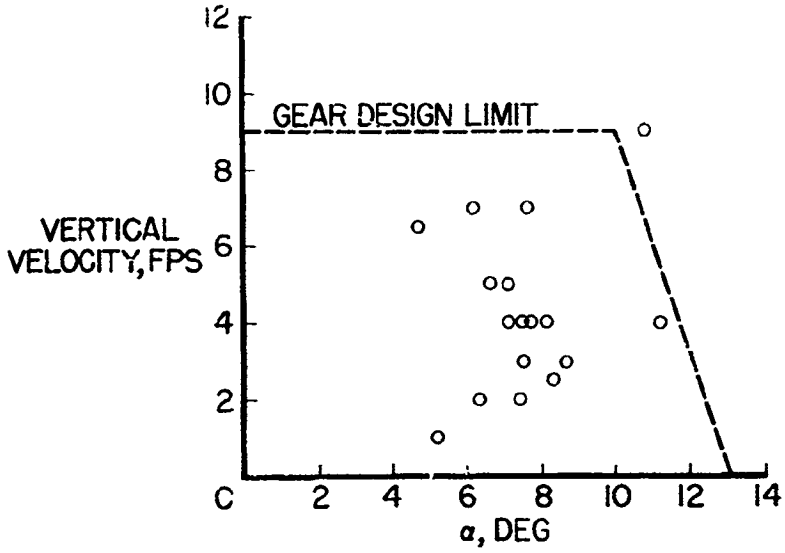

Figure 7

VI. HYPERSONIC CRUISE VEHICLES

By John M. Swihart and John R. Henry

Langley Research Center

INTRODUCTION

Interest has been recently expressed in the military use of hypersonic cruise vehicles as bombers, transports, reconnaissance aircraft, and perhaps recoverable boosters. The purpose of this paper is to give a very brief summary of the state of the art in aerodynamics, aerodynamic heating, propulsion, and to indicate the performance possibilities of such an aircraft based on this state of the art. A great deal of research applicable over broad regions of the hypersonic speed range is in progress (refs. 1 and 2, for example) but for the present purpose, discussion will be confined to cruising vehicles which are boosted to cruise speed and altitude. For this purpose a Mach number of 6 has been chosen as the design point, which is considered to be about the limiting Mach number for the use of hydrocarbon fuel and is also considered to be a logical starting point for the use of liquid hydrogen fuel.

SYMBOLS

A_0	inlet capture area
$C_{D,a}$	afterbody drag coefficient
$C_{D,0}$	drag coefficient at zero lift
C_L	lift coefficient
C_m	pitching-moment coefficient
D	drag
D_0	inlet capture diameter
F	internal thrust
L	lift
M	Mach number

q	dynamic pressure
R	Reynolds number
R_T	transition Reynolds number
W_G	gross weight
α	angle of attack
β	boattail angle
ϵ	emissivity
η_{KI}	inlet kinetic energy efficiency
η_{KN}	nozzle kinetic energy efficiency
Λ_{LE}	wing-leading-edge sweep

RESULTS AND DISCUSSION

Figure 1 illustrates a configuration concept for a hydrocarbon-fuel vehicle. This relatively high-fineness-ratio high-fuel-density model has a 70° single-wedge-slab delta wing with a thickness ratio of 2 percent. The fuselage is shown mounted on top of the flat-bottom wing; however, by interchanging fuselages and wing camber positions, several models were obtained and were investigated. There were no engine nacelles mounted on these models.

Figure 2 illustrates a configuration concept for a liquid-hydrogen-fuel vehicle. It has the same kind of wing as the hydrocarbon-fuel model, except the leading-edge sweep has been increased to 74°, the wing tip has been clipped, and the very large fuselage necessary for the low-density hydrogen fuel has been placed symmetrically on the wing.

A calculated drag breakdown for these two designs at a Mach number of 6 is as follows:

[redacted]

Design	Typical $C_{D,0}$	Component drag coefficient, percent $C_{D,0}$						
		Body		Tail		Wing		Skin friction
		Wave	Base	Wave	Base	Wave	Base	
Hydrocarbon fuel	0.0030	4	5	1	2	2	20	66
Hydrogen fuel	0.0056	30	16	2	1	4	4	43

Typical values of full-scale minimum drag coefficient $C_{D,0}$ are shown for each configuration and the contribution of the body, tail, and wing to the minimum drag are listed as percentages. This table serves to illustrate that for a hydrocarbon-fuel design, the skin-friction drag is all important and no roughness drag above the level for turbulent boundary layers (which has been discussed previously in part III of this volume) can be tolerated. The skin-friction drag for the hydrogen-fuel design is still very important; however, the wave drag associated with the large fuselage has become an appreciable part of the minimum drag. For both configurations, the base drag for these slab wings, tails, and bodies is quite high.

The effect of boattailing on afterbody drag is shown in figure 3. These data are for a Mach number of 6 with a fully turbulent boundary layer, and the afterbody drag coefficient obtained by integrating the pressures along the afterbody and across the base are plotted against the boattail angle. The data were measured on a two-dimensional slab wing and the sketch in figure 3 shows how the model was boattailed with the base dimension corresponding to a boattail angle of 12°. For the flat base, $\beta = 0°$, the drag is nearly equal to the estimated vacuum value of the pressure coefficient, or $(-1/M^2)$; however, as at lower Mach numbers, substantial gains are realized from boattailing and a 33 percent reduction is shown in $C_{D,a}$ by incorporating a boattail angle of 6°.

Figure 4 shows the aerodynamic characteristics for the high-density hydrocarbon-fuel model. These data were obtained in the Langley Unitary Plan Wind Tunnel at a Mach number of 4.63 and a Reynolds number of 7×10^6 based on the mean aerodynamic chord of the wing. Figure 5 shows data obtained in the Langley 300-MPH 7- by 10-foot tunnel at a Mach number of 0.25 and a Reynolds number of 2.5×10^6. The data in figures 4 and 5 are for a configuration with the fuselage below and above the delta wing untrimmed and with no vertical tail. The L/D is slightly higher with the body above than with the body below the wing, but the

configuration with the body below the wing gives a higher value of C_m at zero lift. Many methods have been devised in the past to reduce the trim drag that would be associated with the body above the wing; and one of these, nose cant, for example, could be applied here. Shifting the body position changes the lift-curve slope slightly as would be expected and changes the position of zero lift by about $\pm 1^\circ$. An important point to be noted in figures 4 and 5 is that the data appear to be very smooth and show no radical nonlinearities, either at subsonic or high supersonic speeds.

Figure 6 has been prepared to give an indication of the magnitude of the lift-drag ratios that have been obtained. Solid and dashed lines are calculations for flat plates at a Reynolds number of 90×10^6. The transition Reynolds number was assumed to be zero (leading edge) for the solid-line curve and 10×10^6 for the dash-line curve. This value of transition is probably as high as can be expected, inasmuch as high values of leading-edge sweep tend to have a detrimental effect on laminar flow. (See part III.) Some preliminary data obtained at a Mach number of 5 with a 70° delta wing indicate that transition occurred at a Reynolds number of about 3×10^6. These flat-plate data set an upper limit to be expected on L/D and show a value of L/D of about 10 at a Mach number of 6. The model data shown are not for complete models in the usual sense in that they have no engine nacelles; however, in a subsequent part of this discussion, the nacelle external drag has been subtracted from engine thrust, and the interference drag is believed to be very small. The data indicate that for high-density hydrocarbon-fuel vehicles, values of L/D of about 8 can be obtained at a Mach number of 6, whereas for low-density liquid-hydrogen-fuel models the values of L/D are near 6 or less over the speed range up to a Mach number of 10.5. This level of aerodynamic performance is shown subsequently to be high enough to provide desirable ranges for cruising vehicles.

Figure 7 is concerned with the aerodynamic heating of the basic vehicle structure. The equilibrium surface temperatures calculated for a Mach number of 6 with an emissivity of 0.9 are tabulated for the wing of the hydrocarbon-fuel vehicle at an angle of attack of 5°. The wing leading-edge diameter is 1 inch. The tabulated values indicate that the leading-edge temperature would be about $1,750^\circ$ F, that the lower-surface temperatures from immediately in back of the leading to the trailing edges would range from $1,200^\circ$ F to $1,400^\circ$ F, and that the upper-surface temperatures would range from 700° F to 900° F. The leading edge might have to be made of some refractory material; however, the rest of the vehicle could probably be constructed of one of the super alloys such as René 41, and perhaps the upper surface of the wing and also the body, if mounted above the wing, could be constructed of titanium. Construction of such a vehicle is consequently believed to be within the capability of the aviation industry at the present time.

The propulsion systems for a vehicle of this type are next to be considered. The propulsion systems discussed are limited to the conventional ramjet type of engine. Other engine types are under study by various organizations throughout the United States; however, these other types are intended to operate either over a range of flight Mach numbers or at speeds substantially higher than a Mach number of 6.

Figure 8 presents a sketch of the propulsion unit under consideration. It consists of three principal parts: the hypersonic inlet, the subsonic combustion chamber, and the exhaust nozzle. Much research has yet to be done on the hypersonic propulsion unit. With regard to the inlet, in addition to the usual determinations of optimum configurations for missions of interest, questions and problems exist relative to the effects of boundary-layer cooling on the inlet performance, the method of handling the cooling, the design of structural and variable-geometry configurations, and the optimum compromises between boundary-layer bleed and total pressure recovery. Essentially no information is available on combustion chamber design, for example. Much information is needed on recombination rates for the gases flowing through the exhaust nozzle and the associated effects on exhaust-nozzle design requirements. The matter of the appropriate combination of special materials and cooling arrangement to be used for the diffuser, nozzle throat, and combustion chamber is under study. Recent research (ref. 3) by Connors and Obery of the NASA Lewis Research Center indicated that the heat-transfer rate at the nozzle throat of a ramjet engine would need to be about 400 Btu per square foot per second in order to maintain a wall temperature of 1,500° F. This cooling rate is approximately one-fourth that being sustained in rocket engines for short duration; therefore, Connors and Obery concluded that it should be possible to cool ramjet engines for indefinite periods of time. For the hypersonic ramjet engine to be really promising, a high-energy fuel with a large heat sink and no coking problems is required. Ordinary hydrocarbons do not fulfill these requirements and liquid hydrogen has many logistic disadvantages. However, all of these problems which have been listed appear to be subject to solution with sufficient investment in research and development.

The proportions of the exhaust nozzle indicated in figure 8 were determined from an analysis using real-gas Mollier diagrams (ref. 4) and three-dimensional characteristic computations for the external nacelle drag. The dimensions given apply to either hydrocarbon or hydrogen fuels because the proportions were nearly the same for the two fuels. The exit diameter of $1.3D_0$ corresponds to an underexpanded nozzle and represents the maximum thrust-minus-drag configurations. As the nozzle diameter is increased beyond this value, the external drag increases at a higher rate than the internal thrust. The ratio of nozzle exit to throat diameter corresponds to an area ratio of 13.8, an exit Mach number of 3.3, and an exit static-pressure ratio of about 2.0. Hypersonic ramjet engines have been designed in the industry for

internal pressures up to 500 pounds per square inch absolute; therefore, the combustion-chamber stagnation pressure of 98 pounds per square inch absolute for this unit should incur no additional structural problems. The inlet stagnation temperature of 2,600° F and the combustion temperature of 4,800° F will pose cooling problems and special materials, and perhaps regenerative cooling will be required. In this regard liquid hydrogen possesses ideal cooling properties and studies have shown that liquid hydrogen will provide sufficient cooling up to Mach numbers of 8 or perhaps 9. Other fuels such as frozen methane also offer possible solutions.

In relation to the hypersonic-inlet problem, figure 9 contains sketches of two inlet types which are under active consideration. The sketch at the left of the figure represents a three-dimensional all-external-compression spike-type inlet. The spike consists of a conical tip followed by an isentropic compression surface, and boundary-layer bleed may or may not be used on the shoulder. Because of the local flow inclination the cowl lip may be set at a fairly high angle to avoid a strong reflected shock. This design will incur appreciable external drag and the thin annular throat may be subject to special structural and cooling problems. The great advantage of this inlet is that no variable geometry is required because no appreciable amount of internal compression occurs. The sketch in the right-hand half of the figure represents the same general type of inlet; however, the high cowling drag has been eliminated by reducing the external compression and substituting internal compression. This effort to attain increased thrust minus drag results in a variable geometry requirement for starting the inlet. The United Aircraft Corporation has investigated both of these inlet types (refs. 5 and 6) and the NASA Lewis Research Center has tested the all-external-compression inlet (ref. 7). Some representative data on these inlet types and on two-dimensional research inlets are presented in figure 10.

Total pressure recovery is given as a function of free-stream Mach number in figure 10, and curves of constant inlet kinetic energy efficiency based on real air computations are superimposed on the plot. The key in this figure indicates the source of the data: The United Aircraft Corporation data (labeled UAC) are from references 5 and 6. The Langley data are from an unpublished work by John R. Henry, Lowell E. Hasel, and Ernest A. Mackley of the Langley Research Center, which was presented at a classified session of the SAE National Aeronautical Meeting (New York) in April 1960. The Lewis data are from references 7, 8, 9, and an unpublished investigation conducted by L. E. Stitt and D. L. Chubb at the Lewis Research Center.

The type of inlet ranging from all-external to all-internal compression is listed and whether or not the flow field is two dimensional (2-D) or three dimensional (3-D). The solid symbols are for fixed-geometry

inlets and the flagged symbols represent inlets with no boundary-layer bleed. For the cases with bleed, the measured recoveries were reduced by an amount appropriate to the excess drag associated with the bleed flow in order to obtain a true comparison between data with and without boundary-layer bleed. This adjustment to the data was accomplished on an equal thrust-minus-drag basis. The principal conclusion to be drawn from this figure is that inasmuch as the bulk of the data correspond to kinetic-energy efficiencies of 92 percent or higher, an assumption of 92 percent for computations of net thrust, range, and performance is very reasonable.

The engine-nacelle net-thrust coefficient based on capture area is presented in figure 11 as a function of inlet-kinetic-energy efficiency for stoichiometric mixtures of hydrogen and hydrocarbon fuels. The drag component of the net-thrust coefficient includes both the pressure drag and friction drag for fully turbulent flow on the external surface of the axisymmetric nacelle. In addition, the drag coefficient was increased by 0.05 as an allowance for a drag increment due to the rounding of the cowl leading edge in order to maintain a temperature of 2,000° F or less. Mollier diagrams for real air and gases were used in making the computations (ref. 4). No attempt was made to determine optimum cruise equivalence ratios; however, other studies have shown that the optimum values are probably somewhat less than the value of 1 used in this analysis. A nozzle-kinetic-energy efficiency of 0.975 was assumed in the computations. The ticks and numbers appearing on the two curves give the values of specific fuel consumption associated with the particular thrust coefficients.

The primary purpose of this figure is to show the general level of thrust coefficient and specific fuel consumption obtainable for each of the fuels at the inlet-kinetic-energy efficiency of interest, 92 percent. The thrust coefficient for hydrogen is 0.98 which is only 11 percent higher than the value for hydrocarbon fuel of 0.88; however, the specific fuel consumption of 1.15 for hydrogen is only 38 percent of the value of 3.05 for the hydrocarbon fuel. This advantage of hydrogen, of course, is offset to some extent by its low-density high-storage volume requirements.

The values for the aerodynamic characteristics of hypersonic configurations which have been presented earlier herein have been combined with the propulsion unit-performance values just presented to give the range-payload-mission potentialities. The ranges have been computed by using the Breguet range equation and do not include increments of range obtained during the boosted portion of the flight or the glide letdown at the end of the mission. The unit hardware weights used are consistent with previous work on hypersonic glide vehicles and with industry studies on hypersonic cruise vehicles.

The results of these performance computations are given in figure 12 which presents range in nautical miles as a function of payload for assumed gross weights of 200,000 and 250,000 pounds for both hydrogen and hydrocarbon fuels. The curves shown should be regarded as approximate indications of the level of performance obtainable, inasmuch as no detailed design work has been done on these configurations. It should also be noted that the weight of the solid propellant booster required to lift these vehicles to a design cruise speed of Mach number 6 at an altitude of approximately 80,000 to 100,000 feet is roughly twice the weight of the vehicle itself, so that for the 200,000-pound machine, the gross take-off weight of the cruise vehicle and its booster would be about 600,000 pounds. This booster weight could be cut in half by boosting only to a Mach number of 3.0 and paying the weight penalty of the variable-geometry inlet required to make the ramjet self-accelerating. The booster weight could also be reduced by about one-half by incorporating an all-liquid system and using liquid hydrogen as fuel.

The hydrogen fuel provides approximately 30 percent more range than the hydrocarbon fuel over the entire range of these calculations. This result shows that the low specific fuel consumption of hydrogen has outweighed the adverse effect of high-volume storage requirements on the aerodynamic characteristics of the vehicle; however, it cannot be concluded that hydrogen is best because of the many logistics problems involved for military applications. Military missions of roughly 10,000 nautical miles and 25,000 pounds of payload are of considerable interest and the curves clearly show that this type of mission is obtainable with a boosted hypersonic cruise vehicle. Smaller ranges and payloads such as those applicable to reconnaissance missions could be accomplished with much smaller gross weights than have been indicated here. It is possible that these smaller vehicles could be launched from a recoverable booster such as has been under study for Dyna-Soar and other space missions.

CONCLUSIONS

It is recognized that there are many problem areas for a hypersonic cruise vehicle which will require intensive research for satisfactory solutions; however, it appears that:

1. The state of the art is such that lift-drag ratios of sufficient magnitude to give satisfactory range can be obtained.

2. The thermodynamics of the propulsion units yield values of propulsive efficiency which, when coupled with the aerodynamic efficiency,

indicate desirable range-payload possibilities. Unfortunately research data on the materials and cooling methods for this engine are not well documented.

3. The aerodynamic heating of the vehicle is low enough to allow construction of such a vehicle within the present capability of the aviation industry.

REFERENCES

1. Armstrong, William O., and Ladson, Charles L. (With Appendix A by Donald L. Baradell and Thomas A. Blackstock): Effects of Variation in Body Orientation and Wing and Body Geometry on Lift-Drag Characteristics of a Series of Wing-Body Combinations at Mach Numbers From 3 to 18. NASA TM X-73, 1959.

2. Rainey, Robert W., Fetterman, David E. Jr., and Smith, Robert: Summary of the Static Stability and Control Results of a Hypersonic Glider Investigation. NASA TM X-277, 1960.

3. Connors, James F., and Obery, Leonard J.: Some Considerations of Hypersonic Inlets. Paper presented at 4th AGARD Combustion and Propulsion Colloquium on High Mach Number Air-Breathing Engines (Milan, Italy), Apr. 1960.

4. Hall, Eldon W., and Weber, Richard J.: Tables and Charts for Thermodynamic Calculations Involving Air and Fuels Containing Boron, Carbon, Hydrogen, and Oxygen. NACA RM E56B27, 1956.

5. Kepler, C. Edward: Performance of a Mach 4.0 Variable-Geometry Axisymmetric Inlet Having External-Plus-Internal Compression. Rep. R-1285-12 (Contract NOa(s) 55-133-c), United Aircraft Corp., Sept. 1959.

6. McLafferty, George H.: Hypersonic Inlet Studies at UAC Research Laboratories. Rep. M-2000-113, United Aircraft Corp., Dec. 1959.

7. Stitt, Leonard E., and Flaherty, Richard J.: Experimental Investigation of a Mach 5 Isentropic Spike at and Below Design Speed. NASA TM X-4, 1959.

8. Connors, James F., and Anderson, Leverett A., Jr.: Performance of an Axisymmetric External-Compression and a Two-Dimensional External-Internal-Compression Inlet at Mach 4.95. NASA Memo 12-18-58E, 1959.

9. Connors, James F., and Allen, John L.: Survey of Supersonic Inlets for High Mach Number Applications. NACA RM E58A20, 1958.

HIGH-FUEL-DENSITY MODEL

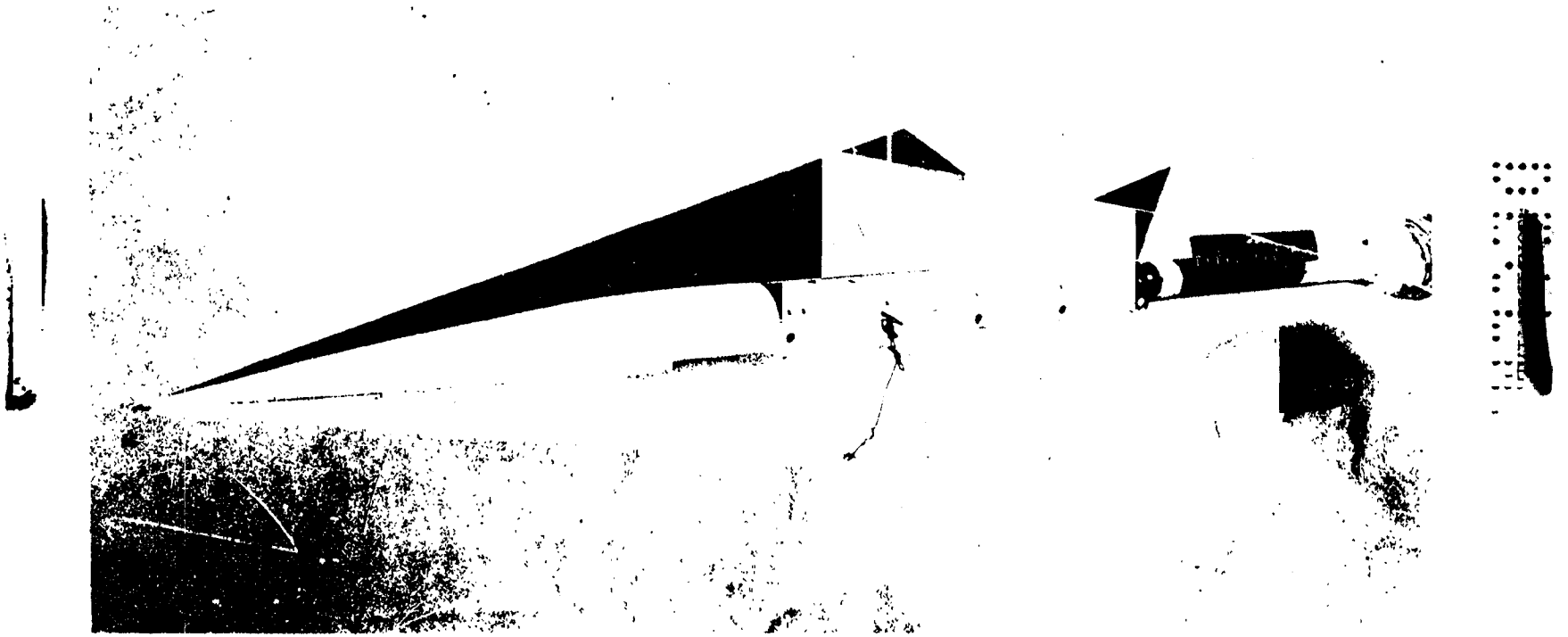

Figure 1

L-60-3035.S

LOW-FUEL-DENSITY MODEL

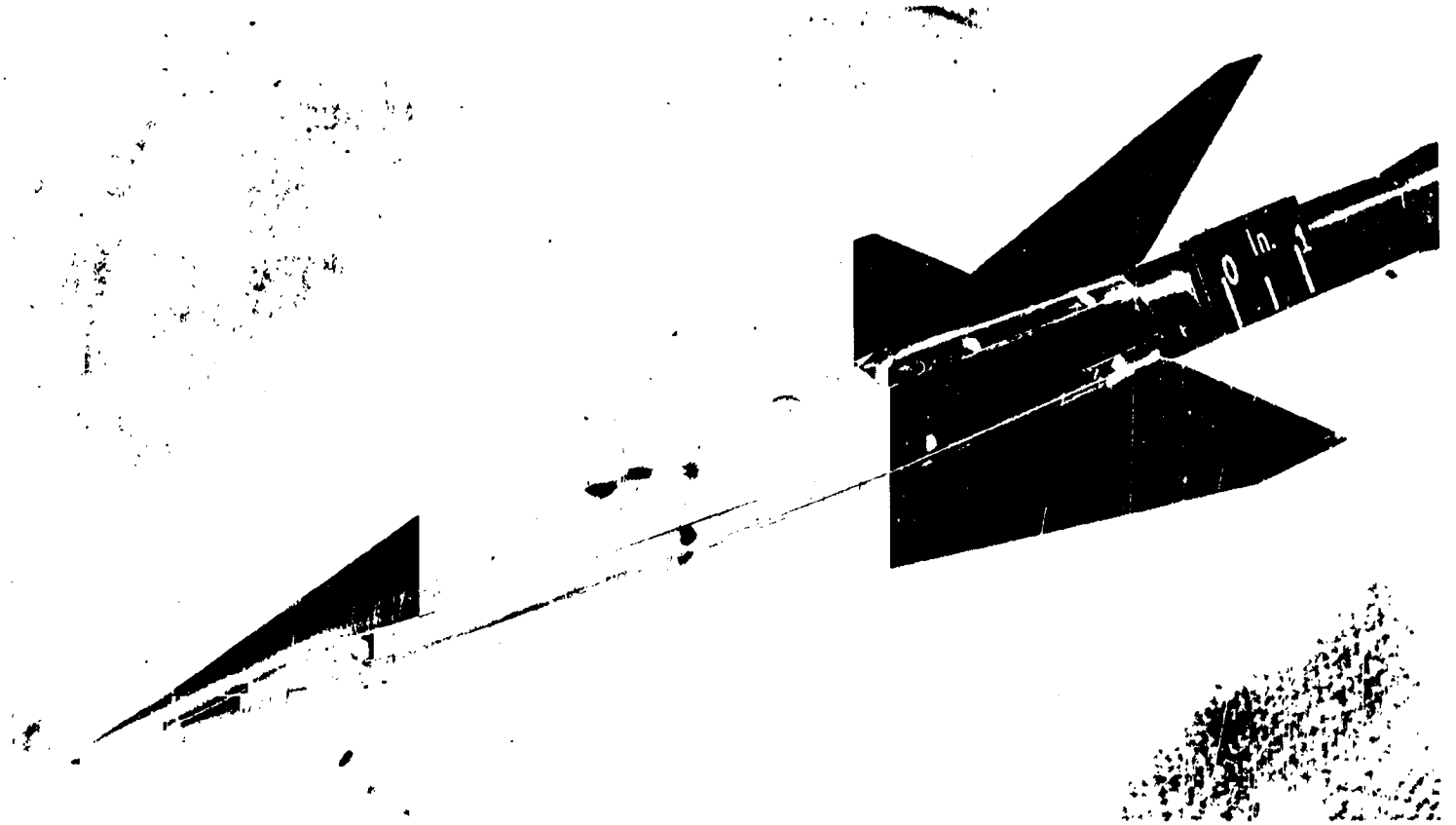

Figure 2

L-60-4267.S

EFFECT OF BOATTAIL ANGLE ON AFTERBODY DRAG

WING TRAILING EDGE;
M = 6.0, TURBULENT FLOW

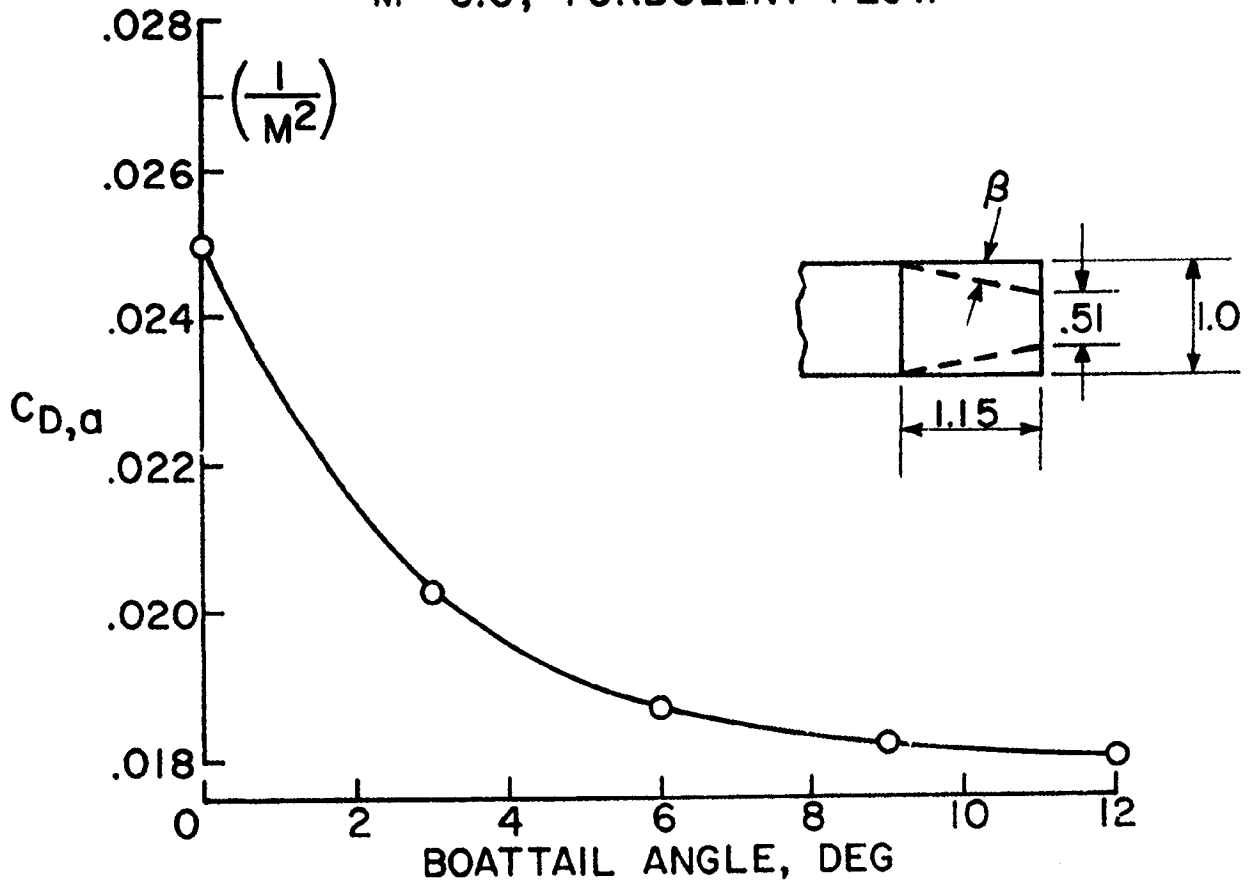

Figure 3

AERODYNAMIC CHARACTERISTICS OF HIGH-DENSITY MODEL

UNTRIMMED - NO VERTICAL TAIL; M = 4.63; R = 7×10^6 BASED ON MAC

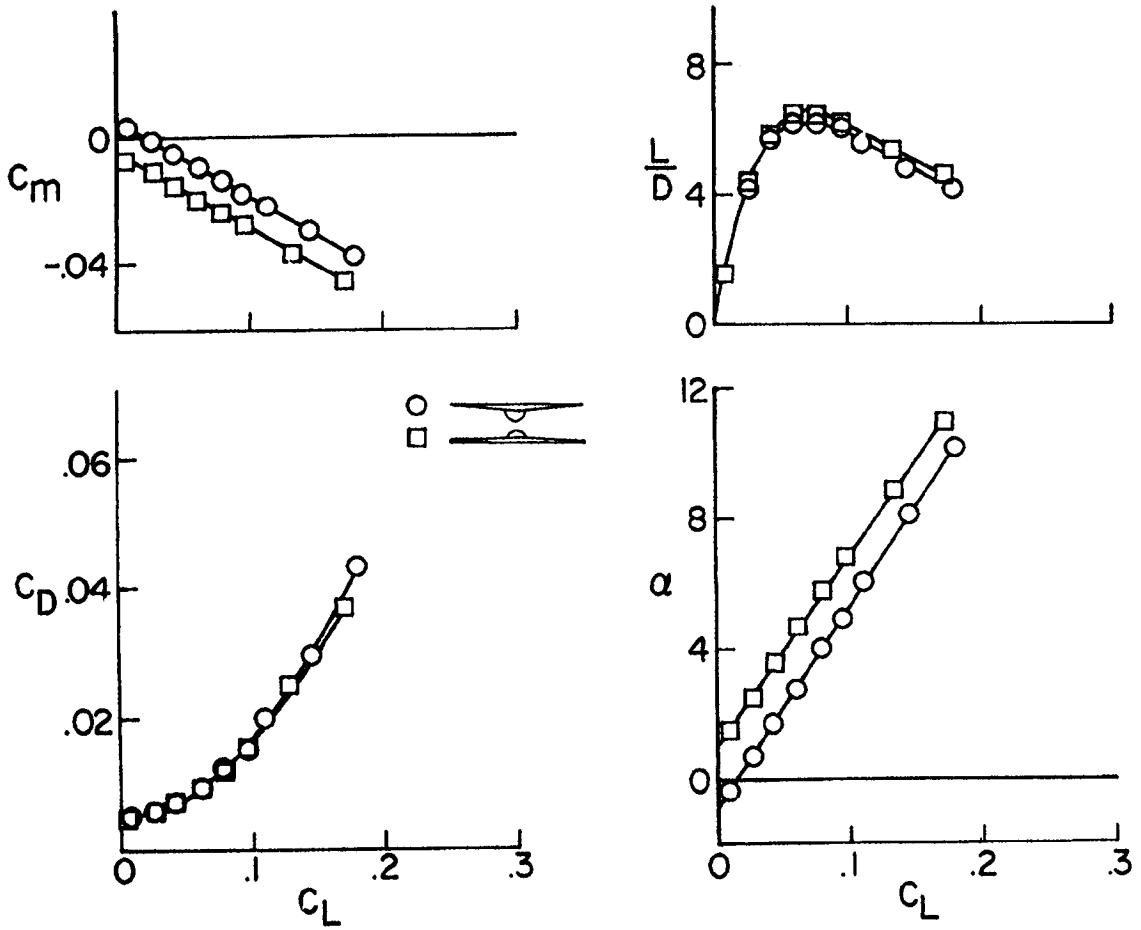

Figure 4

AERODYNAMIC CHARACTERISTICS OF HIGH-DENSITY MODEL

UNTRIMMED; M = 0.25; R = 2.5×10^6 BASED ON MAC

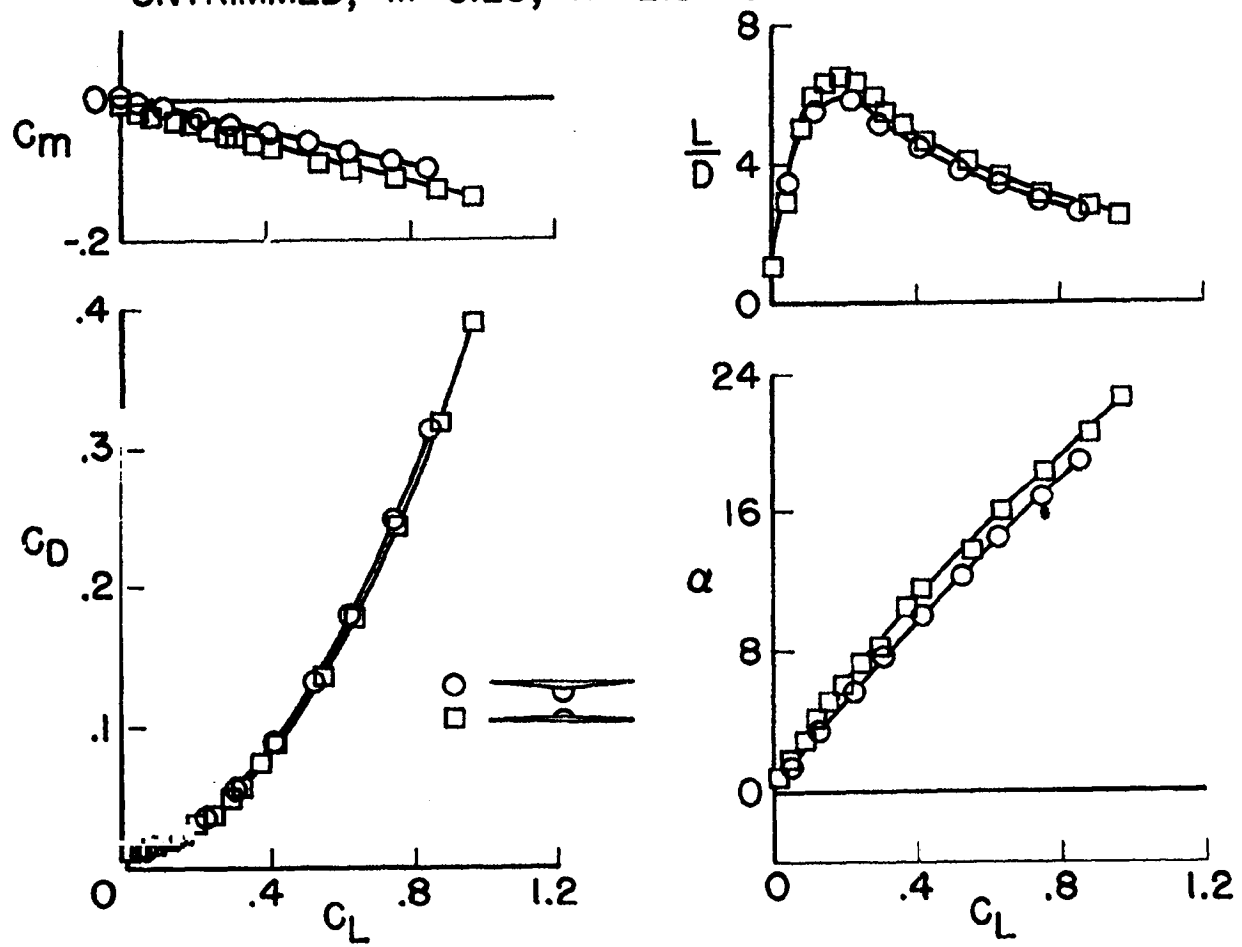

Figure 5

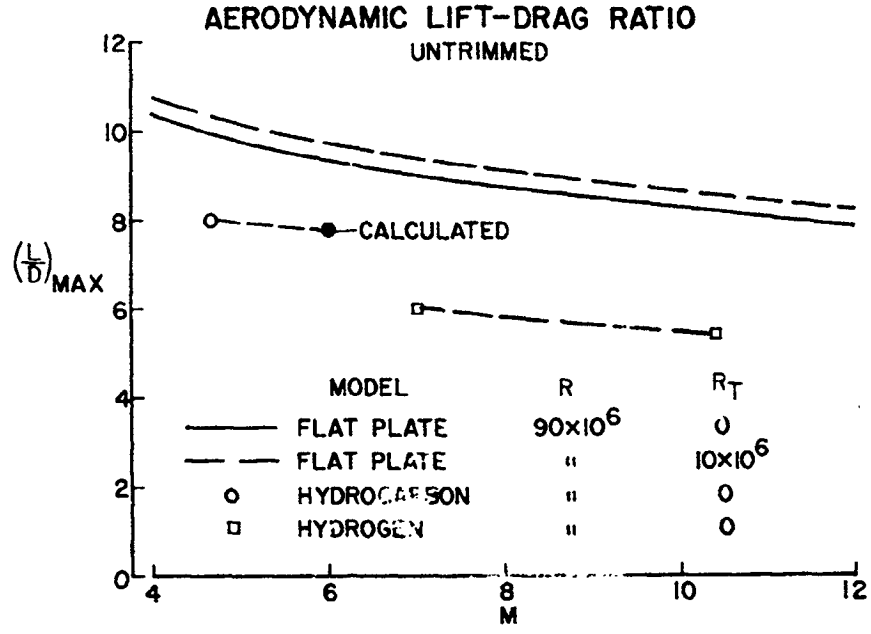

Figure 6

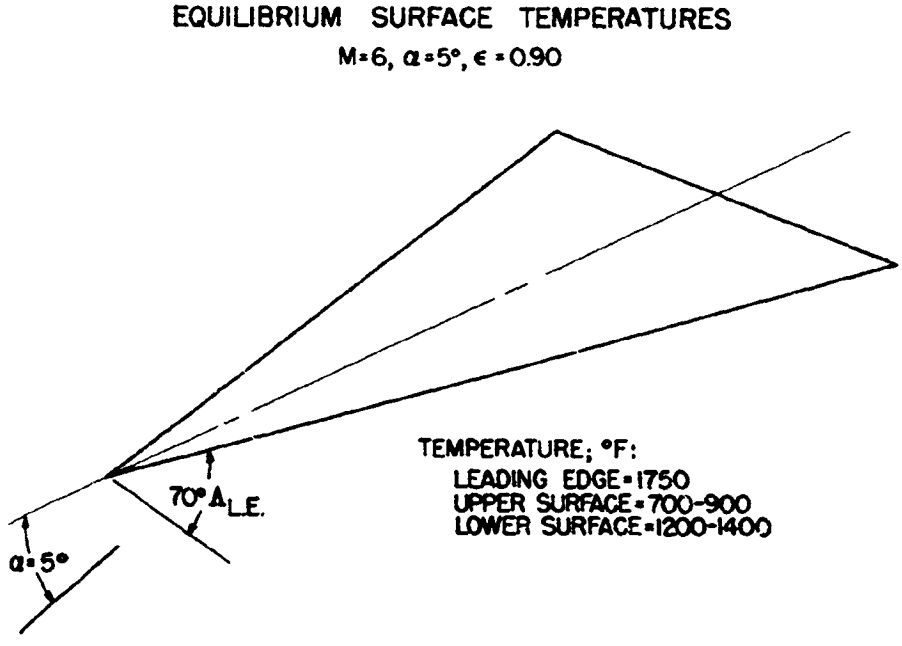

Figure 7

DIAGRAM OF PROPULSION SYSTEM
M=6.0

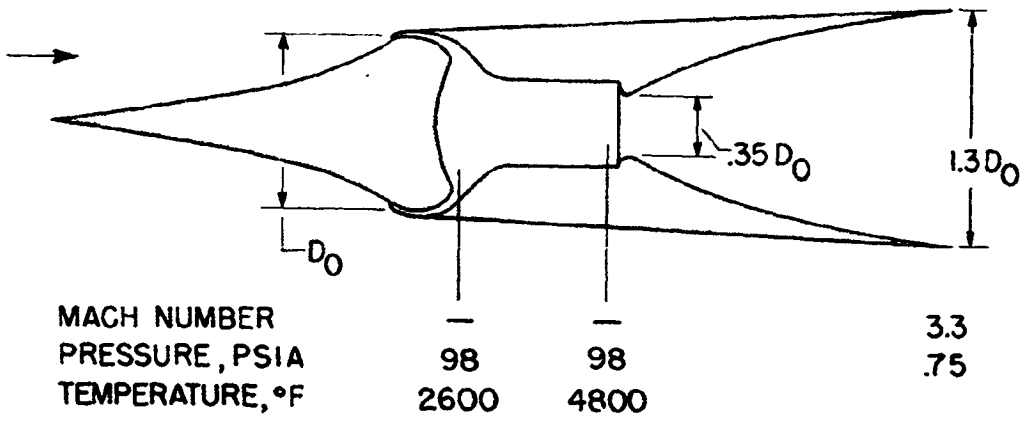

Figure 8

HYPERSONIC INLET DESIGNS

SPIKE-EXTERNAL

SPIKE-EXTERNAL-INTERNAL

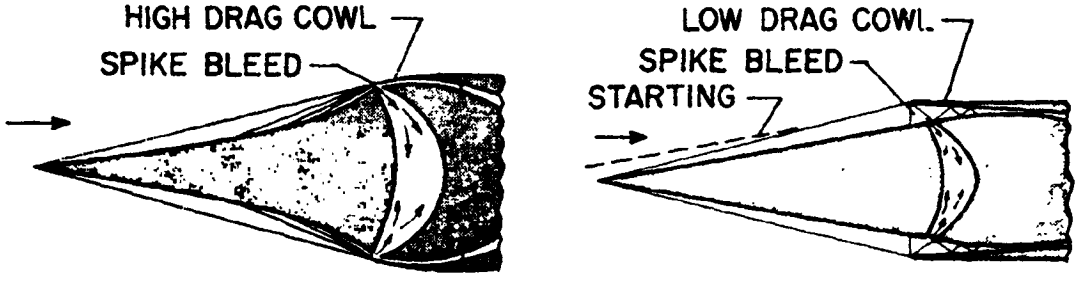

Figure 9

HYPERSONIC INLET DATA ADJUSTED FOR BLEED DRAG

FILLED SYMBOLS, FIXED GEOMETRY INLETS
FLAGGED SYMBOLS, NO BOUNDARY-LAYER BLEED

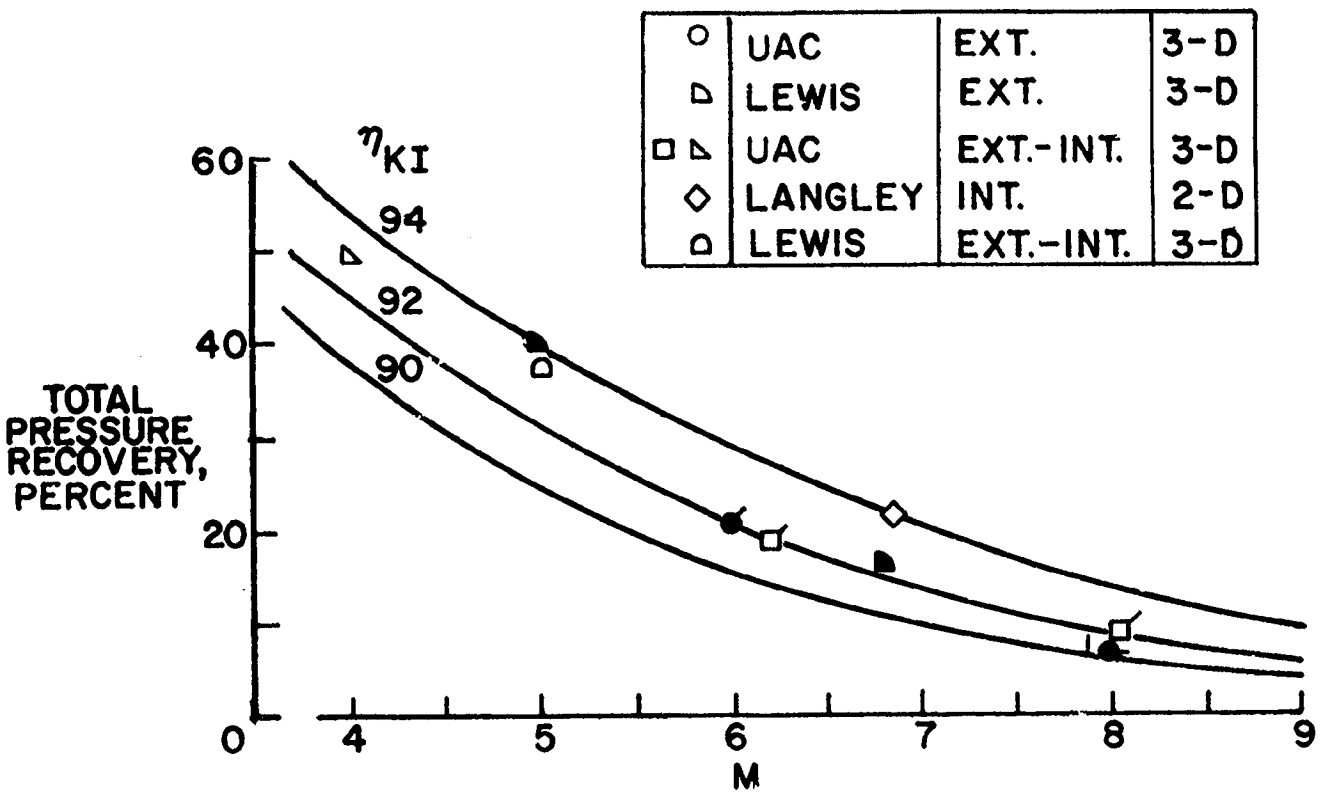

Figure 10

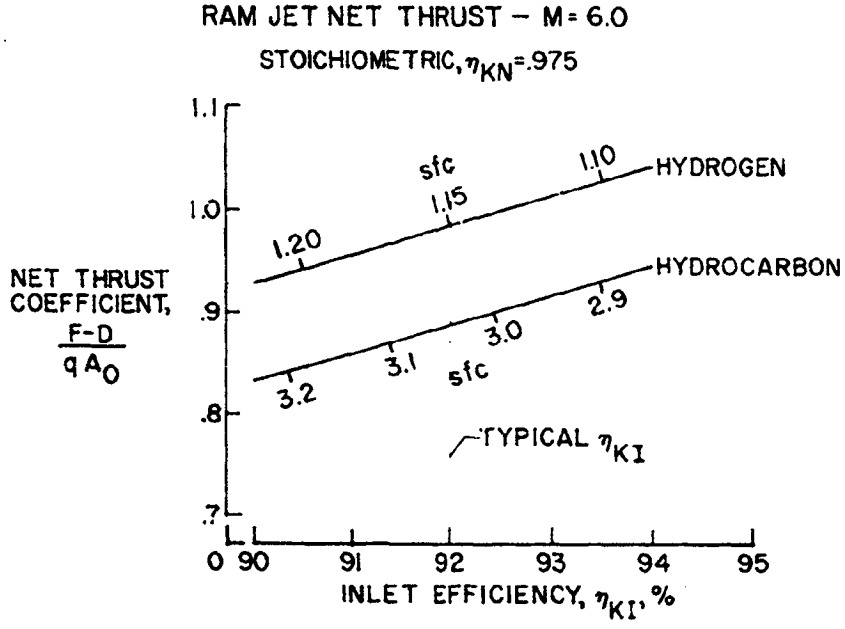

Figure 11

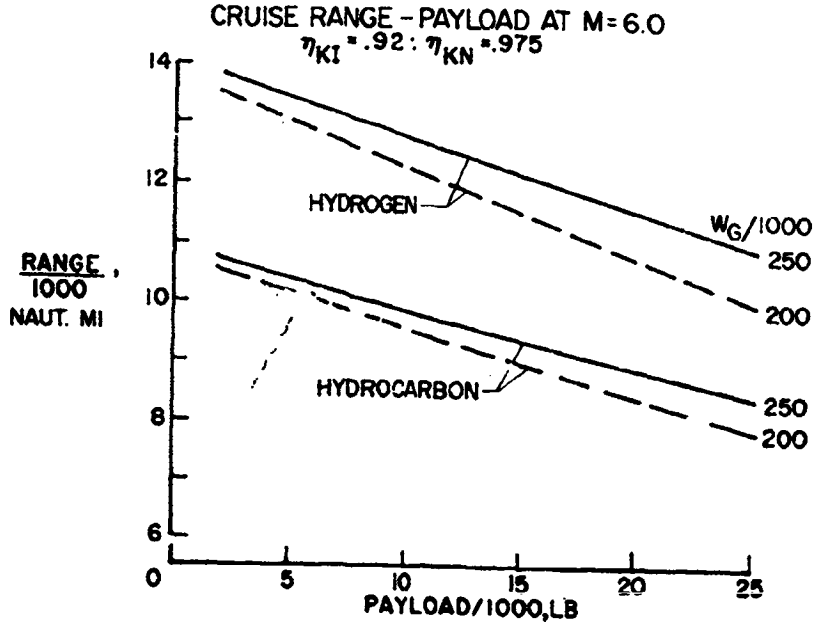

Figure 12

VII. SOME STRUCTURAL AND MATERIALS CONSIDERATIONS FOR MANNED MILITARY AIRCRAFT

By Eldon E. Mathauser, Richard A. Pride, and Avraham Berkovits

Langley Research Center

INTRODUCTION

The design of lightweight, efficient structures is one of the fundamental requirements for achievement of high performance in military aircraft. In this paper some of the structural and materials considerations that are important to the strength, weight, and integrity of aircraft structures are reviewed. A comparison of some structural materials is made on the basis of weight-strength and tear resistance. In the area of structural design, the relative weights of several types of construction that are of current interest are reviewed and the influence of different materials and the effects of elevated temperatures on structural weight are indicated. Lastly, other factors that are of importance in structural design of future aircraft are discussed. These include strength under nonuniform temperatures, creep, sonic fatigue, and panel flutter.

MATERIALS

Weight-Strength Comparison

The relative efficiency of structural materials is frequently determined on a weight-strength basis by use of plots of the type shown in figure 1. Relative weight is plotted against temperature for 7075-T6 aluminum alloy, 6Al-4V titanium alloy, PH 15-7 Mo stainless steel, René 41 nickel alloy, and a material of considerable structural interest, beryllium. This comparison is made on the basis of density and ultimate tensile strength and provides a means for selection of minimum-weight tensile members. For the selection of members under compressive loading, material properties such as Young's modulus and yield strength would be utilized.

Note that the stainless steel and the titanium alloy are either competitive or superior weightwise to the aluminum alloy at room temperature and that relatively little weight increase is obtained with these two materials for temperatures up to 600° F or 700° F. At

higher temperatures, a change to nickel alloy materials, such as René 41, appears desirable in order to conserve weight.

Weight-strength considerations such as these are of interest in the selection of structural materials; however, other factors are becoming increasingly important.

Tear Resistance

Tear resistance is of concern for transport-type aircraft because of the possibility of catastrophic failures of aircraft in service. It is expected to be of concern when high-strength, thin-gage sheet materials are used in the structure.

The tear resistance of some structural materials is presented in figure 2. (See ref. 1.) The average- or gross-area failure stress σ_f for sheet containing a crack, divided by the ultimate tensile strength of the material σ_{ULT}, is plotted against the ratio x/b, where x is the crack length and b is the plate width. The line labeled "completely ductile" represents a material that is completely insensitive to the presence of a crack. Among the materials shown here, 6061-T4 aluminum alloy indicates the best tear resistance and 420 stainless steel the poorest. Note that several high-strength steels are superior on this basis to the 2024-T3 and 7075-T6 aluminum alloys in current use.

Data on tear resistance are not available for many of the structural materials of interest; and in some cases, the data cover only a small range as shown, for example, for the PH 15-7 Mo stainless steel and 6Al-4V titanium alloy. Furthermore, very little elevated-temperature data of this type are available. General agreement does not exist as to the significance of this type of information, although it is recognized that structural sheet should resist tearing either from cracks that develop slowly from fatigue or suddenly from penetration by foreign objects. Continuing efforts should be made to identify tear-resistant structural materials at low and elevated temperatures, to standardize test methods, and to establish the significance of this type of data in structural design.

STRUCTURAL DESIGN

Type of Construction

Consideration is next given to structural design. Three types of construction that may be of particular interest for aircraft wings are

[redacted]

shown in figure 3. The view on the left indicates honeycomb-sandwich construction in which the sandwich panels are fabricated either by adhesive bonding for use at relatively low temperatures or by brazing for applications at higher temperatures. Construction utilizing an open-face sandwich panel is indicated in the view in the center. This sandwich panel consists of a single corrugated sheet welded to a face sheet and includes transverse stiffeners attached to the corrugated sheet. The view on the right shows a stiffened panel type of construction utilizing hat-section stiffeners that are either welded or riveted to the face sheet. In all three types of construction the longitudinal webs are corrugated and in the stiffened-panel design the transverse ribs are also corrugated. Corrugated webs and ribs would alleviate thermal stresses that are produced by differences between the temperatures of the upper and lower wing surfaces. All of these designs are characterized by thin-gage sheet and generally close spacing of the supports. These designs also reflect fabrication complexity that is coupled with high cost, particularly for the brazed honeycomb-sandwich type of construction. The relative weights of these types of construction will be examined.

In figure 4 the relative weights of the three types of idealized wing constructions investigated are plotted against the structural or loading index. The weight, divided by the square root of the bending moment, is plotted against the bending moment divided by the square of the wing depth. The honeycomb-sandwich wing indicates the least weight, the minimum weight of the stiffened-panel wing is 15 percent greater, and that of the open-face sandwich wing 35 percent greater. It is significant to note that for a given bending moment the minimum-weight stiffened-panel and open-face-sandwich designs are associated with thinner wings than the minimum-weight honeycomb-sandwich design. In this plot wing designs representative of some of the current high-performance fighters appear at values of the loading index greater than 1.0, where weight is not sensitive to the type of construction but is rather directly dependent upon the yield strength of the material. The wing design of a proposed supersonic bomber falls in the loading-index range between 0.1 and 1.0 where the curves indicate a minimum weight.

The relative weights indicated in figure 4 do not include the weights of attachments between webs and cover panels and do not include the weights of the brazing material and reinforcements that are required with honeycomb-sandwich construction. Some of the indicated weight advantage of the honeycomb-sandwich construction would be nullified by the addition of these weights.

Structural Materials

Next, the influence of structural materials upon structural weight is examined. This comparison is made in figure 5 for several structural

[redacted]

materials utilizing honeycomb-sandwich wing construction. The weight, divided by the square root of the bending moment, is again plotted against the bending moment divided by the square of the wing depth. Note that the aluminum-alloy and titanium-alloy designs are competitive weightwise, whereas the stainless-steel design is 40 percent heavier, and the nickel-alloy design is 75 percent heavier. The significant point in this comparison is that the most efficient aluminum-alloy wing has greater depth than the titanium-alloy or stainless-steel wing. This result is of particular interest because titanium-alloy and stainless-steel designs are generally associated with high-speed aircraft that require thin wings for high performance.

L
1
2
1
4

Elevated Temperatures

Consideration is given next to the effect of elevated temperatures on structural weight. The minimum weights corresponding to the lowest point on curves such as those shown in figure 5 have been obtained over a range of temperatures for the indicated materials. These minimum weights are shown in figure 6. The relative weight of honeycomb-sandwich wings is plotted against temperature. The results are based on materials data for 1,000 hours of exposure at temperature. These weight results suggest that aluminum-alloy construction would be satisfactory up to approximately 200° F, titanium alloy and stainless steel up to 700° F or 800° F, and René 41 up to 1,200° F or 1,300° F. Above these respective temperatures, which may be taken as limiting temperatures for long-time application, very rapid weight increases are obtained. Note that for each material shown only a modest weight change occurs between room temperature and the limiting temperature noted previously for long-time application. These weight changes are on the order of 10 to 20 percent. Greater differences exist between the wing weights at room temperature for some of the indicated materials.

These results on structural design have indicated relative weights of idealized wings for several materials over a range of temperatures. To date, this study has not been extended to cylindrical shells representative of fuselages over the complete range of materials and temperatures indicated in figure 6; however, results approximately similar to those presented would be expected from such an analysis.

OTHER FACTORS

Strength Under Nonuniform Temperatures

The weight comparisons presented in figures 4 to 6 have been obtained under the assumption that the temperature of the structure is

uniform. It is recognized that aircraft structures will be subjected to nonuniform temperatures in flight, and for this reason a brief discussion on the effects of nonuniform temperatures on structural strength is presented next. Experimental studies (refs. 2 and 3) generally indicate that maximum strength is independent of thermal stresses that are induced by nonuniform temperatures, whereas the load for buckling and permanent deformation is reduced by the presence of thermal stresses. Some pertinent results on sandwich plates are now examined (fig. 7). The average stress at maximum load σ_f is plotted against the average temperature $\bar{T}$ for 17-7 Ph stainless-steel corrugated-core sandwiches. The face sheets of these small sandwich specimens were heated to temperatures T_1 and T_2, and the specimens were then subjected to axial compressive loading to determine the crippling strength. Tests were made with temperature differences between the faces of 200° F, 400° F, and 600° F. The dashed-line curve indicates experimental strength of the sandwiches under uniform temperatures, and the solid-line curves are calculated strengths for the indicated face-temperature differences. The calculated curves were obtained from a summation of the strengths of the individual plate elements of the sandwich at the respective temperature of each element. Experimental data were obtained over the indicated temperature range and were in agreement with these calculated curves. These results indicate that thermal stresses did not influence the maximum strength. Although maximum strength was not influenced significantly by thermal stresses in these tests, the importance of thermal stresses in initiating undesirable deformation should not be overlooked. Each structural design will require detailed analysis to evaluate the effects of nonuniform temperatures and further studies with emphasis on design features that minimize thermal stresses but preserve structural strength and stiffness are of interest. An example of such a study is described in reference 4.

Creep

The problem of creep at elevated temperatures has attracted considerable attention during the past few years because of its assumed importance on structural design. Studies made by the NASA in the past have indicated little likelihood that creep will be a major problem. This conclusion was based on both analysis and upon experimental data obtained under constant load and constant temperatures.

This conclusion may be drawn from figure 8. The required weight of a tensile member is plotted against temperature for three structural materials. The solid-line curves indicate the weight required for strength based on ultimate load after 1,000 hours of exposure to temperature. Ultimate load is assumed to be 3.75 times the 1 g load. The

shaded regions define the temperature range for each material where creep may become a factor in structural design. The left boundary of each shaded area indicates the required weight for 0.02 percent creep strain in 1,000 hours at 1 g load and the right boundary, the required weight for creep rupture under the same load and time. Note that the temperature range where creep may become significant for each material is rather narrow. Furthermore, creep does not become a design consideration until temperatures are reached where the strength of the material deteriorates rapidly. It thus appears that when temperatures are encountered in which creep may become a problem, it will generally be necessary to convert to a material suitable for use at higher temper ture for strength reasons, and the creep problem will be eliminated.

Recent studies on structural assemblies utilizing varying loads representative of load-time relations for present fighters and bombers have again supported the conclusion that creep does not appear to be a major structural problem for aircraft. One note of caution is offered. These conclusions are based on relatively short-time results compared with the desired life of some aircraft, particularly transports. Some additional work to extend the experimental work into longer times may be of interest; however, it is believed such results will support the present conclusions.

Sonic Fatigue

In the area of acoustic fatigue, the underlying cause of structural difficulties is the use of increasingly powerful propulsion systems. Considerable effort has been made to obtain a better understanding of this problem and to improve the noise resistance capabilities of aircraft structures. Examples of some detailed design features that minimize noise-induced structural fatigue are presented herein. Methods for fastening the skin to the ribs to determine features that are resistant to sonic fatigue are first considered. In figure 9 are shown several skin-rib joints (ref. 5). The top row of numbers represents the fatigue life in minutes for these various joints at a 160-decibel noise level. The design shown at the right was also tested at a noise level of 170 decibels. The design on the left consists of a sheet and rib stiffener that failed in 17 minutes at the 160-decibel noise level. Addition of a doubler strip shown in the adjacent figure increased the noise fatigue life by a factor of approximately 10. The addition of a second rib stiffener to improve symmetry further increased the fatigue life. Finally, use of bonding rather than riveting to decrease stress concentrations resulted in still further increased fatigue life.

Another form of construction that has been used successfully for many high-intensity noise applications is the honeycomb-sandwich. In figure 10 a honeycomb-sandwich panel is shown at the top with possible

damage areas due to acoustic fatigue indicated. At the bottom are shown various possible schemes for attachment of these panels to the main structure. Fatigue damage may occur at the attachment points, in the bend radius of the edge-former of the panel, and in the bond between the core and face sheet or in the cell walls themselves. Among the different edge treatments indicated, the crushed cell walls are not satisfactory from the fatigue standpoint because the crushed cells are prone to fatigue cracks. Specimens fabricated with a formed doubler at the edge as shown in the upper right-hand view have survived for 50 hours at a noise level of 160 decibels. Other promising edge treatments for which results are as yet unavailable include the metal insert and the densified core.

This brief study of sonic fatigue has indicated some problem areas in structural design that will undoubtedly be of importance to future aircraft. In all probability the acoustic fatigue problem will become more severe as a result of use of high-strength, thin-gage materials, coupled with construction that will utilize large numbers of tiny weld joints that are potential sources for fatigue cracks. More detailed discussion of noise problems associated with manned aircraft is contained in chapter VIII of this volume.

Panel Flutter

Panel flutter has an important bearing on structural integrity. It is of particular importance for structural surfaces that are fabricated from thin sheets of high-strength, high-density materials that are designed to carry small structural loads.

The panel flutter problem will be examined in terms of some experimental information given in figure 11. (See refs. 4 and 6.) The panel-flutter parameter in the ordinate is a modified thickness-length ratio where t_{EFF} is an effective panel thickness, L is the panel length, M is the Mach number, E is Young's modulus for the panel material, and q is the dynamic pressure at flutter. The parameter on the abscissa is a length-width ratio where L is the panel length and B_{EFF} is the effective width of the panel. An envelope curve has been drawn to enclose the upper limits of more than 100 flutter tests on both flat and corrugation-stiffened panels. The flutter region lies below this envelope curve.

The purpose of figure 11 is to demonstrate the influence of corrugation orientation relative to the airflow on panel flutter. Two tests are singled out for consideration. Identical square panels fabricated from thin-gage sheet were tested in the Langley Unitary Plan wind tunnel. The panel shown at the lower right was mounted so that the airflow was perpendicular to the corrugation axis. Panel flutter developed during

the test and the model was destroyed. The second panel was mounted so that airflow was parallel to the axis of the corrugations and at the same dynamic pressure showed no indication of flutter. On the basis of this flutter parameter, a 20-fold increase in dynamic pressure would be required to move this test point into the flutter region.

The X-15 research airplane has corrugation-backed fairing panels along the sides of the fuselage with the corrugations perpendicular to the airflow. Wind-tunnel flutter tests of this fairing panel, shown by the test point indicated that flutter could occur within the operating range of the X-15.

Figure 12 shows the fairing panels on the X-15 as well as an enlarged view of the interior side of the panels. The panels consist of a flat outer sheet welded to an inner sheet that contains the corrugations. Indications of flutter were obtained in flight tests. This flutter has been stopped or at least considerably alleviated by the addition of a longitudinal stiffener riveted to the crests of the corrugations. It is of interest to note that fatigue cracks are developing in these particular panels. These fatigue cracks originate at holes that were drilled on the crest of each corrugation near the panel ends to relieve gas pressure during heat treatment. These fatigue cracks continue to develop subsequent to the addition of the transverse stiffener. In view of these flutter and fatigue difficulties, it is apparent that continued efforts are needed to obtain further insight into these problems and to define structural designs that are resistant to flutter and fatigue.

CONCLUDING REMARKS

Several structural and materials problems that are of interest for manned military aircraft have been reviewed and pertinent analytical and experimental results have been presented. Further efforts in these problem areas have been indicated in order to guarantee structural integrity and high performance in manned military aircraft of the future.

REFERENCES

1. Melcon, M. A.: A Survey of the Structural Properties of Some High Strength Sheet Steels. Rep. 101, AGARD North Atlantic Treaty Organization (Paris), Apr. 1957.

2. Zender, George W., and Pride, Richard A.: The Combinations of Thermal and Load Stresses for the Onset of Permanent Buckling in Plates. NACA TN 4053, 1957.

3. Pride, Richard A., and Hall, John B., Jr.: Transient Heating Effects on the Bending Strength of Integral Aluminum-Alloy Box Beams. NACA TN 4205, 1958.

4. Pride, Richard A., Royster, Dick M., and [illegible]ns, Bobbie F.: Experimental Study of a Hot Structure for a Reentry Vehicle. NASA TM X-314, 1960.

5. Edson, John R.: Review of Testing and Information on Sonic Fatigue. Structural Dev. Note No. 38 (Doc. No. D-17130), Boeing Airplane Co., Mar. 7, 1957.

6. Kordes, Eldon E., Tuovila, Weimer J., and Guy, Lawrence D.: Flutter Research on Skin Panels. NASA TN D-451, 1960.

WEIGHT-STRENGTH COMPARISON FOR STRUCTURAL MATERIALS

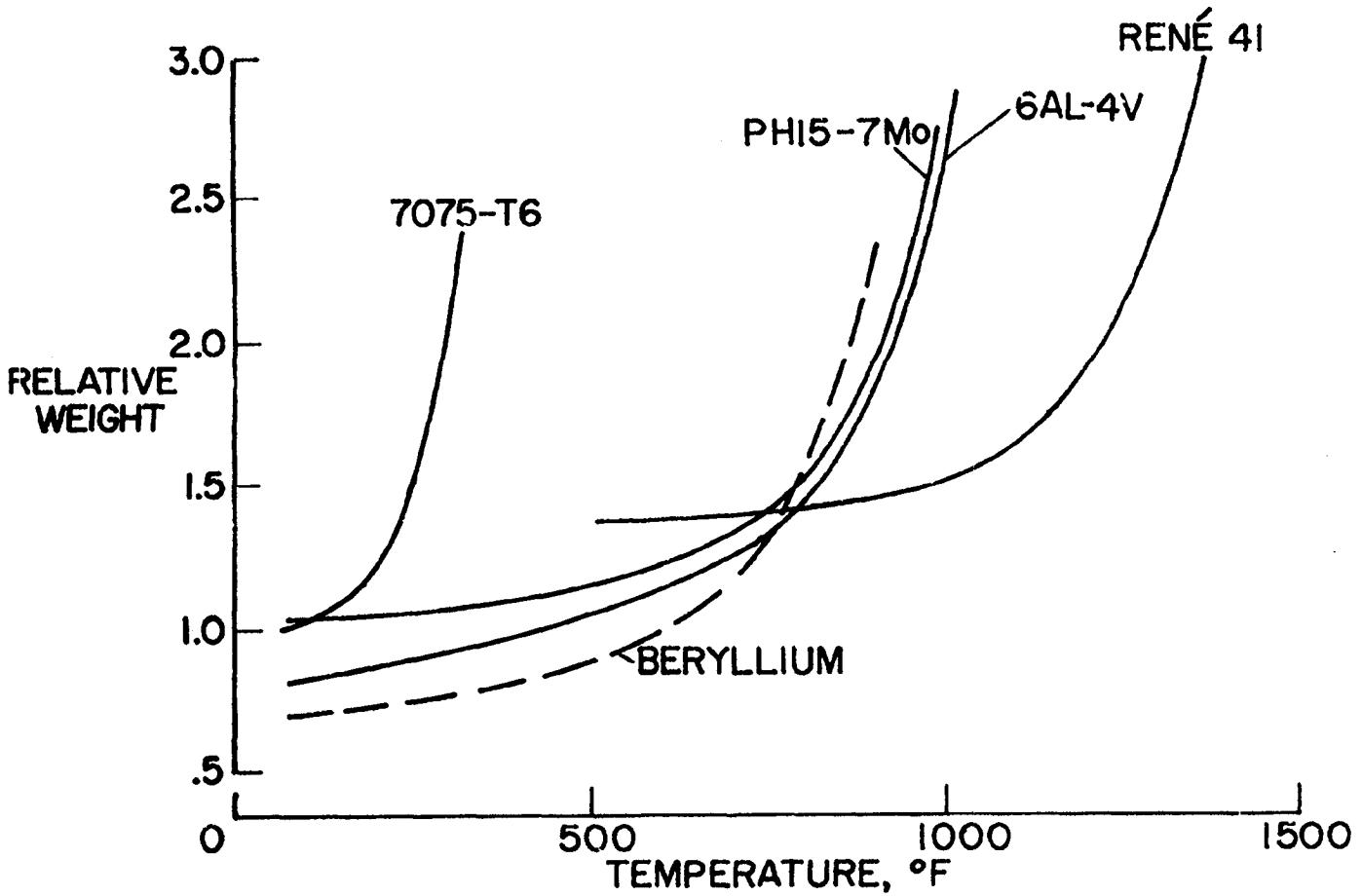

Figure 1

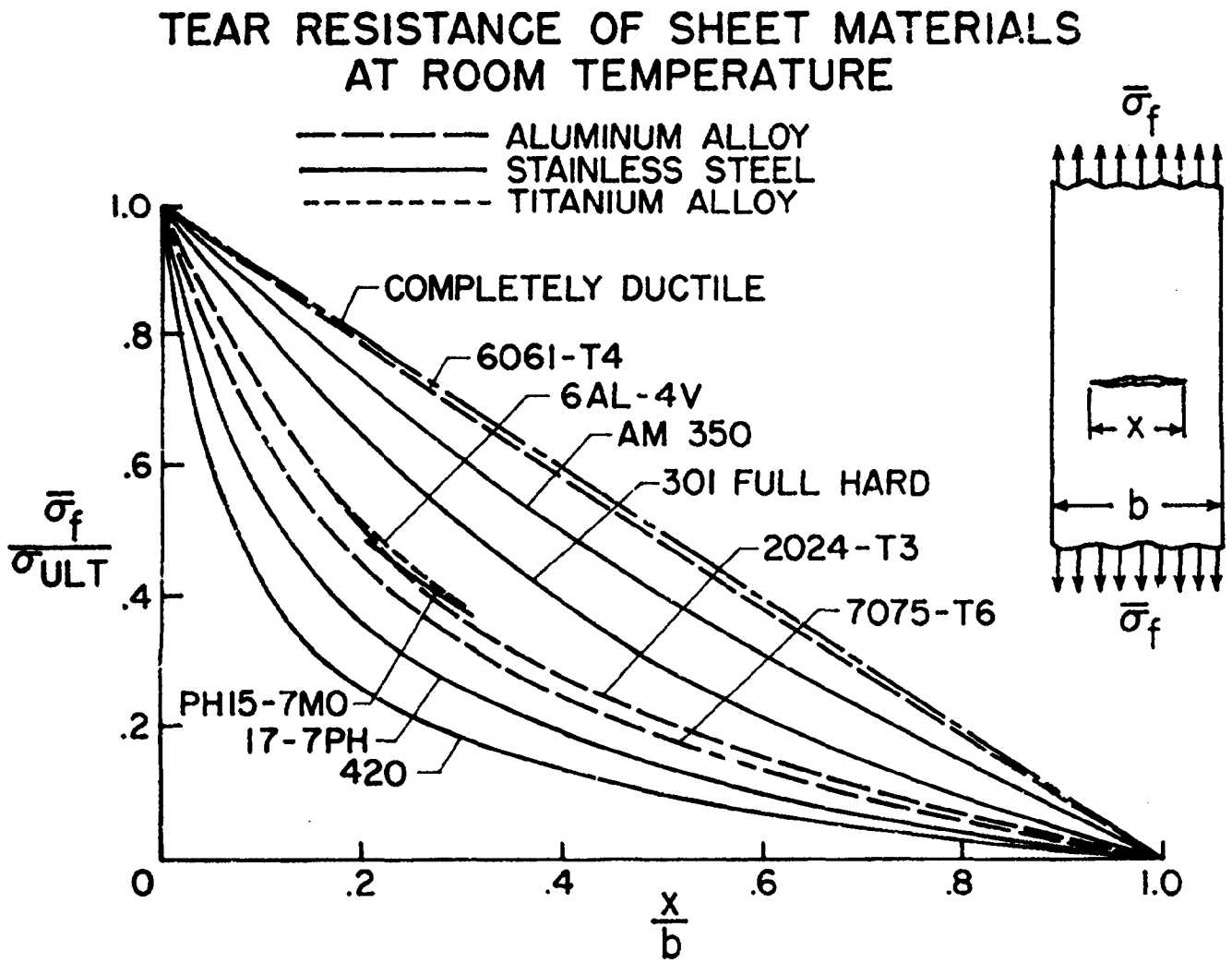
TEAR RESISTANCE OF SHEET MATERIALS
AT ROOM TEMPERATURE
ALUMINUM ALLOY
STAINLESS STEEL
TITANIUM ALLOY
COMPLETELY DUCTILE
6061-T4
6AL-4V
AM 350
301 FULL HARD
2024-T3
7075-T6
PH15-7MO
17-7PH
420
1.0
.8
.6
.4
.2
0
.2
.4
.6
.8
1.0
$\frac{\bar{\sigma}_f}{\sigma_{ULT}}$
$\frac{x}{b}$
$\bar{\sigma}_f$
x
b
$\bar{\sigma}_f$

Figure 2

TYPES OF WING CONSTRUCTION

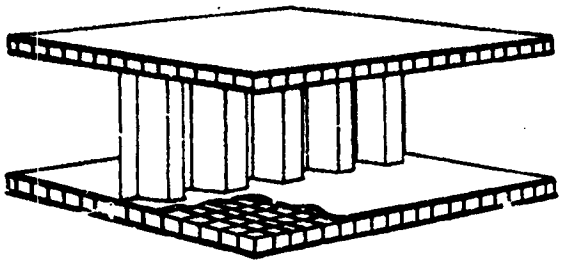

HONEYCOMB SANDWICH

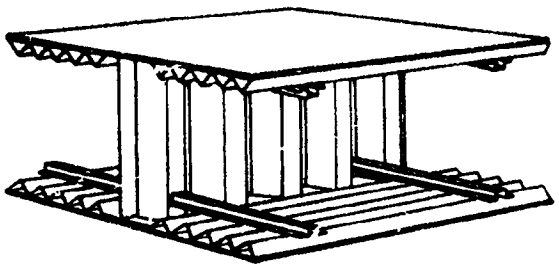

OPEN-FACE SANDWICH

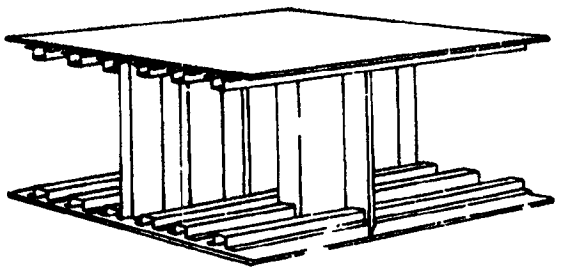

STIFFENED PANEL

Figure 3

WEIGHT COMPARISON FOR THREE TYPES OF WINGS

PH 15-7 MO STAINLESS STEEL, 75° F

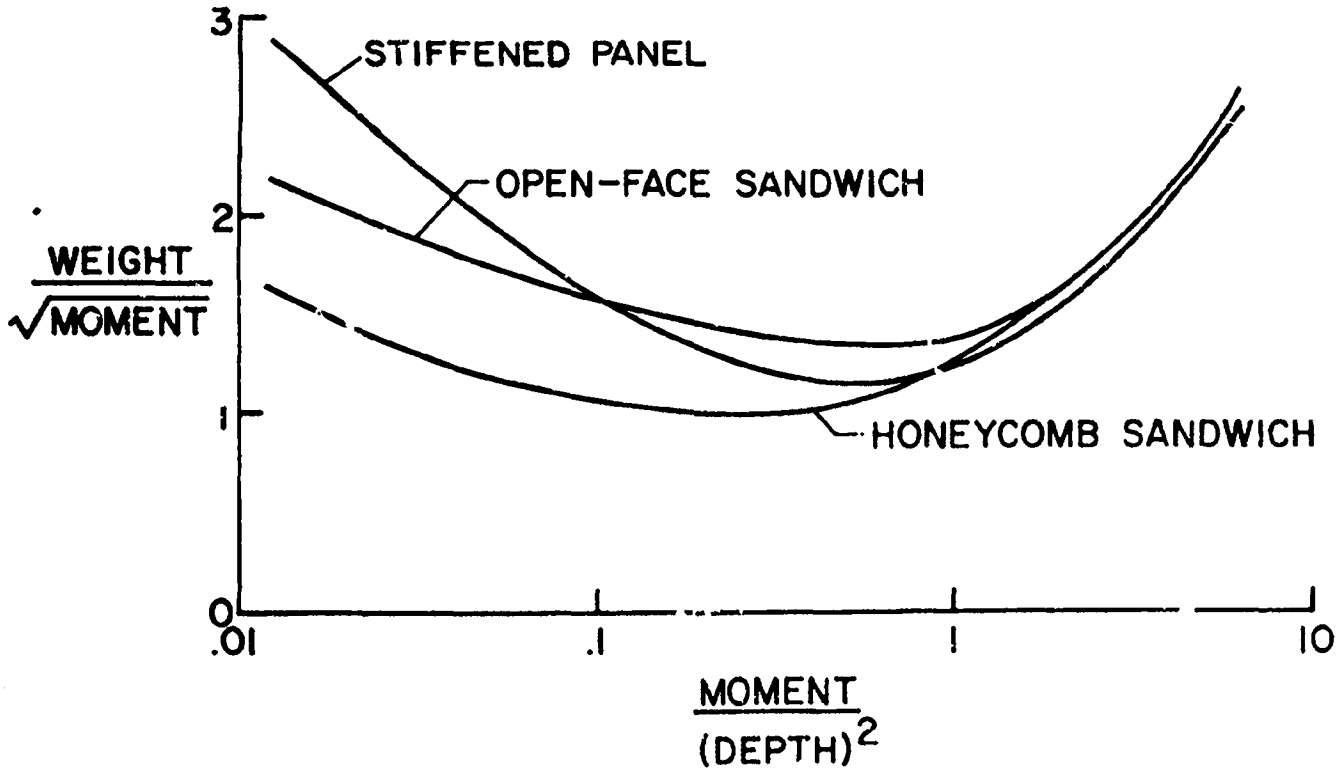

Figure 4

WEIGHT COMPARISON FOR HONEYCOMB-SANDWICH WINGS OF FOUR MATERIALS, 75° F

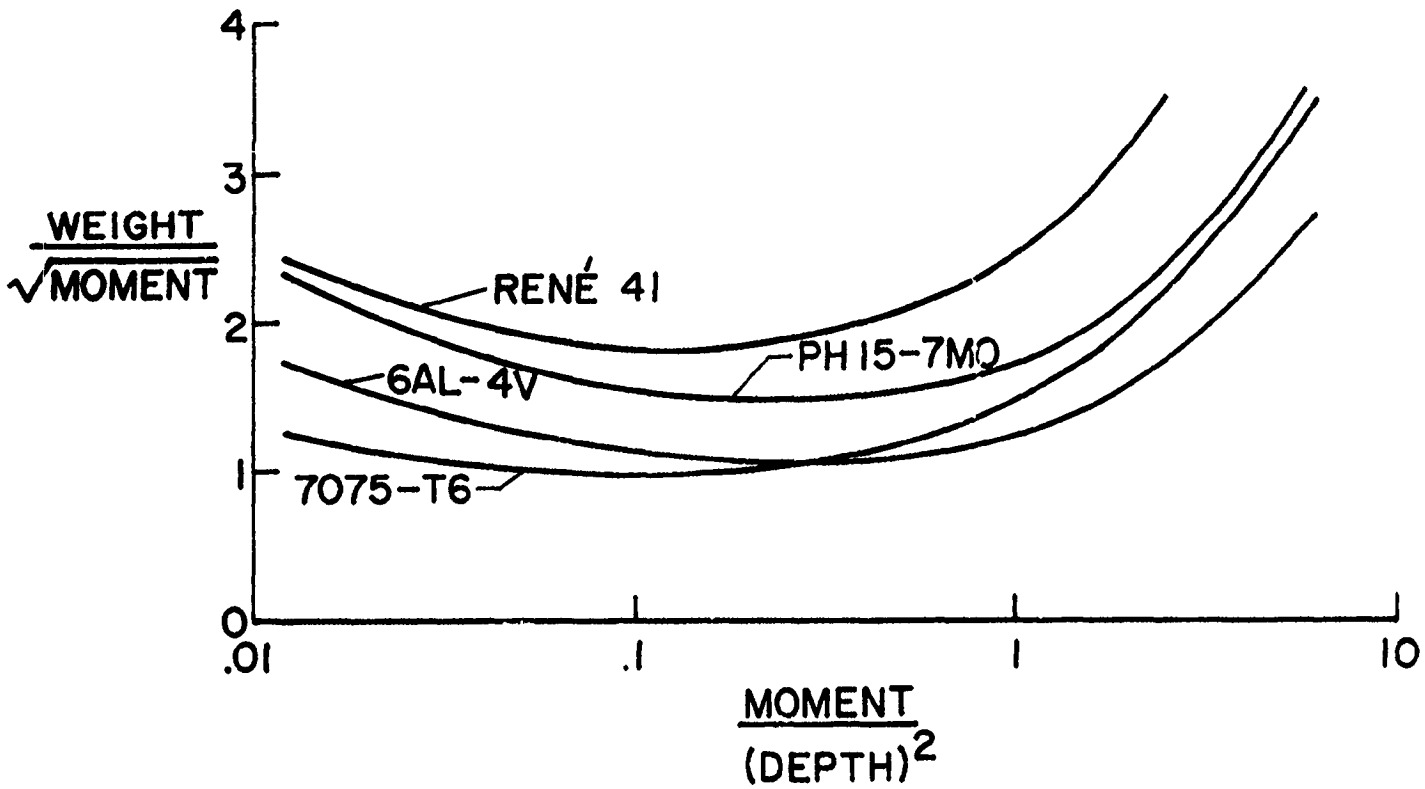

Figure 5

EFFECT OF ELEVATED TEMPERATURES ON MINIMUM WING WEIGHT

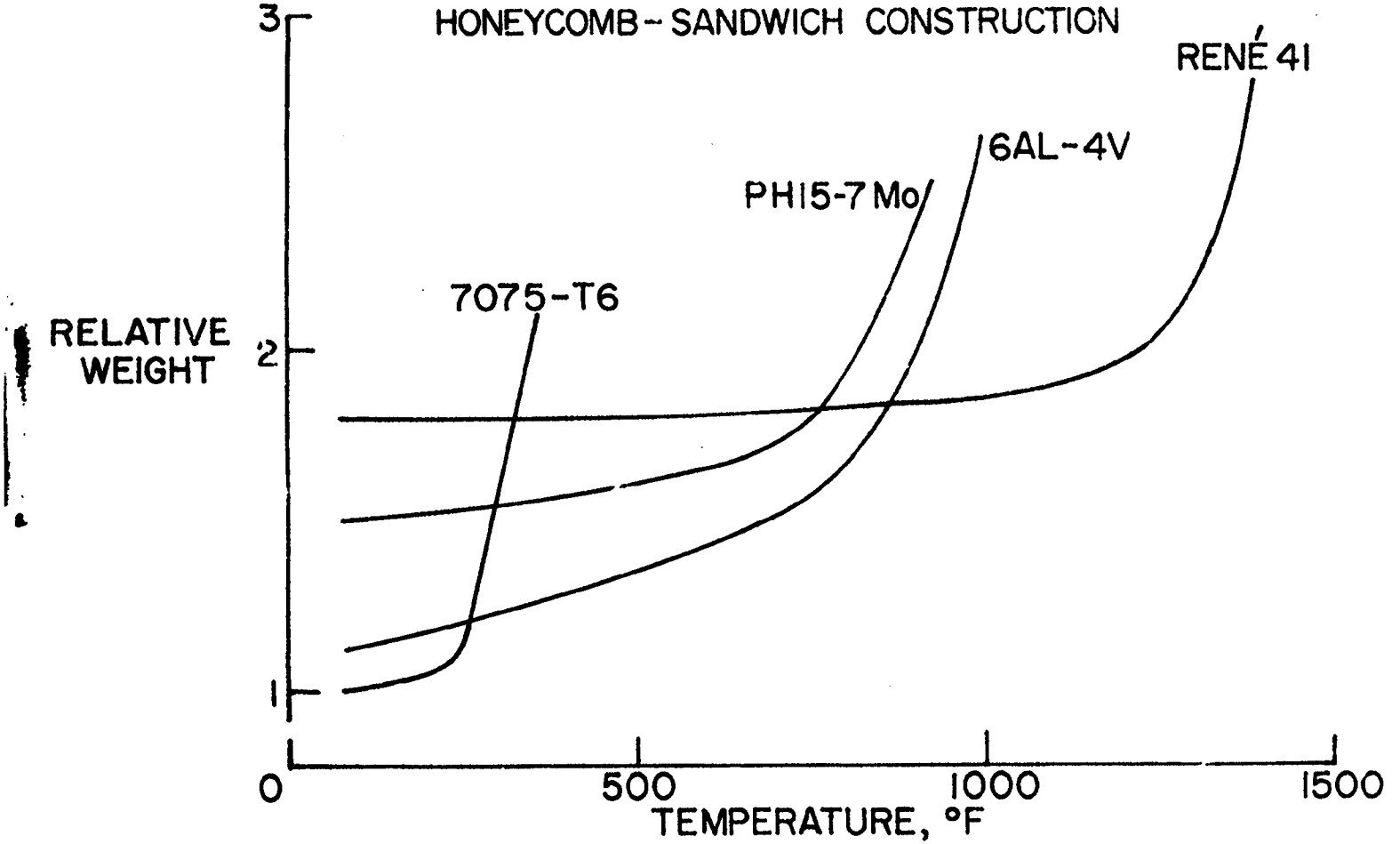

Figure 6

MAXIMUM STRENGTH OF SANDWICH PLATES UNDER NONUNIFORM TEMPERATURES

17-7PH STAINLESS STEEL

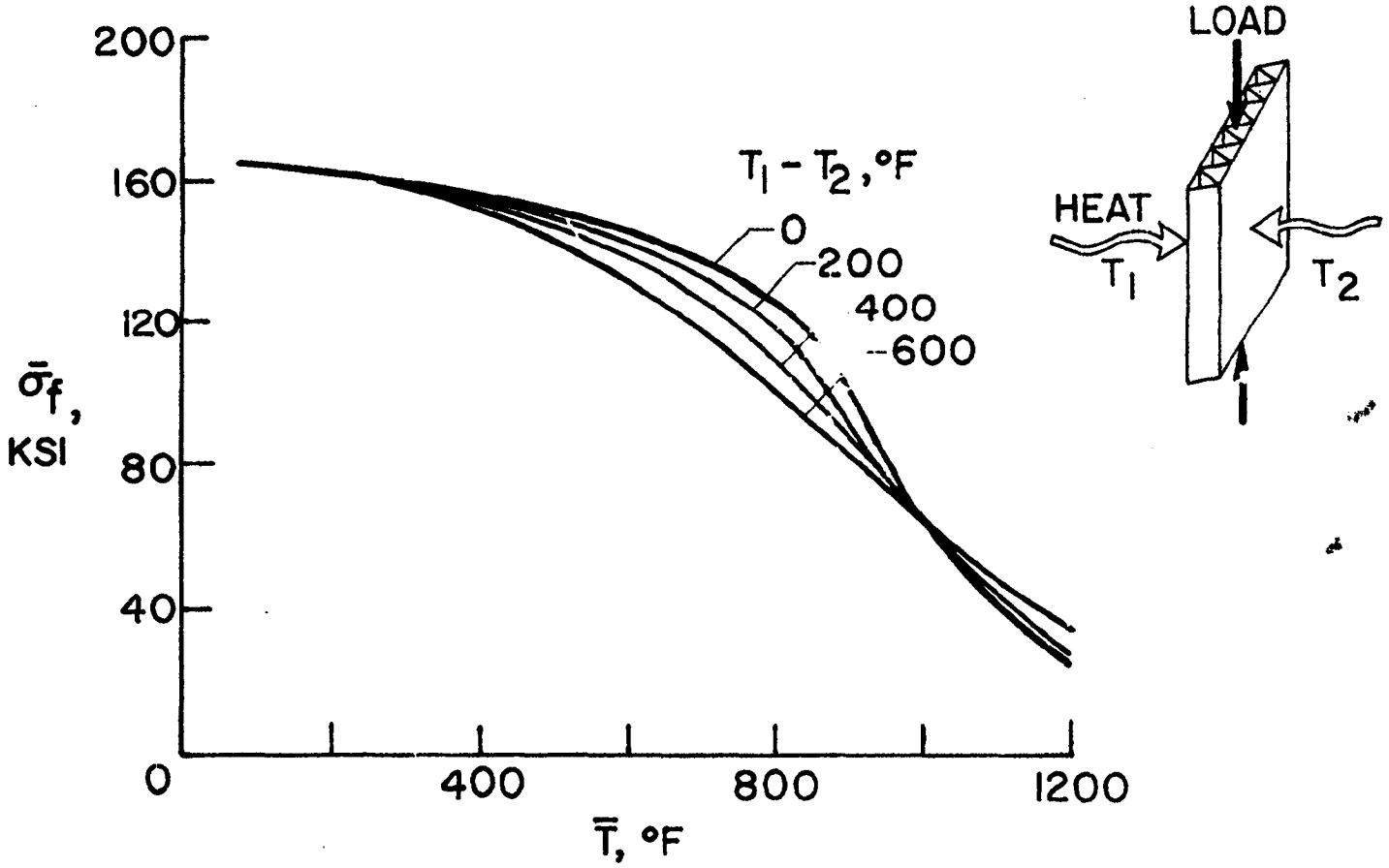

Figure 7

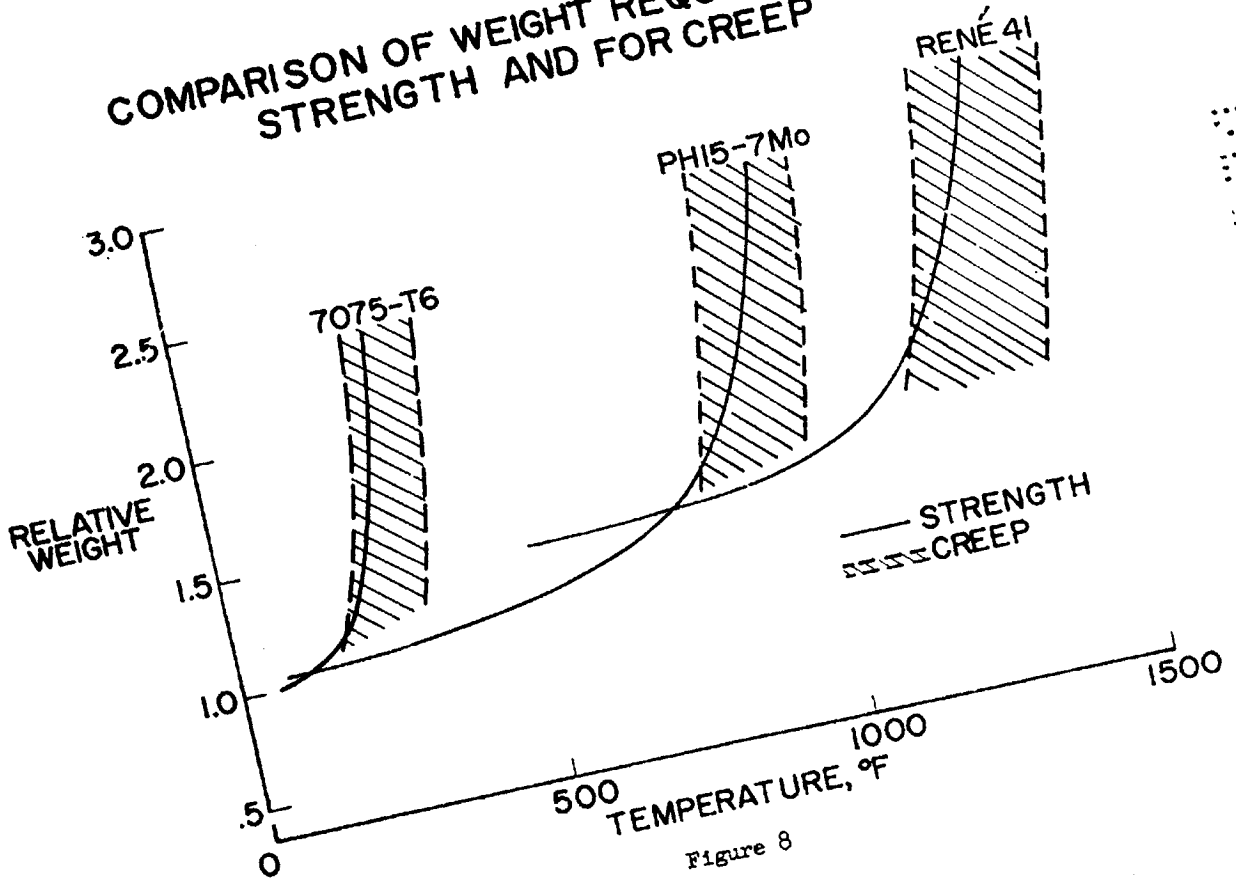
COMPARISON OF WEIGHT REQUIRED FOR STRENGTH AND FOR CREEP
RENÉ 41
PH15-7Mo
7075-T6
3.0
2.5
2.0
1.5
1.0
.5
0
RELATIVE WEIGHT
STRENGTH
CREEP
500
1000
1500
TEMPERATURE, °F

Figure 8

SKIN-RIB JUNCTURES

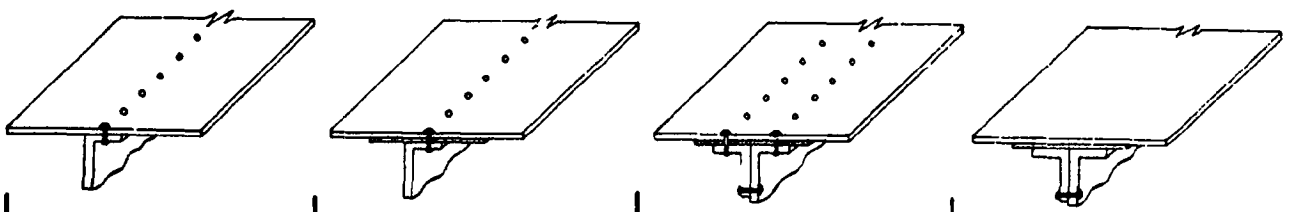

NOISE LEVEL, db				
160	17	180	1,500	3,000
170	—	—	—	23

TIME TO FAILURE, MINUTES

Figure 9

HONEYCOMB PANEL CONFIGURATIONS

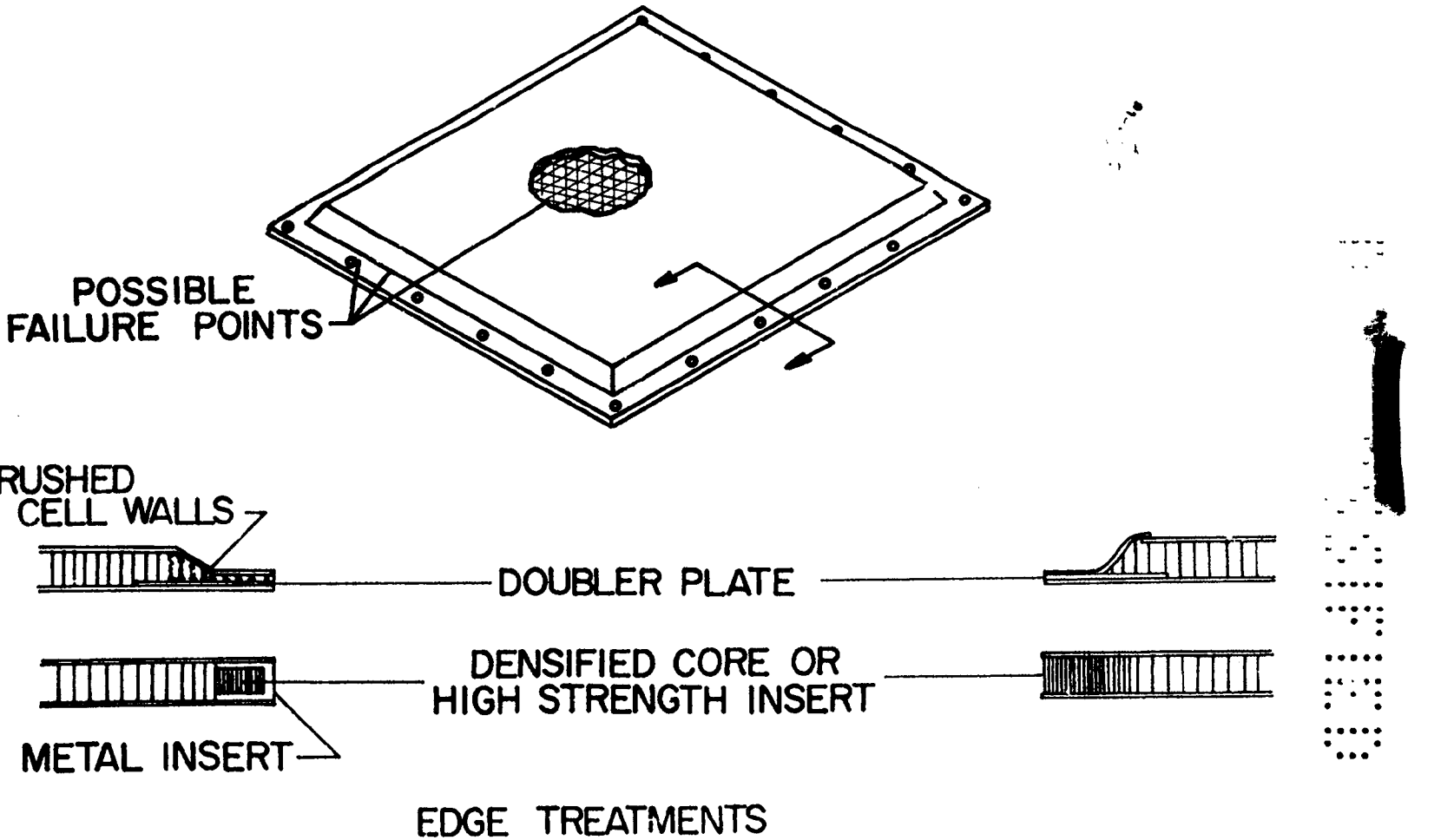

Figure 10

PANEL FLUTTER

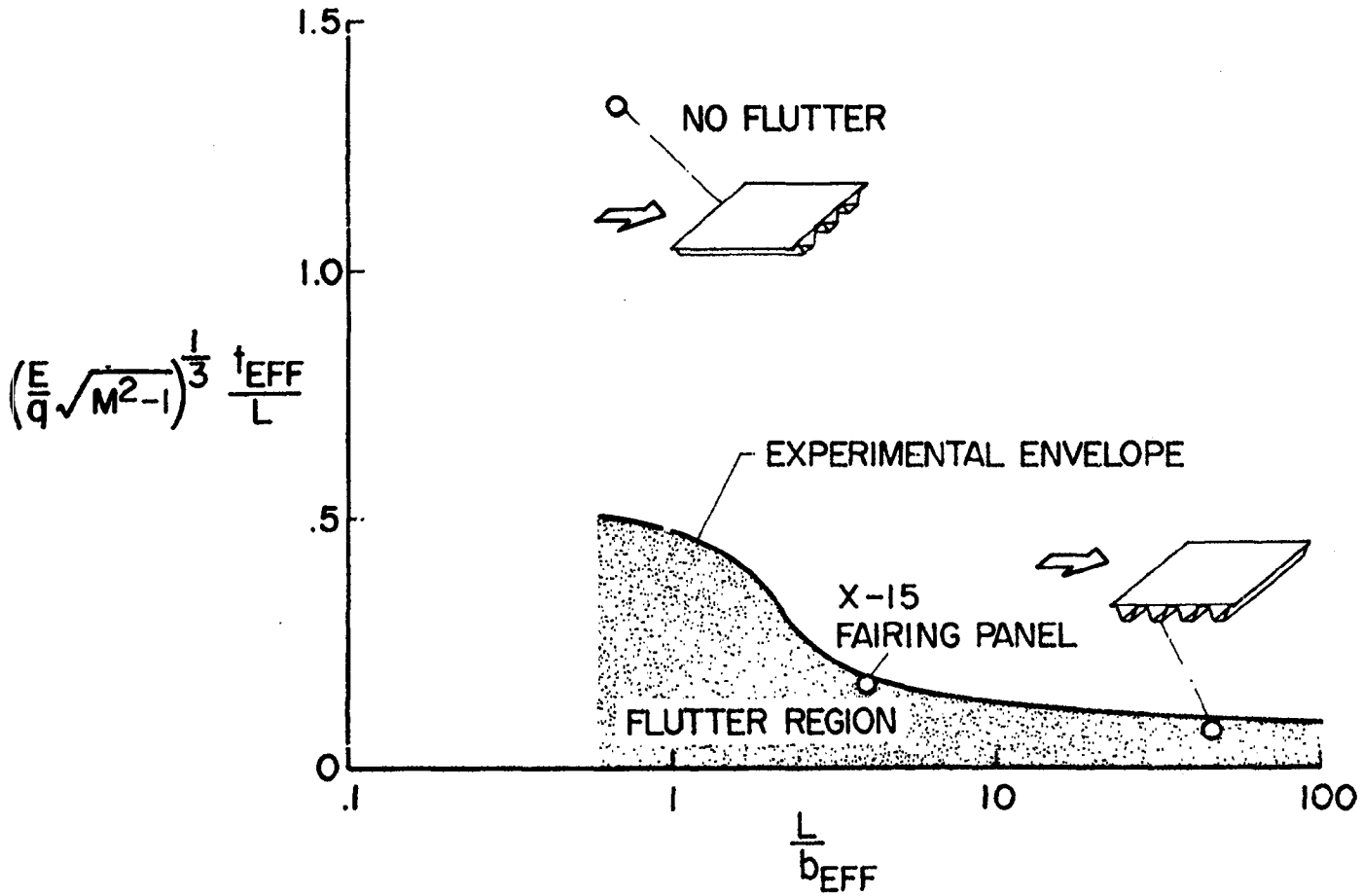

Figure 11

X-15 FAIRING PANEL FLUTTER

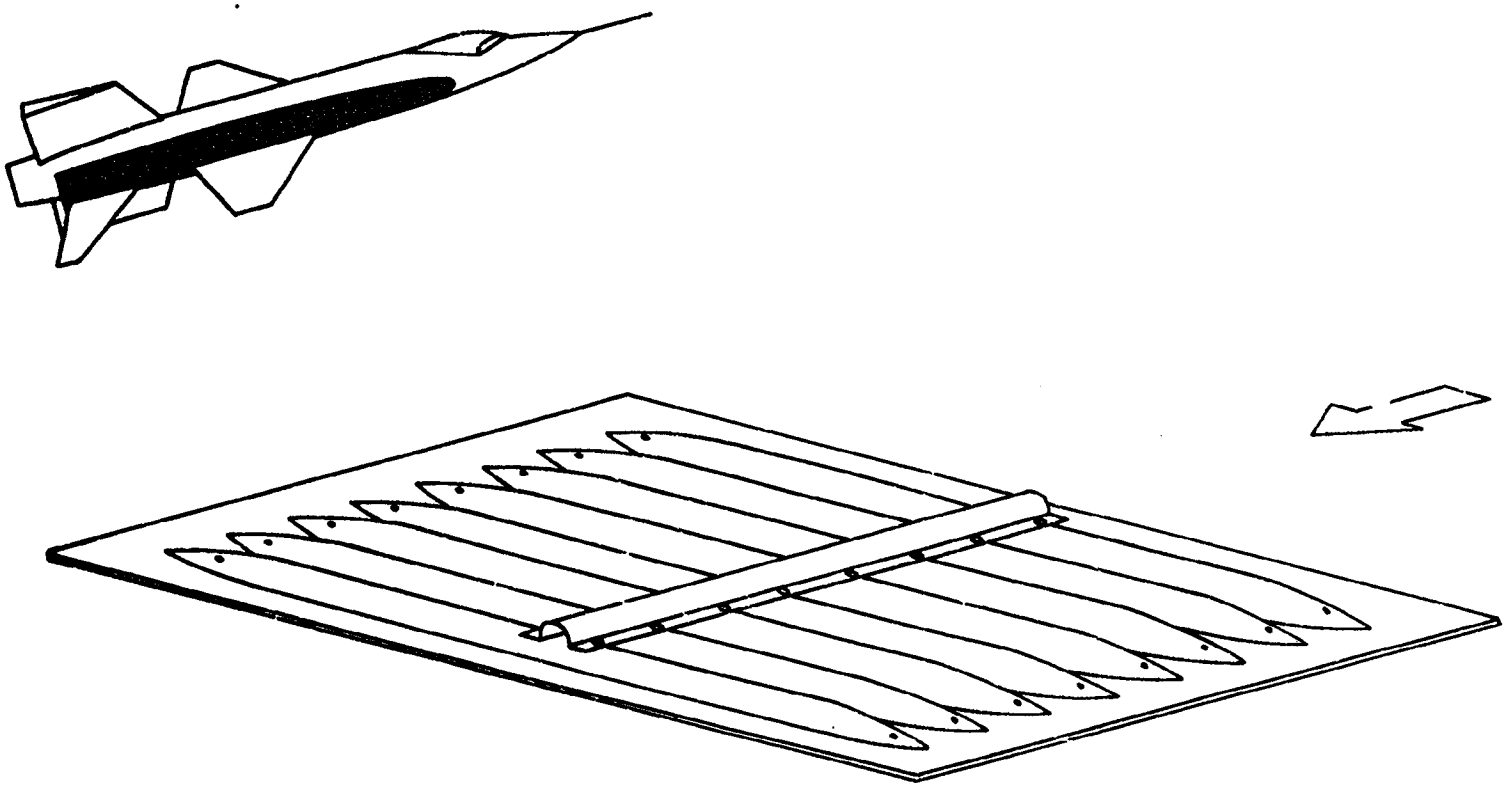

Figure 12

VIII. NOISE CONSIDERATIONS FOR FUTURE MANNED AIRCRAFT

By Harvey H. Hubbard and Domenic J. Maglieri

Langley Research Center

INTRODUCTION

Past experience has indicated that the noise problems of an aircraft are closely related to its design and the manner in which it is operated. Thus, in order to assess properly the potential noise problems of a future aircraft, a knowledge of the main features of its aerodynamic configuration is required as well as an appreciation for the various mission profiles assigned to it.

The material of figure 1 has been taken from various configuration studies, and the values listed are thought to be representative of three future aircraft types to which the discussions of the present paper will be limited. These are subsonic propeller- and jet-powered V/STOL aircraft, large high-altitude supersonic-cruise aircraft, and special mission aircraft capable of supersonic flight at low altitudes. The values given in figure 1 do not apply to any specific designs but are believed to be realistic for these various aircraft types. In this paper there will be no attempt to document the noise problems anticipated for each of these aircraft completely, but rather the discussion will be limited to those problem areas that are inherently associated with each because of its design and the missions to be performed.

Figure 2 indicates the main sources of noise for each aircraft type. For the V/STOL type aircraft, the main noise sources are the power plants. Adverse community reaction to noise during take-off and landing may be a problem for all three aircraft and will be discussed specifically for the V/STOL and supersonic transport. Although sonic fatigue due to the power plants will not be covered in this paper, it should be pointed out here that the problems for the V/STOL aircraft are similar in nature to those for current aircraft. Placing power plants in the rear of the airframe, as has been indicated in many proposed supersonic-transport designs, will tend to minimize but not necessarily eliminate the problem. For aircraft operating at high dynamic pressures, boundary-layer noise is the main concern and will be discussed for a range of operating conditions of interest for both high-altitude and low-altitude supersonic aircraft. Shock-wave-noise problems are, of course, only of concern for supersonic-flight operations. These will be discussed from the standpoint of minimizing annoyance and property damage during routine supersonic-flight operations, and also from the standpoint of maximizing shock-wave-induced damage for special military missions.

Of particular concern in the operation of V/STOL aircraft is the possible adverse community reaction around airports due to power-plant noise during take-off and landing operations. Estimates have been made of the noise characteristics of two proposed V/STOL aircraft in an attempt to evaluate their noise problems for commercial-type operations. Some of the operating rules assumed for these aircraft are illustrated in figure 3. It is assumed that they would operate from either conventional airports or short-haul terminals. All V/STOL aircraft are assumed to climbout at a 10° geometric angle. This climbout angle is maintained to an altitude of 1,500 feet at which point a transition is made to level flight. This level-flight condition is continued out beyond the area of air traffic congestion before the climb to cruising altitude is made. The reverse of this procedure is used during the landing phase to the point where the approach is initiated, and then a 6° geometric approach angle is assumed.

Estimated noise data for STOL take-offs and landings are presented in figures 4 and 5. The data of the figures apply directly to the STOL conditions; the principal conclusions, however, also apply to V/STOL conditions except in the areas close to the terminal. Perceived noise levels (PNdb) for the location along the ground track of the aircraft are plotted in figure 4 as a function of distance from the point of lift-off in miles. Also shown on the figure for comparison are available data for conventional four-engine transport aircraft (ref. 1). It is assumed that the STOL aircraft has two turboprop engines or two turbofan engines. The horizontal line of small dashes in the center of each figure corresponds to an acceptable noise level in some communities for daylight and early evening operations. Note that levels below the line are considered acceptable whereas levels above the line are not considered acceptable. The main objective is to operate in such a way that the perceived noise levels on the ground become equal to or less than the acceptable level in as short a ground distance as possible. It will be noted from figure 4 that the propeller- and jet-powered STOL aircraft achieve acceptable noise levels in a shorter distance from lift-off than conventional transports. These reductions result mainly from the different noise spectra and the steeper climbout capability of the STOL aircraft.

Similar data are presented for landing in figure 5. The objective in landing is to operate the aircraft so that the noise levels remain at acceptable values within as short a distance as possible from the point of touchdown. It can be seen that at a given distance from the point of touchdown the perceived noise levels associated with propeller-driven STOL aircraft are somewhat higher than those for the conventional propeller transports. This increase in noise level is mainly due to

the higher power settings required during landing. The jet-powered STOL aircraft has lower noise levels than current jet transports because of different noise spectra and a steeper approach angle.

The airspeed of the STOL aircraft during landing is considerably lower than that for conventional aircraft, and hence the duration of noise exposure for an observer on the ground is proportionately longer. There is, thus, a possibility that the acceptable noise level for V/STOL type operations would tend to be lower than the acceptable level for conventional airplane operations. Also of concern is the fact that STOL operations may be carried on at local terminals in the vicinity of which the noise tolerance may be less than in more densely populated areas. It should be noted that the STOL aircraft in landing at a conventional airport would probably touchdown about one mile closer to the center of the airport than the conventional aircraft. Hence, its noise at a given distance from the end of the runway would generally be lower than that for conventional transports.

There is a similar concern for the community reaction to supersonic-transport-type operations near conventional airports. Climbout will be made at about a 10° geometric angle, and the approach path will be at about a 3° geometric angle.

In figure 6, perceived noise levels are plotted as a function of horizontal distance in miles from the point of lift-off and touchdown. Comparisons are again made with available data for conventional transport-type aircraft which are indicated by the hatched areas in the figure. For the take-off condition, the turbofan-powered supersonic transport (SST) is seen to have lower perceived noise levels than the current jet-transport aircraft. This results mainly from the fact that the larger thrust-to-weight ratio of the supersonic transport makes it capable of a steeper climbout angle.

For the landing condition in which the approach angles are about equal to those presently being used, the estimated range of perceived noise levels for the supersonic transport are shown by the crosshatched area in figure 6. A range of values is included because of the uncertainty in evaluating the airframe noise component. If noise from the airframe were not significant, then it is believed that the overall perceived noise levels during landing could be reduced to values near the lower extremity of the crosshatching in figure 6.

If turbojet engines with noise suppressors were used, it is believed that the obtainable perceived noise levels would only approach those of the upper extremity of the crosshatched area in the figure. Furthermore, the problem of providing acceptable noise suppressors for this type of aircraft is a formidable one because of the requirements for variable area exits and retraction during cruise flight.

[redacted]

BOUNDARY-LAYER NOISE

On current airplanes the boundary-layer noise is mainly of concern from the standpoint of passenger comfort. For future aircraft, particularly those capable of supersonic-flight speeds, there is a concern not only for passenger comfort but also for noise-induced damage to the skin structure of the airplane.

Results from a large number of experimental investigations have suggested that the boundary-layer-noise pressures on an aircraft surface are roughly proportional to the local dynamic pressures (ref. 2). A brief summary of existing information relating to surface-pressure levels is given in figure 7 for a range of dynamic pressures of interest for future aircraft. In this figure, the term $\sqrt{\overline{p}^2}$ is the mean square of fluctuating pressure and q is the dynamic pressure. Experiments at subsonic speeds have indicated that the noise pressures are approximately equal to 0.006 times the dynamic pressure. This relationship is illustrated by the solid line in figure 7. Recent wind-tunnel and flight tests have indicated that the empirical constant in the above relation may be as low as 0.002 at supersonic speeds. This difference is equivalent to about 10 db, as indicated by the hatched area below the solid line. On the other hand, recent measurements from Project Mercury space vehicles have indicated that in regions of separated flow the surface-pressure levels may be as high as 10 db above those indicated by the solid line. (See figs. 8 and 9 of ref. 3.) This increase due to flow separation is indicated by the crosshatched area above the solid line. Thus, at any given value of dynamic pressure, a wide range of surface-pressure levels may exist depending on the flow conditions. Shown also on figure 7 is a horizontal dashed line at a surface-pressure level of 140 db. It is believed that pressure levels higher than this may, under some conditions, cause structural damage. The locations of the ticks and the sketches at the bottom of the figure indicate the approximate maximum dynamic-pressure values associated with each aircraft type. It can be seen that the STOL type aircraft will probably encounter little, if any, damage to the structure because of boundary-layer noise. On the other hand, the supersonic transport and special mission aircraft will probably have large areas of surface structure over which the pressure levels are sufficiently high to cause damage.

Further considerations relating to the boundary-layer-noise problem are illustrated in figure 8. Boundary-layer thickness and surface pressures are indicated as a function of distance along the airplane fuselage. At the front of the aircraft, there is a region of laminar flow in which the surface-pressure levels are relatively low. Where the shading begins there is then a transition to turbulent boundary layer a short distance back along the fuselage and this turbulent

[redacted]

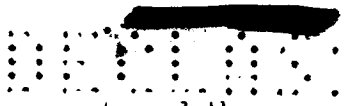

boundary layer thickens up toward the rear of the aircraft. Measurements have suggested that the overall fluctuating surface-pressure magnitudes are essentially constant along the fuselage although the spectrum shape varies considerably with boundary-layer thickness. As a result of this spectrum change, the surface pressures vary as indicated schematically in the bottom part of the figure. Near the front of the airplane, where the boundary layer is thin, the high frequencies predominate and the low- (audible) frequency pressures are small. Toward the rear of the aircraft where the boundary layer is thicker, the low frequencies predominate and the high- (ultrasonic) frequency pressures are small (ref. 2). The problems of acoustic fatigue of the skin surfaces and noise insulation of the interior compartments both involve the dynamic responses of the structure which are usually in the audible-frequency range. Thus, it would appear that both the acoustic-fatigue problem and interior-fuselage noise would be more troublesome in the aft portions of the aircraft.

SHOCK-WAVE NOISE

Additional sources of noise in the operation of supersonic aircraft are the shock waves which result in sonic booms. Although these resulting sonic-boom disturbances may be observed throughout all supersonic phases of the flight, the most serious problems appear to be associated with the climb phase where sonic booms may be produced at reduced altitudes (ref. 4).

The material of figure 9 suggests an approach to solving the sonic-boom problem for the supersonic transport during the climb phase. The hatched area represents combinations of Mach number and altitude which may result in damage to structures on the ground. The shaded area above the hatching represents combinations of Mach number and altitude for which sonic booms will be observed on the ground and which may be annoying but will not cause damage.

The main objective in this flight operation is to travel from ground level to cruise conditions without intersecting the damage area. This may be accomplished by climbing subsonically to some intermediate altitude, accelerating to supersonic speeds in level flight, and then finally climbing and accelerating to cruise conditions. This altitude of 35,000 feet is considered an absolute minimum value and for a large airplane should probably be in the vicinity of 45,000 feet.

There has been some concern about being able to make predictions of the sonic-boom pressures for the case of a large airplane at high altitudes for which it has been shown theoretically that the lift component of the boom pressure might be relatively large (ref. 5). Experimental data under realistic flight conditions are urgently needed for

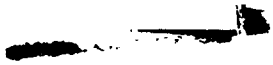

correlation with results of analytical studies and to evaluate the atmospheric propagation losses. An extrapolation of data from fighter airplanes at high altitudes suggests that cruise-flight altitudes in the vicinity of 60,000 to 70,000 feet may be acceptable for the supersonic transport.

Because of the increased performance capability of some proposed aircraft, it will be possible to operate at supersonic Mach numbers at very low altitudes. The question has arisen as to the possibility of doing enough damage as a result of the sonic boom to warrant its use as a tactical weapon in a manner illustrated in figure 10. The airplane would be flown on a low-altitude pass over a suitable target area in such a manner as to expose it to damaging pressures in a short interval of time. Such an operation might have the effect of temporarily inerting some types of enemy activity on the ground over fairly large areas.

Indications of the nature of the pressures obtainable and their effects are given in figure 11. When the airplane is at a relatively high altitude, that is several thousand feet, the pressure signature has the characteristic "N" wave shape as illustrated in the lower sketch. Peak overpressures Δp up to about 10 lb/sq ft are obtainable. In this pressure range, humans and animals are startled, and damage has occurred to large plate glass windows and to plaster walls.

When the airplane is at a relatively low altitude, the pressure signature has a shorter period and is much more complex in nature as illustrated in the upper right-hand sketch of figure 11. Peak overpressures Δp up to about 100 lb/sq ft have been obtained for fighter planes operating overhead at a vertical distance of about 150 feet. Up to overpressures Δp of 100 lb/sq ft, no lasting physiological effects were noted for people repeatedly exposed, although they were startled and may have suffered some temporary hearing loss. Widespread window damage has occurred, and in some cases buckling of wall and roof panels has occurred. There have also been incidents of malfunction of nonruggedized pressure-sensitive electronic equipment. Measurable vertical and horizontal earth motions have been recorded for a wide range of supersonic-flight conditions.

CONCLUDING REMARKS

In conclusion, some of the principal noise problems anticipated for future aircraft types such as the subsonic V/STOL airplane, the supersonic transport, and the special mission aircraft capable of supersonic flight at low altitudes have been discussed. The main noise sources are noted to be the power plants, the boundary layer, and the shock waves. Engine-noise problems will be of particular concern in

commercial-type operations of V/STOL and the supersonic transport, particularly during the landing operation. Boundary-layer noise is of importance for aircraft such as the supersonic transport and any special mission aircraft that fly at high dynamic pressures. Special provision will have to be made in the design of the supersonic transport to allow it to operate at sufficient altitudes so as to minimize sonic-boom disturbances on the ground and to avoid damage. The ability of the sonic boom to create some types of structural damage may be used to advantage for special tactical missions.

REFERENCES

1. Anon.: Studies of Noise Characteristics of the Boeing 707-102 Jet Airliner and of Large Conventional Propeller-Driven Airliners. Bolt Beranek and Newman Inc., Oct. 1958.

2. Richards, E. J., Bull, M. K., and Willis, J. L.: Boundary Layer Noise Research in the U.S.A. and Canada; A Critical Review. USAA Rep. No. 131, Univ. of Southampton, Feb. 1960.

3. Hilton, David A., Mayes, William H., and Hubbard, Harvey H.: Noise Considerations for Manned Reentry Vehicles. NASA TN D-450, 1960.

4. Lina, Lindsay J., Maglieri, Domenic J., and Hubbard, Harvey H.: Supersonic Transports - Noise Aspects With Emphasis on Sonic Boom. 2nd Supersonic Transports (Proceedings), S.M.F. Fund Paper No. FF-26, Inst. Aero. Sci., Jan. 1960.

5. Walkden, F.: The Shock Pattern of a Wing-Body Combination, Far From the Flight Path. Aero. Quarterly, vol. IX, pt. 2, May 1958, pp. 164-194.

[redacted]

AIRCRAFT TYPES

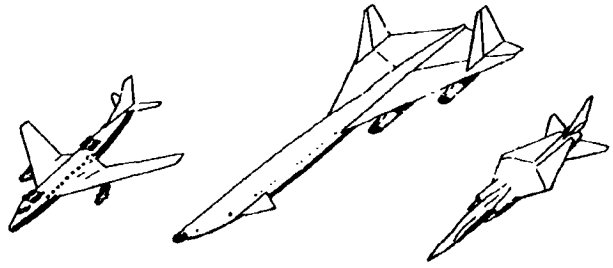

THRUST, LB	65,000	120,000	40,000
WEIGHT, LB	55,000	350,000	60,000
M	0.6	3.0	0.9-2.5
ALTITUDE, FT	40,000	70,000	100

Figure 1

PRINCIPAL NOISE SOURCES

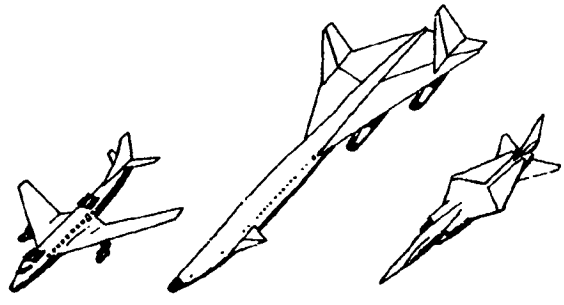

POWER PLANTS	✓	✓	
BOUNDARY LAYER		✓	✓
SHOCK WAVES		✓	✓

Figure 2

V/STOL OPERATIONS

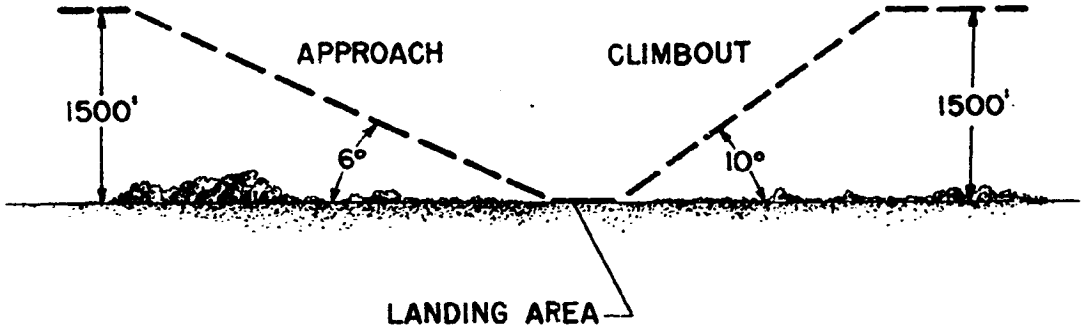

Figure 3

V/STOL TAKE-OFF NOISE

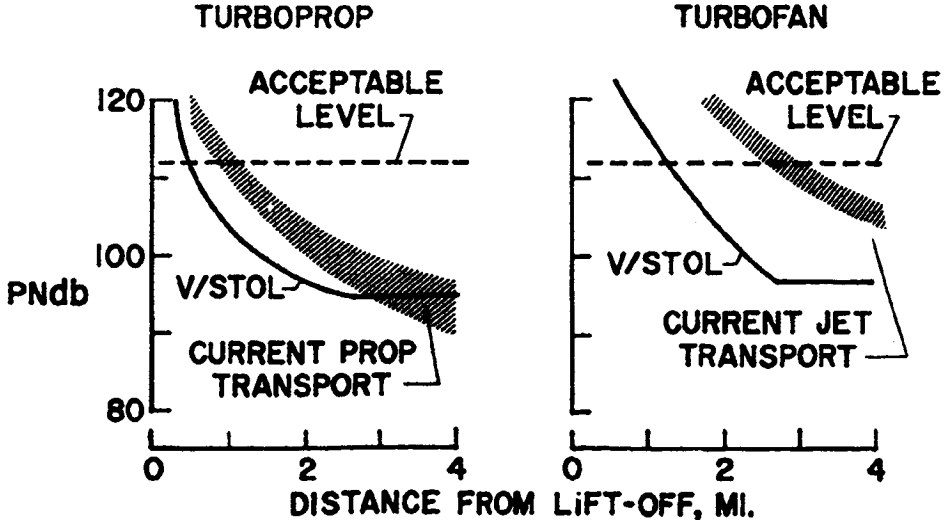

Figure 4

[redacted]

V/STOL LANDING NOISE

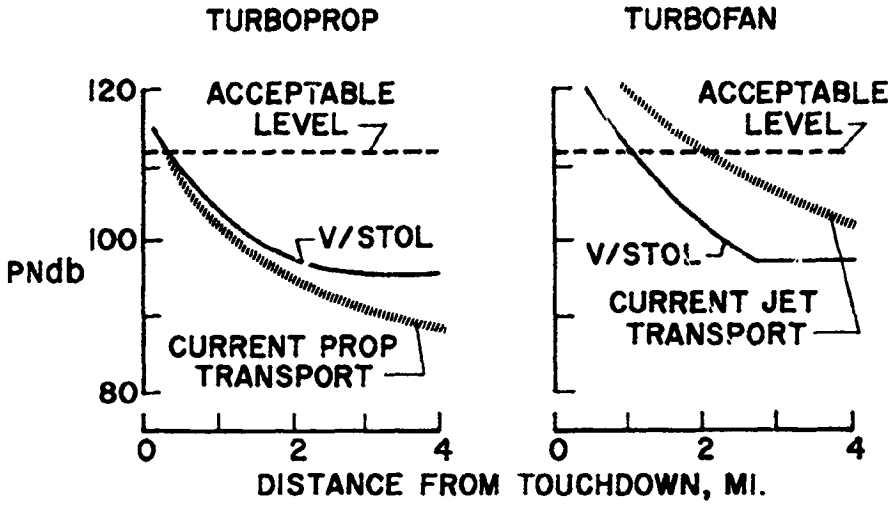

Figure 5

SUPERSONIC-TRANSPORT ENGINE NOISE

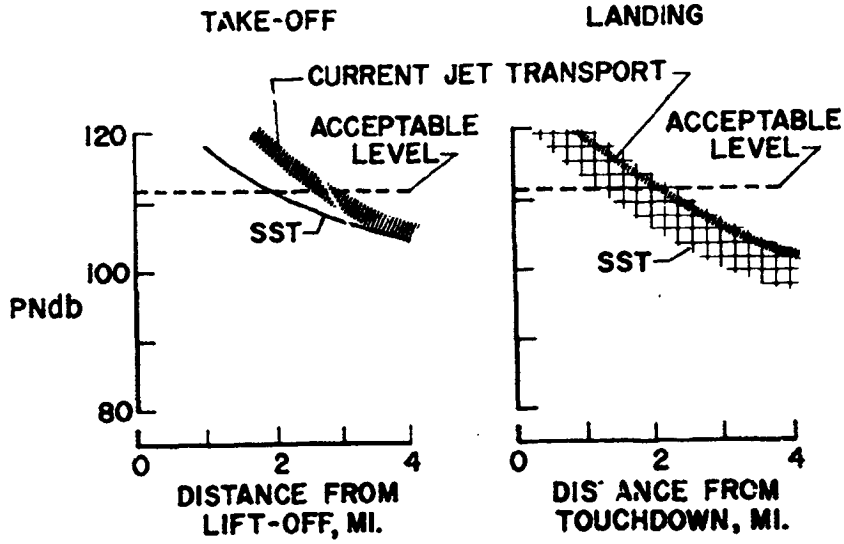

Figure 6

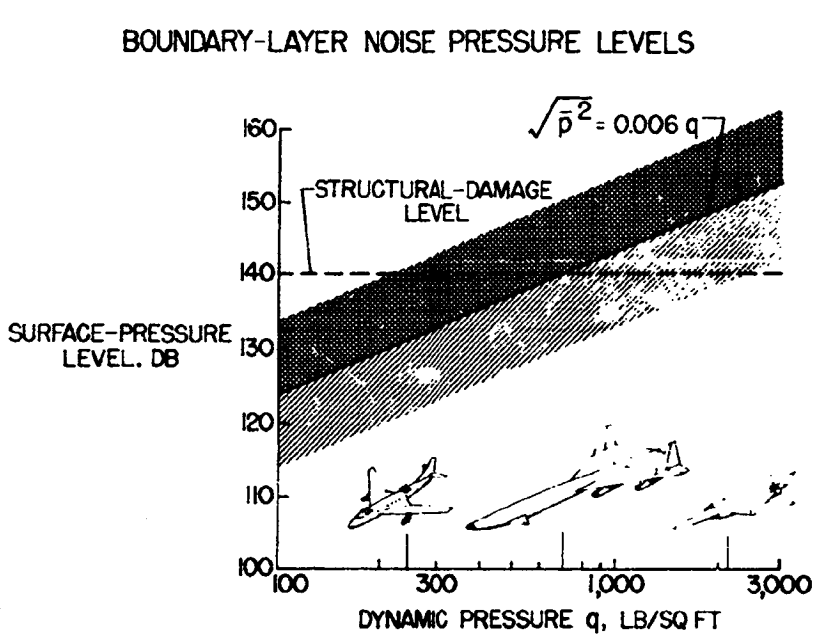

Figure 7

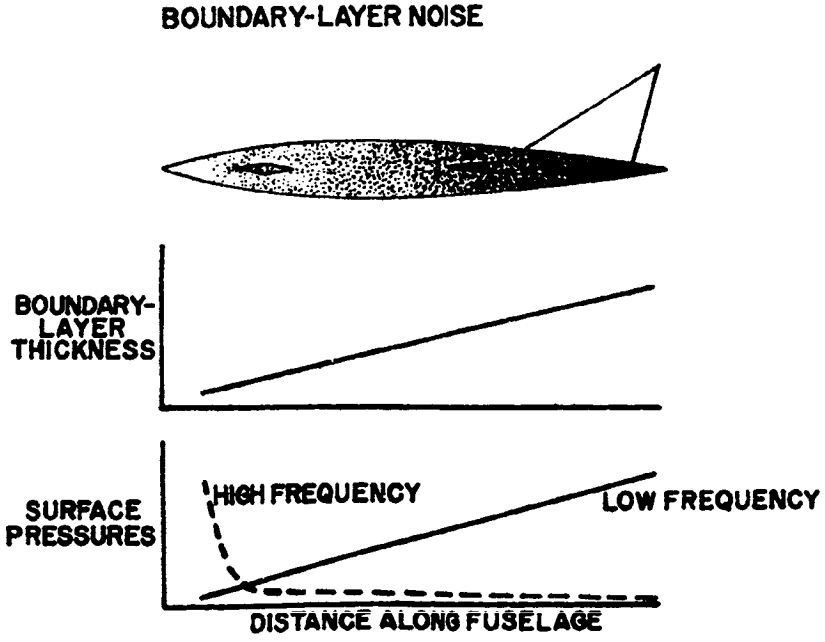

Figure 8

[redacted]

SUPERSONIC-TRANSPORT CLIMB SCHEDULE

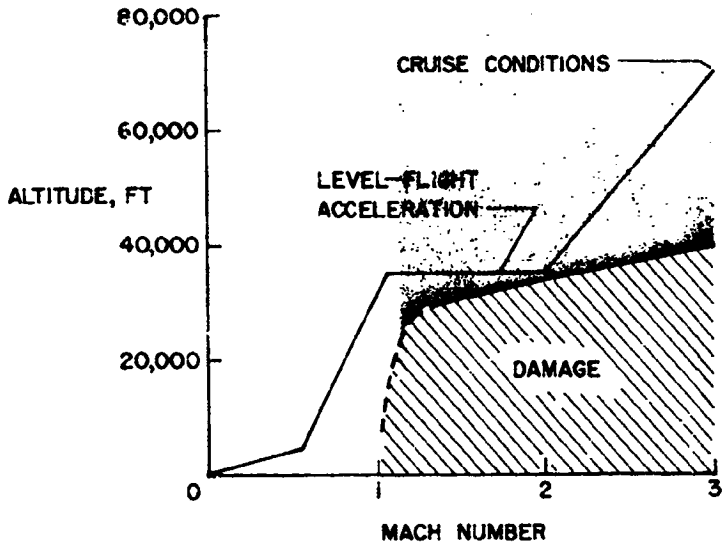

Figure 9

SONIC-BOOM DAMAGE

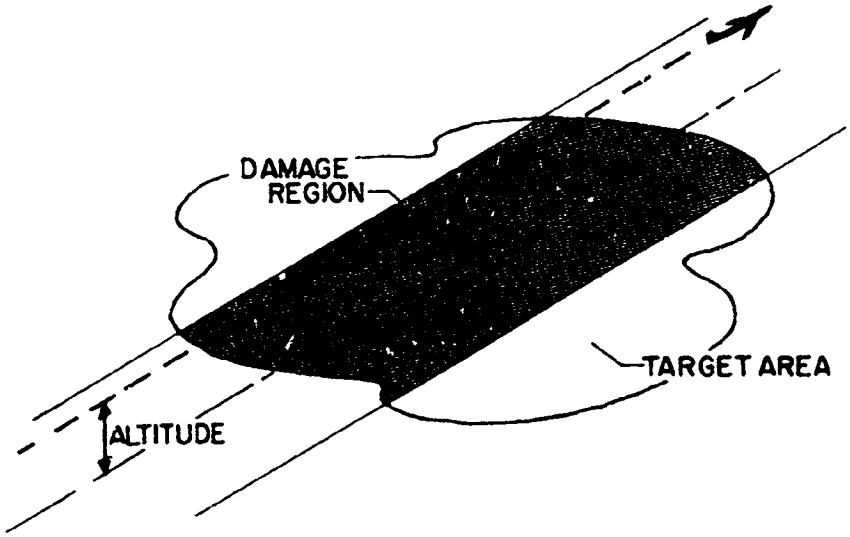

Figure 10

[redacted]

SONIC-BOOM EFFECTS

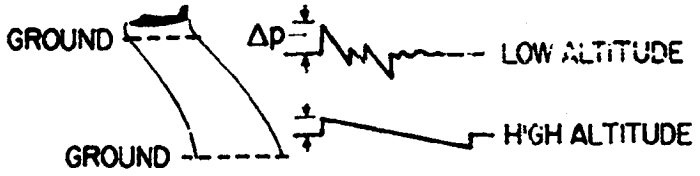

Δp, LB/SQ FT	EFFECTS
1 – 10	STARTLE HUMANS & ANIMALS DAMAGE TO LARGE PLATE GLASS SOME PLASTER DAMAGE
10 – 100	NO LASTING PHYSIOLOGICAL EFFECTS WIDESPREAD WINDOW DAMAGE BUCKLING OF WALL & ROOF PANELS SOME MALFUNCTION OF ELECTRONICS MEASURABLE EARTH MOTIONS

Figure 11

IX. SIMULATION REQUIREMENTS FOR THE DEVELOPMENT OF ADVANCED MANNED MILITARY AIRCRAFT

By Euclid C. Holleman
Flight Research Center

and Melvin Sadoff
Ames Research Center

INTRODUCTION

Paralleling the large increase in the performance capability of present airplanes has been the increase in the problems connected with the design and operation of these airplanes. Many methods have been devised to study these problems, but perhaps no single method of analysis has achieved the success and universal acceptance accorded the flight simulator as a design and research tool. The simulation of flight is a relatively new art which depends to a large extent on the ingenuity of the designer of the simulator. Of course, the use of a flight simulator will never replace actual flight. However, because of the increased usefulness of the simulator for airplane design and for the reduction of flight time, much more effort is being expended to improve the realism of the flight simulator and to increase its flexibility.

Some of the most useful simulations have involved the pilot in the control loop. A drawing illustrating a pilot-operated flight simulator is presented in figure 1. Illustrated is the flow of information from the computer to the pilot and back to the computer. The pilot is the key link in closing the control loop.

The National Aeronautics and Space Administration has had considerable experience with a wide variety of piloted-flight simulators from simple, inexpensive, fixed-chair types to complex and expensive human centrifuges and variable stability and control airplanes. As is indicated in figure 2, these simulators fall logically into two groups, ground based and airborne, by virtue of their operating environment. The fixed-base simulator setup is described in figure 1. The moving visual environment (fig. 2) refers to a dome-type simulator or a television-camera sensor with appropriate projection on a screen in front of the pilot's cockpit. The moving-base simulators provide linear acceleration, such as the normal-acceleration chair or the human centrifuge at the Naval Air Development Center, Johnsville, Pa. Other simulators provide angular acceleration or attitude; an example is the pitch-roll chair. The flight vehicles refer to variable-stability

airplanes (for example, the NASA modified F-100C airplane) a variable-stability helicopter, and a variable-stability VTOL (the X-14). Variable-control-system airplanes have also been tested, as has a variable-control helicopter. The low-dynamic-pressure airplane refers to reaction-control tests with the F-104, whereas the low-lift-drag-ratio landing tests refer to the simulation of the X-15 landing with the F-104.

Some of the typical aircraft design problems that have been studied in varying degrees by using flight simulators are as follows: basic stability and damping requirements, piloting techniques, emergency procedures, evaluation of displays, primary control systems, augmentation systems, landing techniques, and performance and ranging. Much effort has been spent in the areas of stability and control, piloting techniques, and augmentation systems. This backlog of experience has provided considerable information on, and insight into, the simulator complexity required for a wide variety of aircraft design problems. The purpose of this paper is to review some of the more recent simulator results with emphasis on the airplane-design problem areas. Some of the simulator requirements for V/STOL and a low-altitude attack airplane will also be presented. Areas requiring additional effort are discussed briefly. Simulators for crew training, however, are not considered in this paper.

SYMBOLS

b reference lateral length, ft

C_l rolling-moment coefficient

$$C_{l_p} = \frac{\partial C_l}{\partial\left(\frac{pb}{2V}\right)}$$

$$C_{l_{\delta_a}} = \frac{\partial C_l}{\partial \delta_a}$$

C_m pitching-moment coefficient

$$C_{m_q} = \frac{\partial C_m}{\partial\left(\frac{qc}{2V}\right)}$$

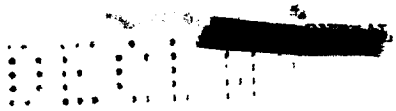

$C_{m_{\delta_e}} = \frac{\partial C_m}{\partial \delta_e}$

c reference longitudinal length, ft

I_X inertia in roll, slug-ft^2

I_Y inertia in pitch, slug-ft^2

H 1 8 3

$L_p = \frac{q_O S b^2}{2VI_X} C_{l_p}$, per sec

$L_{\delta_a} = \frac{q_O S b}{I_X} C_{l_{\delta_a}}$, per sec^2

$M_q = \frac{q_O S c^2}{2VI_Y} C_{m_q}$, per sec

$M_{\delta_e} = \frac{q_O S c}{I_Y} C_{m_{\delta_e}}$, per sec^2

p rolling velocity, radian/sec

q pitching velocity, radian/sec

q_O dynamic pressure, lb/sq ft

S reference area, sq ft

V velocity, ft/sec

δ_a maximum lateral-control deflection, radian

δ_e maximum longitudinal-control deflection, radian

ζ damping ratio

ω_n undamped natural frequency, radian/sec

DISCUSSION

To be effective, a flight simulator should prompt pilot response and comment similar to that obtained during actual flight. Pilot opinion, then, is the prime measuring device for determining the effectiveness of the simulation. Therefore, program results will be reviewed where pilot-opinion comparisons between simulator and flight are available.

By using simulators and variable-stability airplanes, the stability and damping requirements for both the longitudinal and the lateral directional modes of airplanes have been studied. Representative results are presented in figure 3 showing areas, obtained in flight with a variable-stability airplane, that were considered by the pilots to have satisfactory, unsatisfactory, unacceptable, and uncontrollable longitudinal characteristics. In order to determine the effectiveness of the simulators, this same range of airplane dynamics has been investigated by the same pilots by use of a fixed-base and a moving-base simulator (the pitch-roll chair). Figure 4 correlates the pilot-opinion results obtained with the piloted simulator with those obtained in flight. The correlation of both simulators with flight is near perfect until the region of poor airplane dynamic characteristics is reached, where the fixed-base-simulator correlation becomes poor. The moving-base simulator correlates to extremely poor dynamics. In fact, dynamic characteristics which were unflyable with the fixed-base simulator were controllable with the moving-base simulator and in flight; thus, there is a need for motion stimulus in the case of very poor dynamics. The fixed-base simulator, however, was completely satisfactory for a wide range of airplane dynamics including the unstable range of airplane characteristics and gave at least qualitative pilot ratings even in the poorest areas such as high-frequency low damping. Investigations have also been conducted for lateral and directional airplane dynamics and lateral-control coupling, and similar results were obtained.

In addition to the work on conventional aircraft, considerable ground-based simulator work has been completed recently to define control requirements for V/STOL type aircraft. Concurrent flight tests of these V/STOL aircraft have permitted a preliminary comparison between single-degree-of-freedom simulator results and the hovering-control requirements from flight tests.

Data obtained during this study are shown in figure 5. It should be noted that the important parameters are control power and damping. Also shown are the basic control power and damping characteristics measured in flight for several VTOL aircraft. Although the flight data are limited, the single-degree-of-freedom simulator results would indicate that airplanes C and D fall in the region of satisfactory pitch-control

characteristics, whereas aircraft A and B would be expected to be unsatisfactory. Similarly, the roll control of airplanes A and C appears to be satisfactory, whereas aircraft B is definitely in an unsatisfactory region. Actual flight evaluations of the pitch and roll controllability of these aircraft are correlated with the pilot opinions from the moving-base simulator in figure 6. Generally, the predicted ratings from the moving-base simulator tests are in fairly good agreement with those from flight; however, they appear, in general, to be optimistic; that is, the simulated airplane was easier to fly than the actual airplane. Some of these differences might be attributed to such factors as control-system "deadband" and friction, which were not simulated.

Although no quantitative comparisons are available for fixed- or moving-base simulators and flight evaluations of overall hovering and transition characteristics of V/STOL airplanes, it is felt that a brief qualitative resumé of experience to date may be of interest. From the pilots' point of view, an analytical six-degree-of-freedom simulation with a moving cockpit which provides pitch and roll motion has proven very valuable for pilots' practice of expected control problems prior to initial flight tests. The simulator also permitted the pilot to determine piloting techniques for recovery from unusual flight conditions. However, because the simulation did not include an adequate presentation of the external visual references that the pilots would have in flight, the pilots observed no direct correspondence between hovering height control and transition in the simulator and in flight. When definite limitations in the simulation have been noted on the piloted-flight simulator such as just described, it has been helpful for the pilot in evaluating a new configuration to fly the simulation of an airplane with which he has had recent flight experience. This procedure serves to orient or calibrate the pilot to the limitation of the simulation so that he can evaluate objectively the relative difficulty of the new airplane control task.

Recent pilot evaluations of fixed-cockpit simulators, which provide six-degree-of-freedom simulated external visual environment, have indicated that this type of simulator is admirably suited to the V/STOL simulation problem, particularly for accurately evaluating the hovering and transition characteristics of the airplane. The addition of three-axis angular motion may be desirable but, perhaps, is not essential for this problem.

Another design problem in which the simulator has been used is for checking the pilot's presentation. Tests have been made with an airplane, a moving-base simulator, and a fixed-base simulator to compare the pilot's performance while tracking with an inside-out and an outside-in target display. The performance of the pilots was very poor with the outside-in display for both the flight and moving-base simulator, whereas the

performance with the inside-out display was acceptable. These results did not correlate, however, and thus some basic deficiency in the presentation or motion stimulus was indicated. With the fixed-base simulator the pilot's performance with either of the displays was comparable and showed the absence of motion-stimulus effects. From these tests, it was concluded that a fixed-base simulator should not be used for the evaluation of tracking displays and that the results from moving-base simulators should be extrapolated to flight only with reservation.

The fixed-base simulator has also been used during the design of airplane instrument displays. Early in the piloted simulator program of the X-15 airplane a scanning problem was noted by the pilots and, as a result, a rearrangement and a consolidation of the panel instruments was made. Tests with a moving-base simulator (centrifuge) confirmed the improvement afforded by these changes. No new presentation deficiencies have arisen during current flight tests.

A requirement has been indicated for several types of manned military airplanes. One example is the low-altitude attack airplane. This airplane is not too unlike conventional airplanes and, as with any new development program, design and operational problems are expected. Some of these problems are longitudinal- and lateral-control sensitivity, response to turbulence, and control and aerodynamic coupling.

Previous programs have indicated that these problems can be resolved by using a fixed-base simulator with one exception, the piloting problem encountered with a high-performance airplane in turbulent air. Recent tests have shown that both controllability and pilot fatigue are important under these conditions. A moving-base simulator which duplicates the normal acceleration of the airplane will be required for this problem. Figure 7 illustrates such a simulator, the NAA g-seat. This type of simulator is a relatively inexpensive piece of hardware and could, it appears, justify its cost for the investigation of this one problem. The inclusion of pitch and bank angle of this simulator would add realism but would probably not be required.

Thus far, specific-design problem areas that have been investigated on simulators and in flight have been discussed. In order to illustrate further the importance of the piloted-flight simulator, a design program that probably would not have been possible without the piloted-flight simulator - the X-15 research airplane program - is considered briefly. Flight simulators dictated many important design changes to the airplane, but perhaps their most important contribution was to emphasize the need for a complete simulation. The difficulty of the control task during certain parts of the flight envelope showed the need for a moving-base simulation program to investigate the capabilities of the pilot while subjected to the accelerations expected of the airplane. Consequently,

a program was conducted by utilizing the human centrifuge to impose the expected acceleration on the pilot while piloting the simulated X-15 mission. The mechanization of the centrifuge for this program is shown in figure 8. During this simulator program it was determined that, even at the highest acceleration expected, there was little deterioration in the pilot's performance; thus, if the accelerations are below the physiological limit of the pilot, his performance will be unaffected. Exposure to the expected accelerations increased the pilot's confidence in his ability to cope with the problems of actual flight. Experience from several centrifuge programs has shown that, to determine the tolerance limit to acceleration, a centrifuge is necessary; however, for the investigation of airplane control problems with the centrifuge, serious problems have been noted because of spurious motion cues.

At present, a complete six-degree-of-freedom fixed-base X-15 simulator, including the control-system hardware, an airplane-like cockpit with functional pilot's controls, and actual electronic components of the stability-augmentation system, is being used for flight planning, pilots' practice for flight, and for verification of airplane flight behavior after flight. The pilots have enthusiastically endorsed the use of the fixed-base piloted-flight simulator for becoming acquainted with the piloting task before actual flight. Perhaps the most significant contribution of the X-15 simulator program will be correlation of the data from flights, moving base simulators, and fixed-base simulators for defining the simulator requirements for the design of future manned military and research airplanes.

Some results of simulator studies which have provided information concerning the type of simulator best suited for different investigations have been described. A few areas where continued effort would result in large dividends will now be discussed.

While investigating the steep-glide approach to a landing, by using the piloted-flight simulator, it was necessary to resort to actual flight with a test airplane because of the lack of realism of the simulator with a conventional presentation. In this area the simulation of the airplane flight environment by televised projection would be admirably suited. While a moving visual environment is being considered, another area requiring continued study is the blending of visual and motion stimuli on the simulator. An example of the effective use of this blending is the DC-8 simulator, in which the initial angular-acceleration motion is simulated and the motion effect is continued by the visual environment. Pilots report that this simulation of flight is very realistic.

In order to simulate adequately problems of long duration that cover a wide range of operating conditions (navigation, for example), greater accuracy of the analog computer is required. Digital-computer elements

and converters are available; however, the present cost of this equipment for most piloted-flight-simulator applications may be prohibitive.

CONCLUDING REMARKS

The fixed-base simulator with adequate presentation and controls is satisfactory for the investigation of a wide range of airplane problems; however, there are areas where realism can be enhanced by suitable motion and visual-environment stimuli. Concerted effort to increase the usefulness and realism of the simulation will yield large dividends in the form of reduced costs of design and flight test of manned airplanes. Finally, caution should be exercised in mechanizing the piloted-flight simulator to avoid unnecessary complexity and costs which would actually retard the development of the airplane.

BIBLIOGRAPHY

Brown, B. Porter: Ground Simulator Studies of the Effects of Valve Friction, Stick Friction, Flexibility, and Backlash on Power Control System Quality. NACA Rep. 1348, 1958. (Supersedes NACA TN 3998.)

Brown, B. Porter, and Johnson, Harold I.: Moving-Cockpit Simulator Investigation of the Minimum Tolerable Longitudinal Maneuvering Stability. NASA TN D-26, 1959.

Brown, B. Porter, Johnson, Harold I., and Mungall, Robert G.: Simulator Motion Effects on a Pilot's Ability To Perform a Precise Longitudinal Flying Task. NASA TN D-367, 1960.

Creer, Brent Y., Heinle, Donovan R., and Wingrove, Rodney C.: Study of Stability and Control Characteristics of Atmosphere-Entry Type Aircraft Through Use of Piloted Flight Simulators. Paper No. 59-129, Inst. Aero. Sci., Oct. 5-7, 1959.

Creer, Brent Y., Stewart, John D., Merrick, Robert B., and Drinkwater, Fred J., III: A Pilot's Opinion Study of Lateral Control Requirements for Fighter-Type Aircraft. NASA MEMO 1-29-59A, 1959.

Douvillier, Joseph G., Jr., Foster, John V., and Drinkwater, Fred J., III: An Airborne Simulator Investigation of the Accuracy of an Optical Track Command Missile Guidance System. NACA RM A56G24, 1956.

Douvillier, Joseph G., Jr., Turner, Howard L., McLean, John D., and Heinle, Donovan R.: Effects of Flight Simulator Motion on Pilots' Performance of Tracking Tasks. NASA TN D-143, 1960.

Eggleston, John M., Baron, Sheldon, and Cheatham, Donald C.: Fixed-Base Simulation Study of a Pilot's Ability To Control a Winged-Satellite Vehicle During High-Drag Variable-Lift Entries. NASA TN D-228, 1960.

Foster, John V., Fulcher, Elmer C., and Heinle, Donovan R.: An Air-Borne Target Simulator for Use With Scope-Presentation Type Fire-Control Systems. NACA RM A57C19, 1957.

Hardy, James D., and Clark, Carl C.: The Development of Dynamic Flight Simulation. Aero/Space Eng., vol. 18, no. 6, June 1959, pp. 48-52.

Holleman, Euclid C., Armstrong, Neil A., and Andrews, William H.: Utilization of the Pilot in the Launch and Injection of a Multistage Orbital Vehicle. Paper No. 60-16, Inst. Aero. Sci., Jan. 25-27, 1960.

Holleman, Euclid C., and Boslaugh, David L.: A Simulator Investigation of Factors Affecting the Design and Utilization of a Stick Pusher for the Prevention of Airplane Pitch-Up. NACA RM H57J30, 1958.

Holleman, Euclid C., and Stillwell, Wendell H.: Simulator Investigation of Command Reaction Controls. NACA RM H58D22, 1958.

James, Harry A., Wingrove, Rodney C., Holzhauser, Curt A., and Drinkwater, Fred J., III: Wind-Tunnel and Piloted Flight Simulator Investigation of a Deflected-Slipstream VTOL Airplane, the Ryan VZ-3RY. NASA TN D-89, 1959.

Matthews, Howard F., and Merrick, Robert B.: A Simulator Study of Some Longitudinal Stability and Control Problems of a Piloted Aircraft in Flights to Extreme Altitude and High Speed. NACA RM A56F07, 1956.

McFadden, Norman M., Pauli, Frank A., Deinle, Donovan F.: A Flight Study of Longitudinal-Control-System Dynamic Characteristics by the Use of a Variable-Control-System Airplane. NACA RM A57L10, 1958.

McNeill, Walter E., and Creer, Brent Y.: A Summary of Results Obtained During Flight Simulation of Several Aircraft Prototypes With Variable-Stability Airplanes. NACA RM A56C08, 1956.

Rathert, George A., Jr., Creer, Brent Y., and Douvillier, Joseph G., Jr.: Use of Flight Simulators for Pilot-Control Problems. NASA MEMO 3-6-59A, 1959.

Sadoff, Melvin: The Effects of Longitudinal Control-System Dynamics on Pilot Opinion and Response Characteristics As Determined From Flight Tests and From Ground Simulator Studies. NASA MEMO 10-1-58A, 1958.

Stillwell, Wendell H., and Drake, Hubert M.: Simulator Studies of Jet Reaction Controls for Use at High Altitude. NACA RM H58G18a, 1958.

Weil, Joseph, and Day, Richard E.: An Analog Study of the Relative Importance of Various Factors Affecting Roll Coupling. NACA RM H56A06, 1956.

White, Maurice D., and Drinkwater, Fred J., III. A Comparison of Carrier Approach Speeds As Determined From Flight Tests and From Pilot-Operated Simulator Studies. NACA RM A57D30, 1957.

FIXED-BASE SIMULATOR

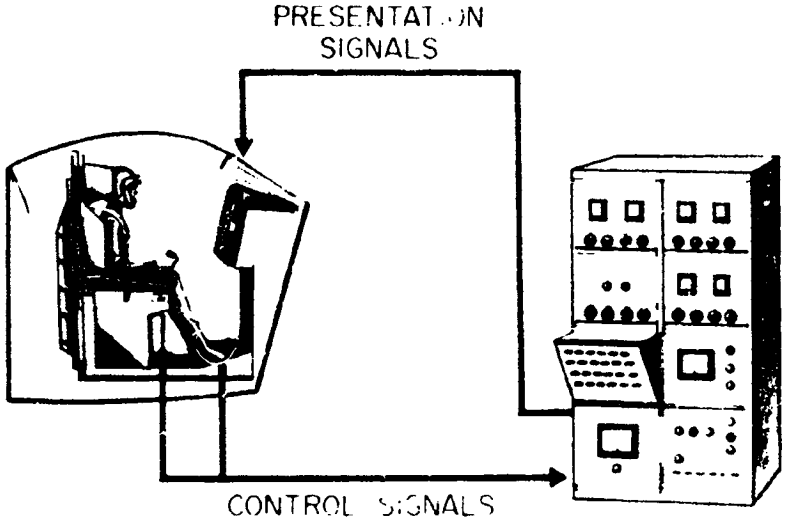

Figure 1

E-5636

TYPES OF SIMULATORS

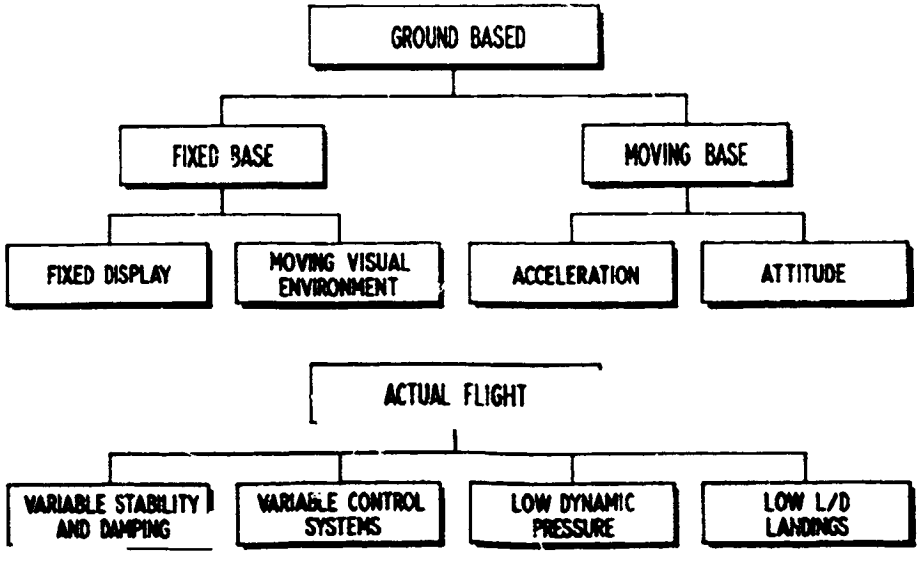

Figure 2

FLIGHT EVALUATION OF AIRPLANE DYNAMICS

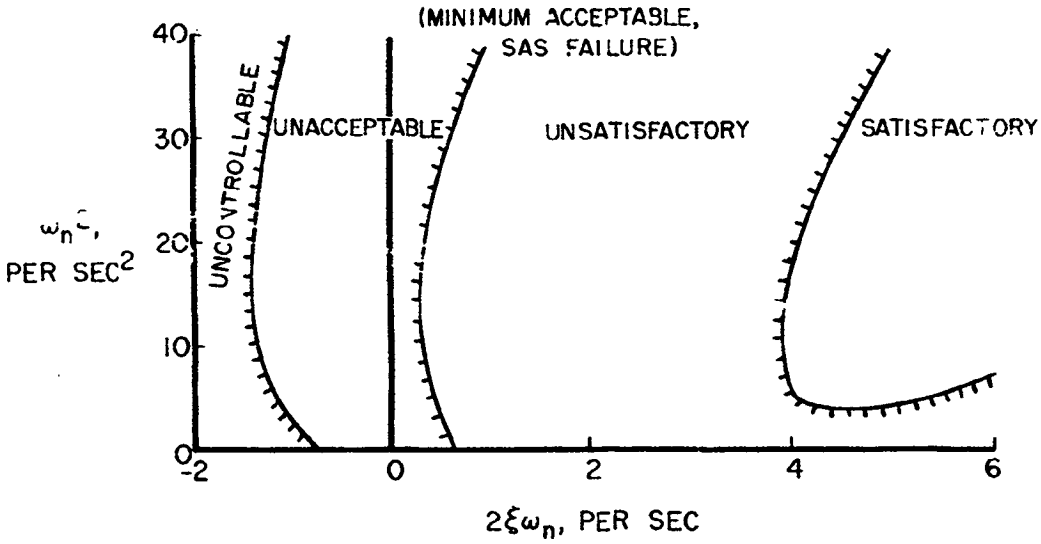

Figure 3

CORRELATION OF PILOT OPINION
LONGITUDINAL DYNAMICS

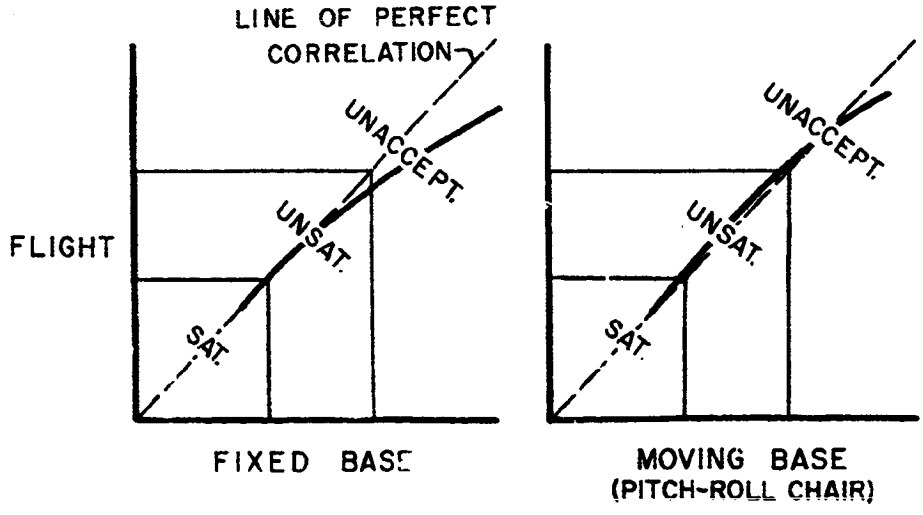

Figure 4

V/STOL HOVERING CONTROL REQUIREMENTS

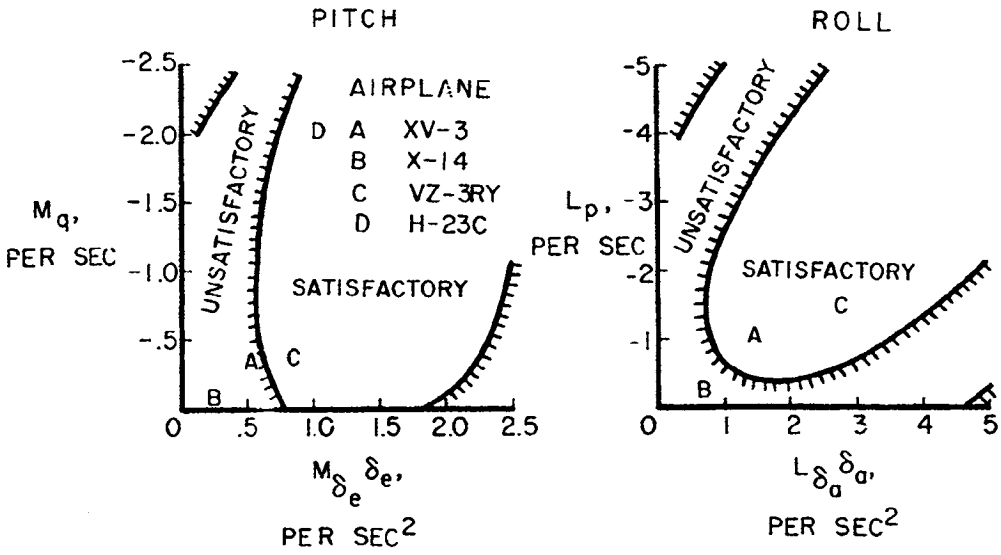

Figure 5

CORRELATION OF PILOT OPINION

V/STOL CONTROL

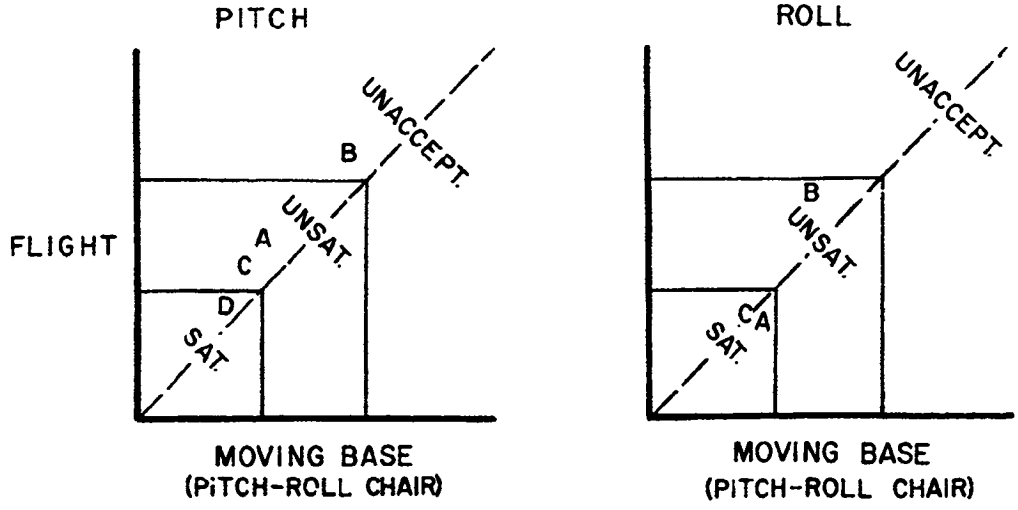

Figure 6

[redacted]

NAA g-SEAT

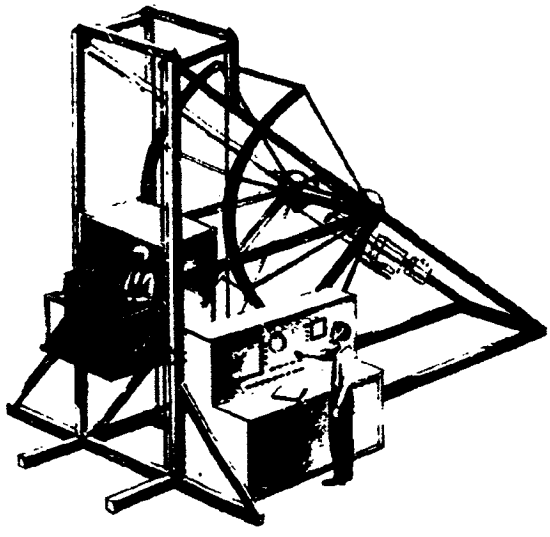

Figure 7 E-5665

CENTRIFUGE DYNAMIC SIMULATION

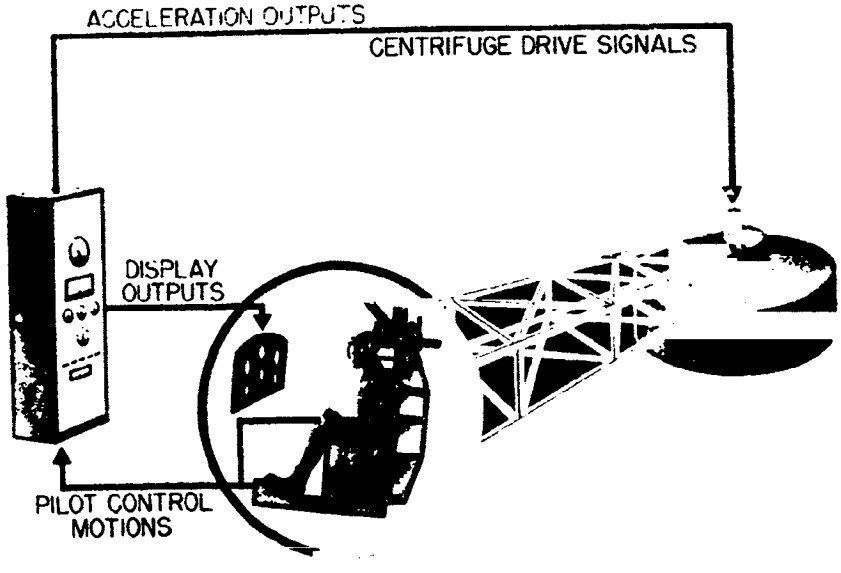

Figure 8 E-5637

RESUMÉ

VTOL aircraft: Helicopters will continue to be the best VTOL for missions where long hovering time is required and where low speed and short range are acceptable. Compound helicopters are expected to give a small increase in cruising speed and range. The propeller-driven tilt-wing and flap configuration is considered to be one of the most promising VTOL types, particularly for use on transport missions where long range is required and where higher speed is advantageous. Although a great deal of research and development will be required before optimum operational VTOL aircraft will be obtained, progress in this field has advanced to the point where operationally useful machines of the most promising types can be designed and built. A great need at the present time is for experience with VTOL aircraft to demonstrate their potentialities and to define more clearly the service requirements in the various areas.

Variable-sweep multimission aircraft: Recent research on variable-sweep wings has led to the development of configurations having acceptable stability and control characteristics over a large wing sweep angle variation without the previously required wing translation. This development opens a new potential for improving the compatibility of the configurations needed for optimum performance at supersonic and subsonic flight conditions, and thus offers greatly improved aircraft versatility. It appears, for example, that one properly designed variable-sweep airplane will be able to accomplish a number of important missions such as transoceanic ferry, extended subsonic patrol or loiter, long-range high-altitude supersonic attack, and long-range low-level supersonic attack. Efficient STOL performance also can be provided in the same aircraft if desired, in order to permit operation out of very small fields. It is estimated that the weight and size of such a multimission aircraft will not appreciably exceed the weight and size of any of the specialized single-purpose aircraft which it can replace.

Supersonic cruise aircraft: Supersonic cruise efficiency comparable to that of present subsonic jet transports has been shown to be attainable within the present state of the art. Recent research indicates further potential gains by reduction of turbulent skin friction through boundary-layer injection and by improvements in drag due to lift. For commercial supersonic transports the major aerodynamic problems are found in the off-design areas, such as take-off and landing, transonic acceleration at high altitude, and subsonic cruise efficiency.

Air-breathing propulsion systems: The current status of propulsion system components designed for Mach 3 flight has been reviewed, and it has been shown that reasonably high levels of on-design performance can be obtained. Off-design performance improvements are necessary and will

require a great deal of individual tailoring. The turbofan engine appears to offer advantages over the turbojet in the areas of take-off noise, off-design specific fuel consumption, higher augmentation ratios at transonic speeds, and lower temperatures during supersonic cruise. Some disadvantages may be a greater frontal area for a given thrust and larger inlet and ducting weights than the turbojet. In spite of these disadvantages, the desirable characteristics appear to make further development of the turbofan highly warranted.

The X-15 flight research program: The research objectives of the X-15 flight program were formulated to provide information over a wide range of conditions pertinent to the development of advanced military aircraft. The flight results obtained thus far indicate reasonable agreement with wind-tunnel predictions regarding aerodynamic forces and heating up to a Mach number of 3. Current plans are to extend the data on the X-15 to these and other aerodynamic, structural, and systems problems in the speed range between Mach numbers of 3 and 6.

Hypersonic-cruise vehicles: Aerodynamic lift-drag ratios have been obtained on both hydrocarbon-fuel and hydrogen-fuel vehicles which are high enough to provide desirable cruise ranges. The thermodynamics of the ramjet units yield values of propulsive efficiency which, when coupled with the aerodynamic efficiency, indicate desirable range-payload possibilities. The aerodynamic heating of the vehicles is low enough that it is within the present construction capability of the aviation industry.

Structures and materials: Structural design and structural materials have an important bearing on the integrity and performance of military aircraft. Weight-strength considerations are useful in the selection of materials; however, other factors such as tear resistance are becoming increasingly important, particularly for transport-type aircraft. Various types of structural construction are of interest for high-density heat-resistant materials. These include honeycomb-sandwich, open-face sandwich, and skin-stringer types. Among these the honeycomb-sandwich construction generally yields the lightest structure. For wing-type structures the most efficient honeycomb-sandwich construction yields a deeper wing than either the most efficient skin-stringer or open-face sandwich. Other factors that are important in aircraft structures include strength under nonuniform temperatures, sonic fatigue, and panel flutter. Creep, on the other hand, will in all probability not be a major structural problem.

Noise considerations: The main noise sources anticipated for future aircraft types such as the subsonic V/STOL airplane, the supersonic transport, and the special mission low-altitude supersonic aircraft, are noted to be the power plants, the boundary layer, and the shock waves. Engine noise problems will be of particular concern in commercial type

operations of V/STOL and the supersonic transport with respect to adverse reactions in communities near airports, particularly during the landing operation. Boundary-layer noise is of importance for aircraft such as the supersonic transport and any special mission aircraft that fly at high dynamic pressures. Special provision will have to be made in the design of the supersonic transport to allow it to operate in such a way as to minimize sonic boom disturbances on the ground and to avoid damage to ground structures. The ability of the sonic boom to create structural damage may be used to advantage for some special tactical missions.

Simulation requirements: The flight simulator has been universally accepted as an effective tool for manned aircraft design and operational research. The fixed-base simulator with adequate presentation and controls has been satisfactorily employed for investigation of a wide range of problems. Furthermore, its value may be enhanced by the inclusion of certain motion and visual-environment stimuli; such studies, for example, would be useful in the evaluation of hovering and transition characteristics of V/STOL aircraft or control and response of the low-level attack airplane. Televised projection techniques and the blending of such visual stimuli with motions are expected to improve the simulation of flight environment for low-level flight and landing approaches. However, caution must be exercised to avoid prohibitive complexity and cost in simulators, even though the technology for provision of more complete simulations is available.

National Aeronautics and Space Administration,
Washington 25, D.C., August 26, 1960.

NASA - Langley Field, Va. L-1210 - 1215, 1279, H-182 - 183